



## City Research Online

### City, University of London Institutional Repository

---

**Citation:** Arnold, P. (2018). Hybrid Radio Resource Management with Limited Channel Feedback Information in Relay enhanced OFDMA Networks. (Unpublished Doctoral thesis, City, University of London)

This is the accepted version of the paper.

This version of the publication may differ from the final published version.

---

**Permanent repository link:** <https://openaccess.city.ac.uk/id/eprint/22229/>

**Link to published version:**

**Copyright:** City Research Online aims to make research outputs of City, University of London available to a wider audience. Copyright and Moral Rights remain with the author(s) and/or copyright holders. URLs from City Research Online may be freely distributed and linked to.

**Reuse:** Copies of full items can be used for personal research or study, educational, or not-for-profit purposes without prior permission or charge. Provided that the authors, title and full bibliographic details are credited, a hyperlink and/or URL is given for the original metadata page and the content is not changed in any way.

---

---

---

City Research Online:

<http://openaccess.city.ac.uk/>

[publications@city.ac.uk](mailto:publications@city.ac.uk)

---

# **Hybrid Radio Resource Management with Limited Channel Feedback Information in Relay enhanced OFDMA Networks**

Paul Arnold

Doctor of Philosophy

School of Mathematics, Computer Science and Engineering,  
City, University of London

August 2018



# Contents

<b>Acronyms</b>	<b>XIII</b>
<b>1 Introduction</b>	<b>1</b>
1.1 Motivation and Overview . . . . .	1
1.1.1 Objectives statement . . . . .	2
1.2 Contribution of the Thesis . . . . .	3
1.3 Thesis structure and content . . . . .	4
<b>2 Relay extended OFDMA Networks</b>	<b>6</b>
2.1 Network architecture in 3GPP . . . . .	6
2.1.1 Core network . . . . .	6
2.1.2 Radio access network . . . . .	7
2.1.3 New study item for 3GPP Release 15/16 revisiting relay nodes . . . . .	9
2.2 Relay types in 3GPP . . . . .	10
2.2.1 Enabling Time Division Multiplexing (TDM) for half duplex RNs in 3GPP . . . . .	15
2.2.2 Full duplex and Half duplex relay operation mode . . . . .	17
2.2.3 Radio channel feedback . . . . .	18
2.2.4 Fixed relay deployment scenarios and commercial aspects . . . . .	20
2.3 Radio resource management in RN extended heterogeneous mobile net- works . . . . .	21
2.3.1 Capacity of mobile networks . . . . .	22
2.3.2 Problem formulation . . . . .	25
2.3.3 Level of centralization and signalling overhead for RRM schemes	28
2.3.4 Inter Cell Interference Coordination . . . . .	33
2.3.5 Buffer aided RN . . . . .	37
2.3.6 MS cell selection in RN extended networks . . . . .	39

2.3.7	Radio resource scheduler . . . . .	39
2.4	Summary . . . . .	50
2.5	Research problem . . . . .	52
<b>3</b>	<b>Methodology</b>	<b>54</b>
3.1	System level simulation processing chain . . . . .	55
3.1.1	Input parameter . . . . .	57
3.1.2	Initialization . . . . .	57
3.2	Scenario loop . . . . .	59
3.2.1	Pre-Processing . . . . .	59
3.2.2	Scenario initialization . . . . .	59
3.3	Snapshot loop . . . . .	65
3.3.1	Event control . . . . .	65
3.3.2	RRM update . . . . .	65
3.3.3	Scheduler update . . . . .	65
3.3.4	SINR calculation . . . . .	66
3.3.5	Analysis update . . . . .	68
3.3.6	Channel update . . . . .	68
3.4	Definition of the key performance indicators . . . . .	69
3.4.1	User Geometry (wideband SINR) . . . . .	70
3.4.2	SINR calculation . . . . .	70
3.4.3	Fairness (Normalized user throughput) . . . . .	71
3.4.4	User throughput . . . . .	72
3.5	Implementation of relay nodes . . . . .	73
3.5.1	Site planning approach . . . . .	73
3.5.2	Different link types . . . . .	74
3.5.3	MBSFN subframe configuration . . . . .	75
3.5.4	Channel feedback delay and HARQ timing . . . . .	75
3.5.5	Buffer structure for the two-hop transmission . . . . .	79
3.5.6	Scheduler for relay enhanced networks . . . . .	80
3.6	Calibration . . . . .	81
3.7	Summary . . . . .	84

<b>4</b>	<b>Design of the effective hybrid RRM scheme</b>	<b>87</b>
4.1	Scenario description . . . . .	88
4.2	Adapted decentralized MS cell selection procedure . . . . .	91
4.3	Network-centralized asynchronous RRM . . . . .	92
4.3.1	Simplified numerical example for the centralized optimization process . . . . .	93
4.3.2	Heuristic approach . . . . .	97
4.4	Cell-centralized synchronous adapted scheduling . . . . .	109
4.4.1	Scheduling strategies for optimized subbands . . . . .	115
4.4.2	Numerical examples for the two-Hop proportional fair metric . . . . .	117
4.5	Additional signalling and overhead consideration . . . . .	122
4.6	Summary . . . . .	124
<b>5</b>	<b>Performance analysis</b>	<b>126</b>
5.1	Assumptions of the network scenario . . . . .	127
5.2	Studies of important aspects in RN extended networks . . . . .	130
5.2.1	Comparison of different cell selection metrics . . . . .	130
5.2.2	Comparison of exclusive backhaul scheduling and co-scheduling . . . . .	132
5.3	Final results of the hybrid radio resource management scheme . . . . .	133
5.3.1	Throughput comparison of different two-hop MS feedbacks forwarded from RN to MBS . . . . .	134
5.3.2	Throughput comparison with different fitness functions and scheduling policies . . . . .	135
5.3.3	Final comparison for best feedback, power reduction pattern and scheduling settings . . . . .	138
5.3.4	SINR comparison for best settings . . . . .	139
5.3.5	Fairness comparison for best settings . . . . .	141
5.3.6	Energy consumption . . . . .	142
<b>6</b>	<b>Conclusions and outlook</b>	<b>143</b>
6.1	Conclusions . . . . .	143
6.2	Future work . . . . .	144
	<b>Appendices</b>	<b>146</b>



# List of Tables

2.1	Summary of further RN type attributes . . . . .	14
2.2	Advantages and Disadvantages of the Radio Resource Management (RRM) centralization level . . . . .	33
2.3	Summary RN RRM design principles . . . . .	51
3.1	Relay planning gain . . . . .	74
3.2	MBSFN subframe patterns (from a to h) and their periodicity . . . . .	75
3.3	An example of an MBSFN assignment for 2 RNs . . . . .	76
3.4	Requirements for investigations of Relay Node (RN) extended large scale network performance . . . . .	85
4.1	Summary of the required additional feedback information for the hybrid RRM scheme . . . . .	123
5.1	System Level Simulation Parameters . . . . .	129
5.2	Summary of the parameters applied for the network-centralized scheme .	130

# List of Figures

1.1	Principle flow chart of the SLS with respect to the hybrid RRM scheme and its decomposed sub-problems . . . . .	5
2.1	EPC Core Architecture [6,7] . . . . .	7
2.2	LTE-Advanced RAN Architecture with RN [9] . . . . .	8
2.3	NG RAN Architecture [12] . . . . .	9
2.4	NG RAN gNB Architecture [13] . . . . .	9
2.5	A heterogeneous network consists of wireline backhauled macro, pico, femto, cells and wireless backhauled RN . . . . .	11
2.6	Defined interfaces for RN extended mobile networks by the Third Generation Partnership Project (3GPP) . . . . .	11
2.7	Layer 1 RN Protocol Stack . . . . .	12
2.8	Layer 2 RN Protocol Stack . . . . .	13
2.9	Layer 3 RN Protocol Stack . . . . .	13
2.10	Downlink half duplex RN radio link operation . . . . .	16
2.11	Use of MBSFN subframe structure to receive data at the RN . . . . .	16
2.12	Full Duplex vs. Half Duplex transmission . . . . .	18
2.13	Fixed RN Deployment Scenarios . . . . .	20
2.14	Link types for an RN-extended Network . . . . .	24
2.15	Downlink resource grid in LTE [47] . . . . .	27
2.16	Level of RRM centralization and corresponding feedback requirement for FDD downlink . . . . .	29
2.17	Level of RRM centralization and corresponding feedback requirement for TDD . . . . .	29
2.18	Example Fractional Frequency Reuse Patterns . . . . .	35
2.19	MS specific buffer structure at the RN . . . . .	38
2.20	Round Robin frequency selective scheduling . . . . .	41

2.21	Radio channel dependent scheduling . . . . .	42
2.22	Max SINR scheduling . . . . .	43
2.23	Two hop proportional fair scheduling . . . . .	45
2.24	Two hop co-scheduling among directly attached UEs and RNs . . . . .	47
3.1	DT System Level Simulator Block Diagram . . . . .	56
3.2	Standard network layout with two rings of MBS sites with three sectors . . . . .	58
3.3	Wrap around technique to prevent border effects . . . . .	58
3.4	Two randomly distributed relays per sector . . . . .	60
3.5	1/3 randomly dropped, 2/3 user hot zone distribution . . . . .	61
3.6	User Geometry for an MBS/RN Scenario during RN receiving mode . . . . .	63
3.7	User Geometry for a MBS/RN Scenario during RN sending mode . . . . .	64
3.8	Exemplary CDF of the user throughput assigned to MBSs . . . . .	69
3.9	Example CDF of the UG assigned to MBSs . . . . .	70
3.10	Example CDF of the SINR assigned to MBSs . . . . .	71
3.11	Example CDF for the normalized MS throughput representing fairness of the network . . . . .	72
3.12	Example CDF for the MS / RN throughput separated in different user groups	73
3.13	Virtual Positioning of RNs . . . . .	74
3.14	CQI Feedback for wireless backhaul . . . . .	76
3.15	Additional Delay caused by CQI Feedback Forwarding for the RN Access Link . . . . .	77
3.16	Additional CQI Feedback for DL MSs . . . . .	78
3.17	No adaptation of HARQ feedback delay necessary . . . . .	79
3.18	Principle two-hop MS specific buffer status . . . . .	80
3.19	3GPP calibration results for the User Geometry . . . . .	82
3.20	3GPP calibration results for the DL normalized user throughput . . . . .	83
3.21	3GPP calibration results for the average SINR per UE . . . . .	83
3.22	3GPP calibration results for the cell average and the cell edge Spectral Efficiency (SE) . . . . .	84
4.1	Possible serving and interfering links during backhaul transmission time . . . . .	88
4.2	Possible serving and interfering links during RN access transmission time . . . . .	89
4.3	Simple network scenario for example optimization approach . . . . .	93
4.4	Flow chart for simplified example optimization approach . . . . .	95

4.5	Numerical example for simplified optimization approach . . . . .	96
4.6	Basic idea of a meta heuristic to find a near optimal solution . . . . .	97
4.7	Flow Chart of the applied genetic algorithm . . . . .	99
4.8	Fitness proportionate selection to create couples of parents . . . . .	104
4.9	One point crossover mechanism to create offspring . . . . .	105
4.10	Sensitivity analysis with different mutation rates . . . . .	106
4.11	Maximum fitness values with different mutation rates . . . . .	106
4.12	Example of GA optimization process with Equation 4.19 . . . . .	107
4.13	Numerical example of an optimized transmission power pattern . . . . .	108
4.14	Example of possible optimized transmission power configuration over time	108
4.15	Example of possible optimized transmission power subband configuration over frequency in the ALSF . . . . .	109
4.16	Flow chart of the adapted two hop proportional fair scheduler . . . . .	110
4.17	Flow chart for the resource allocation considering co-scheduling, two-hop proportional fairness and frequency selectivity . . . . .	113
4.18	Two hop co-scheduling among directly attached UEs and RNs with cor- rect frequency selective decisions . . . . .	115
4.19	Illustration of the compared synchronous scheduling strategies after sub- band power optimization . . . . .	116
4.20	Simple network scenario for numerical examples of the two-hop propor- tional fair metric . . . . .	118
4.21	Example with equal supportable rates among MSs . . . . .	119
4.22	Example with higher supportable rate for MS1 and equal supportable rates of MS2 and two-hop MS3 . . . . .	120
4.23	Example with higher supportable rate for two-hop MS3 and equal sup- portable rates of MS1 and 2 . . . . .	121
4.24	Example with highest supportable rate for two-hop MS3 and equal lowest supportable rates of MS1 and 2 . . . . .	122
4.25	Required signalling for the proposed hybrid RRM scheme . . . . .	124
5.1	Principle flow chart of the DT SLS with respect to the hybrid RRM scheme	126
5.2	Network Layout, 19 MBSs, 3 Sectors/Site, e.g. 4 RNs per Sector . . . . .	127
5.3	MS Cell Selection Rates for the RSRP, the CR and the adapted CR metric	131

5.4	Throughput and fairness of all MSs and RN BH for the different cell selection metrics . . . . .	132
5.5	Throughput and fairness of all MSs and RN BH for with and without co-scheduling functionality . . . . .	133
5.6	Throughput of all MSs and RN BH with different RN AL CQI feedbacks	135
5.7	Throughput of MBS and RN MSs with different RN AL CQI feedbacks .	135
5.8	Throughput of all MSs and RN BH with fitness function o1 and scheduling policy 1,2 and 3 . . . . .	136
5.9	Throughput of all MBS and RN MSs with fitness function o2 and scheduling policy 1,2 and 3 . . . . .	136
5.10	Throughput of all MSs and RN BH with fitness function o2 and scheduling policy 1,2 and 3 . . . . .	137
5.11	Throughput of all MBS and RN MSs with fitness function o2 and scheduling policy 1,2 and 3 . . . . .	138
5.12	Final Comparison of the UE and RN throughput for reduced feedback based on max value and fitness function o2 with scheduling policy 2 . . .	139
5.13	Comparison of the RN BH SINR values for reduced feedback based on max value and fitness function o2 with scheduling policy 2 . . . . .	140
5.14	Comparison of the MBS and RN UE SINR values for reduced feedback based on max value and fitness function o2 with scheduling policy 2 . . .	140
5.15	Comparison of the MBS and RN UE SINR values for reduced feedback based on max value and fitness function o2 with scheduling policy 2 . . .	141
5.16	Final Comparison of the Fairness Criterion . . . . .	142
5.17	Final Comparison of potential MBS and RN transmission power savings on the DL data channel . . . . .	142
A.1	Numerical example for a round robin scheduler . . . . .	147
A.2	Numerical example for a Max-Min scheduler . . . . .	148

In loving memory of my father and sister. To my mother Karin and my son Marlon.

# Acknowledgements

I would like to thank Dr. Veselin Rakocevic and Prof. Dr.-Ing. Joachim Habermann. Their supervision and guidance through the world of academic research were indispensable during the preparation of this dissertation and the whole process of the doctoral studies. In addition I would like to thank Dr. Gerhard Kadel.

## Abstract

In orthogonal frequency division multiple access based mobile networks buffer aided non-transparent in-band half duplex decode-and-forward relay nodes aim to improve coverage and capacity under fairness considerations. The existing centralized radio resource management and inter-cell interference coordination schemes can achieve this goals, although at the cost of a heavy signalling overhead. This cost is a critical issue, particularly for the frequency division duplex downlink transmission. On the other hand, the fully decentralized schemes often focus on different types of frequency reuse schemes with smaller amount of necessary feedback. Here, it is often overseen that in a practical deployment, the backhaul link quality is the bottleneck of the two-hop transmission, and the backhaul link is often modelled way too optimistically. Moreover, it is necessary to allocate radio resources to single hop mobile stations as well, which further limits the possible data rates of the relay-attached users. The research presented in this Thesis aims to improve the backhaul link quality in relay-assisted cellular networks under full consideration of practical constraints. In order to minimize the required channel feedback overhead this work proposes a hybrid radio resource management scheme consisting of three adapted procedures. The hybrid radio resource management scheme includes an adapted decentralized cell selection metric which improves the possibility to gain from the relays in the system for each user. A macro cell-centralized synchronous procedure is proposed, which is responsible to allocate the radio resources in each transmission time interval. Furthermore, an asynchronous network-centralized subband power allocation scheme with very limited feedback is proposed to maximize the wireless backhaul link quality with no losses for single-hop Mobile Station (MS)s. Comprehensive system level simulation results show stable fairness and improved throughput of the proposed hybrid radio resource management scheme. In addition possible energy savings for the shared channel are presented.

# Acronyms

**3GPP** Third Generation Partnership Project

**AC** Admission Control

**ACK** Acknowledgement

**AF** Amplify and Forward

**AL** Access Link

**ALSF** Access Link Subframe

**AoA** Angle of Arrival

**ASA** Angle of Arrival's Spread

**ASD** Angle of Departure's Spread

**AWGN** additive white Gaussian noise

**BHSF** Backhaul Subframe

**BL** Backhaul Link

**BLER** Block Error Rate

**BS** Base Station

**C-RAN** centralized radio access network

**CAPEX** Capital Expenditure

**CDF** Cumulative Distribution Function

**CoMP** Coordinated Multit Point

**CQI** Channel Quality Information

**CR** Composite Rate

**CRE** Cell Range Expansion

**CSI** Channel State Information

**CU** Centralized Unit

**deNB** donor eNB

**DL** Downlink

**dMBS** donor MBS

**DS** Delay Spread

**DT SLS** Deutsche Telekom System Level Simulator

**DU** Decentralized Unit

**eNB** eNodeB

**EPC** Evolved Packet Core

**FD** Full Duplex

**FDD** Frequency Division Duplex

**FFR** Fractional Frequency Reuse

**FFT** Fast Fourier Transformation

**FIFO** First Input First Output

**FSS** Frequency Selective Scheduling

**GA** Genetic Algorithm

**gNB** gNodeB

**HARQ** Hybrid Automatic Repeat Request

**HD** Half Duplex

**HetNet** Heterogeneous Network

**HSS** Home Subscriber Server

**IAB** Integrated Access and Backhaul

**ICIC** Inter Cell Interference Coordination

**IP** internet protocol

**IR** Impulse Response

**ISD** Inter Site Distance

**K** K-factor

**KPI** Key Performance Indicator

**LA** Link Adaptation

**LLS** Link Level Simulation

**LoS** Line of Sight

**LSP** Large Scale Parameter

**LTE** Long Term Evolution

**LTE-A** Long Term Evolution Advanced

**MBS** Macro Base Station

**MBSFN** Multicast Broadcast Single Frequency Network

**MCS** Modulation and Coding Scheme

**MIESM** Mutual Information Effective SINR Mapping

**MIMO** Multiple Input Multiple Output

**MME** Mobility Management Entity

**MS** Mobile Station

**NACK** Negative Acknowledgement

**NG** Next Generation

**nLoS** non Line of Sight

**NP** non-deterministic polynomial

**OFDM** Orthogonal Frequency Division Multiplexing

**OFDMA** Orthogonal Frequency Division Multiple Access

**OPEX** Operational Expenditures

**P-GW** Packet Data Network Gateway

**PA** Power Amplifier

**PAV** Power Adaptation Value

**PBCH** Physical Broadcast Channel

**PDCCH** Physical Downlink Control Channel

**PF** Proportional Fair

**PL** Path Loss

**PMI** Precoding Matrix Indicator

**PRB** Physical Resource Block

**PSO** Partical Swarm Optimization

**QoS** Quality of Service

**QPSK** Quadrature Phase Shift Keying

**RAN** Radio Access Network

**RI** Rank Indicator

**RN** Relay Node

**RR** Round Robin

**RRM** Radio Resource Management

**RSRP** Reference Signal Received Power

**S-GW** Serving Gateway

**SA** Simulated Annealing

**SDMA** Space Division Multiple Access

**SE** Spectral Efficiency

**SF** Shadow Fading

**SFR** Soft Frequency Reuse

**SINR** Signal to Interference plus Noise Ratio

**SISO** Single Input Single Output

**SLS** System Level Simulation

**SNR** Signal to Noise Ratio

**SSP** Small Scale Parameter

**TBS** Transport Block Size

**TCP** Transmission Control Protocol

**TDD** Time Division Duplex

**TDM** Time Division Multiplexing

**TS** Tabu Search

**TTI** Time Transmission Interval

**UE** User Equipment

**UG** User Geometry

**UL** uplink

# Chapter 1

## Introduction

### 1.1 Motivation and Overview

During the last decade the academia and the industry have paid a lot of attention on the improvement of the system capacity of mobile networks. One possibility to satisfy the ever growing data demand and thus, the necessity to increase the capacity is to densify the network, using different kind of small cells also known as heterogeneous networks [1]. Besides pico and femto cells, relay nodes (RN)s have been introduced to mobile networks, to improve coverage and capacity. The difference with the relay nodes is that they are backhauled by a wireless link and therefore they might be an attractive alternative to wired backhauled pico cells [2] for operators to deploy because of reasonable Capital Expenditure (CAPEX) and Operational Expenditures (OPEX). Different kinds of RNs have been designed and standardized in recent years [3,4] in the 3GPP and will be further investigated in an upcoming study item defined as Integrated Access and Backhaul (IAB) [5]. In general, such node types introduce a challenging research topic, primarily how to handle and allocate the available radio resources in the most efficient way and thus, how to gain the most from the additional nodes in the mobile network. Those relay nodes (RN)s operating in the half duplex mode suffer from a loss in transmission time, further explained in Section 2.2.1. Sophisticated means of resource allocation have to be designed to overcome this problem and therefore, to maximize the spectral efficiency of the two hop links. To this end, different targets for the radio resource management (RRM) approaches have been identified, such as the maximization of the capacity, the consideration of fairness, interference mitigation, energy awareness, queueing and Quality of Service (QoS). The main challenge in designing RRM algorithms for relay extended

systems is that typically an optimal solution requires a prohibitively exhaustive solution search. Furthermore, practical limitations have to be carefully taken into account. Various RRM strategies related to the aforementioned targets for all kind of RN types have been intensively studied in the past years.

However, the existing results in the literature are diverging in terms of the correct modelling of the underlying network topology and the system assumptions. Often ideal assumptions of the radio channel knowledge, the feedback delay and the wireless backhaul conditions are assumed. A lot of proposed methods will only work under such idealized conditions and will suffer in real large scale networks. These aspects are the main motivation for the work presented in this Thesis.

### **1.1.1 Objectives statement**

The Thesis therefore contributes an answer to the question if it is possible to improve the overall user throughput of the system by designing a hybrid radio resource management approach under practical limitations for relay-extended networks. To achieve this target a very detailed modelled system level simulation is applied. More specifically the research problem is decomposed in three parts for the hybrid RRM scheme as follows:

- A decentralized improved cell selection scheme.
- A cell-centralized improved short-term radio resource scheduler.
- A network centralized long-term transmission power adaptation algorithm, which improves the quality of the non-ideal wireless relay backhaul link.

The simulation results show that the proposed hybrid RRM scheme achieve performance gains in terms of data throughput of the mobile stations in the overall network under fairness constraints. This is reached by the adapted cell selection scheme, which enables an improved attachment strategy in combination with an increased degree of freedom for the short-term scheduling decisions taking into account fairness between one-hop and two-hop users. In addition, a network-centralized scheme derives an improved transmission power pattern, which increases the wireless backhaul link quality for the relays without decreasing the one-hop MSs performance. Moreover, energy savings can be reached with the proposed solution of this Thesis. However, the performance gains are limited by the realistic practical constraints.

## 1.2 Contribution of the Thesis

The contribution of the Thesis is related to radio resource management (RRM) and Inter Cell Interference Coordination (ICIC) in relay enhanced Orthogonal Frequency Division Multiple Access (OFDMA) heterogeneous networks for the downlink transmission. It aims to improve the non-ideal wireless backhaul connection of relay nodes to the serving donor macro base stations without throughput losses for the users directly connected to the macro base stations. This is a challenging task as the macro users and the relays have to share the available radio resources. The theoretical multi objective optimization problem cannot be solved optimally in practical systems. To this end, the problem is decomposed in three sub-problems to reach an improved system performance. The major contributions of the Thesis are described as follows:

1. The first contribution is a comprehensive system level simulation analysis on different cell selection schemes to improve the overall user throughput of a relay enhanced large scale OFDMA heterogeneous network under practical constraints. Here, buffer enabled half duplex non-transparent decode relay nodes with non-ideal wireless backhails are considered. An adapted cell selection scheme as well as a macro cell-centralized improved two-hop proportional fair scheduling scheme is proposed.

2. The second contribution is the design of a low complexity network-centralized RRM scheme under neglected considerations of practical limitations. Here, a hybrid solution is designed, which consists of a network-centralized and a macro cell-centralized part to improve the overall user throughput. The network-centralized part adapts the transmission power pattern for a subband of the system bandwidth, while the macro cell-centralized part combines the adapted two-hop frequency selective scheduling decisions with scheduling strategies of how to use the optimized subband. The scheme takes into account fairness, relay and user buffer status' and radio channel diversities. In addition it reduces the energy consumption of the transmission without losses and works with a very limited amount of additional channel feedback information.

## 1.3 Thesis structure and content

The Thesis is organized as follows: In Chapter 2 an introduction to the Radio Access Network (RAN) architecture is presented, which has been agreed recently in 3GPP. Then different kind of relay nodes are introduced and possible operating modes are described in detail. A comprehensive summary on the existing literature of solutions for enhanced radio resource management for relay-extended networks is provided. Based on that, relevant existing radio resource management solutions are considered. Finally the research problem is described and the requirements are derived for the novel low complexity hybrid radio resource management scheme proposed in this Thesis.

Chapter 3 explains at first, why a system level simulation is the necessary tool to investigate the defined research problem. It includes the detailed description of the methodology to be used, implying the description of used models, followed by the defined Key Performance Indicator (KPI)s to analyse the results. Then, the System Level Simulation (SLS) is calibrated to verify it as a comparable tool within the 3GPP simulation framework. Afterwords, the extensions done throughout this Thesis are described and analyzed to introduce layer 3 in-band Frequency Division Duplex (FDD) half-duplex RNs.

In Chapter 4 the novel hybrid radio resource management scheme is then proposed, which consists of three decomposed sub-problems: a decentralized, a cell-centralized and a network-centralized part. It is designed to be applied in large scale relay extended mobile networks under practical constraints, such as a non-ideal wireless backhaul, limited available radio channel feedback and additional channel feedback delays of the two-hop connections. The principle flow chart of the conducted simulations with respect to decomposed sub-problems of the hybrid RRM scheme is illustrated in Figure 1.1.

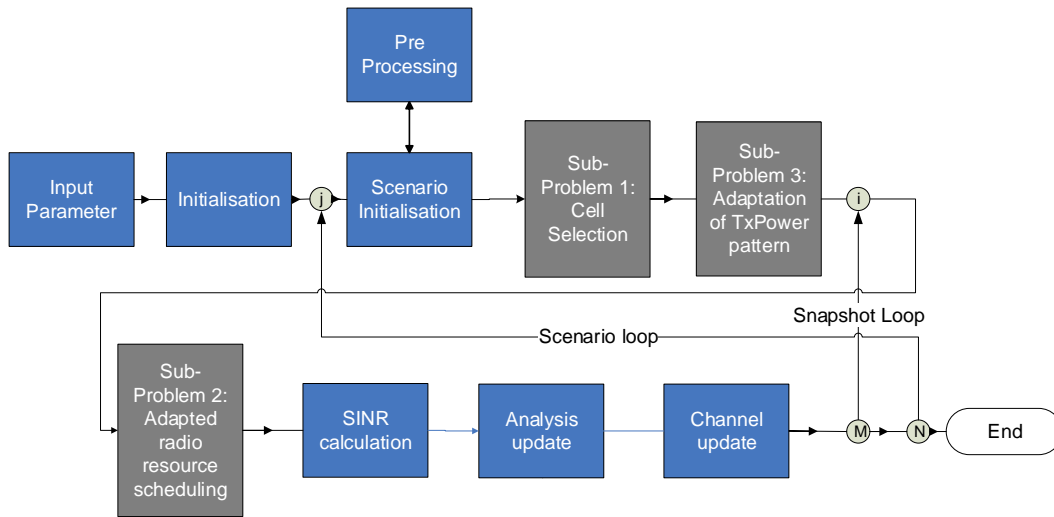


Figure 1.1: Principle flow chart of the SLS with respect to the hybrid RRM scheme and its decomposed sub-problems

Chapter 5 contains a performance analysis of different cell selection schemes and cell-centralized functionalities, followed by the presentation of the final assumptions and results of the carried out SLS analysis for the proposed hybrid radio resource management (RRM) scheme.

In Chapter 6 the conclusions are drawn and an outlook to potential future work is given.

## Chapter 2

# Relay extended OFDMA Networks

In this Chapter an introduction to the RAN architecture is presented which has been agreed recently in 3GPP. Then different kind of relay nodes are introduced and possible operating modes are described in detail. Based on that, relevant existing radio resource management solutions are considered. Finally the research problem is described and the requirements are derived for the novel low complexity hybrid radio resource management scheme proposed in this Thesis.

### 2.1 Network architecture in 3GPP

#### 2.1.1 Core network

The 3GPP defines the global mobile radio telecommunication standard including the core and access network as well as service capabilities of the system. The Long Term Evolution (LTE) specific core network was first introduced in Release 8 of the specification and defined as Evolved Packet Core (EPC) in [6, 7]. The agreed design principle was to have a flat hierarchical architecture, which means to define only a few network nodes to handle the data traffic performance in a more cost efficient manner, compared to previous 3G communication standards, defined in [8]. As a second principle requirement, the EPC architecture depicted in Figure 2.1 handles the payload (user data) and signalling traffic (further referred as control plane) in a separated way to make the scaling of both data types independent to each other. Due to the introduced functional split, dimensioning and adapting the network can be done in a more flexible way and is easier to adapt specific operators' needs.

Figure 2.1 shows the defined core network elements and their corresponding inter-

faces between each other. The Home Subscriber Server (HSS) basically is a database containing user and subscriber specific information, such as authentication and access authorization information, besides others. The Serving Gateway (S-GW) and Packet Data Network Gateway (P-GW) handle the users' data traffic further referred as user plane. Those network elements mainly transport the IP data traffic between the mobile stations and the external networks behind the mobile core. The S-GW interconnects the user plane between the core network and the Radio Access Network (RAN), defined as multiple eNodeB (eNB)s via the S1-u interface, while the P-GW interconnects the EPC with external internet protocol (IP) networks via the SGi interface. The P-GW also supports functionalities such as IP address allocation or policy control and charging. The Mobility Management Entity (MME) is responsible for handling the signalling traffic, further referred to as the control plane. The MME is interconnected to the RAN via the S1-c interface. Mainly, it is defined to support mobility and security for the radio access. Moreover, the MME handles MS tracking and paging when subscribers are connected in idle-mode.

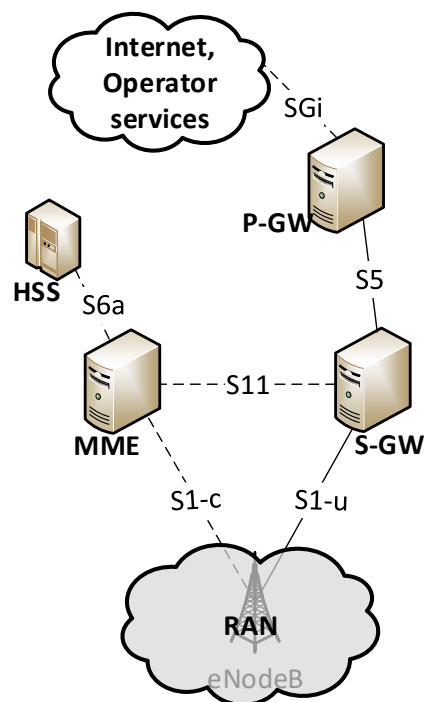


Figure 2.1: EPC Core Architecture [6, 7]

## 2.1.2 Radio access network

In the following, the LTE and Next Generation (NG) RAN architectures are presented. As already mentioned, the eNB is interconnected to the EPC via S1-c and S1-u interface for control and user plane, respectively, as illustrated in Figure 2.2 and defined in [9]. Besides

that, the radio sites are interconnected via the defined X2 interface to exchange different types of control messages for e.g. possible Base Station (BS) interference cooperation and load balancing schemes as well as the handover related information. Further detailed information can be found in [10]. Since this Thesis focuses on relay node RN extended RAN, an RN is depicted as well in Figure 2.2. Relay nodes are introduced to the 3GPP architecture in Release 10 of the specification. The details on the definition of different RN types introduced by 3GPP can be found in [11] and will be discussed in the upcoming Section 2.2 as well. As can be already seen in Figure 2.2, an RN is a node type which is interconnected to the network via a wireless backhaul connection to an eNB, further referred as donor eNB (deNB).

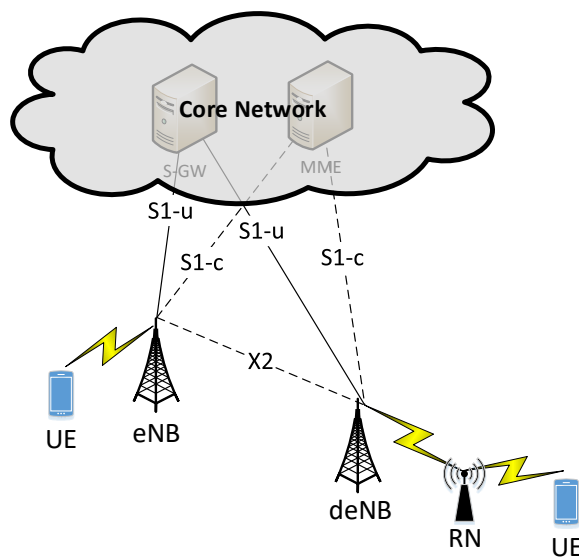


Figure 2.2: LTE-Advanced RAN Architecture with RN [9]

With 3GPP's newest mobile communication standard Release 15 a new NG RAN architecture has been introduced, recently. Based on [12, 13] a novel architecture is defined and a new type of BS is described, further referred as gNodeB (gNB). Besides evolved ng-eNBs based on the Long Term Evolution Advanced (LTE-A) specification the gNB is introduced to the NG RAN in [12]. Figure 2.3 shows the novel overall NG RAN architecture. Both node types are basically connected to the core network by the NG interface, while the Xn interface provides interconnection between each other. In Figure 2.4 further details on the design of the newly introduced gNB are presented. A gNB consists of a Centralized Unit (CU) interconnected with a new interface, defined as F1, to multiple Decentralized Unit (DU)s. The termination point for the NG interface which connects the gNB with the core network is always the CU. Two important aspects can be seen within the novel RAN architecture. First, the LTE eNB is still part of the next generation mobile

network, which means that LTE is a part of the 5G system. Second, due to the newly introduced CU in the NG RAN higher flexibility in data forwarding to transmission points as well as better possibilities to coordinate resource allocation among DUs are introduced.

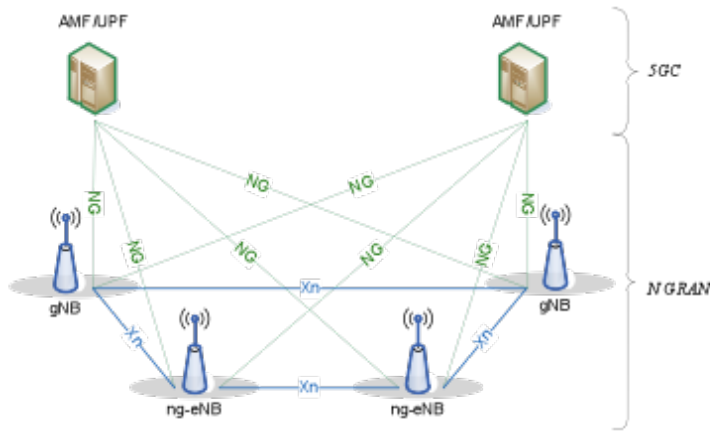


Figure 2.3: NG RAN Architecture [12]

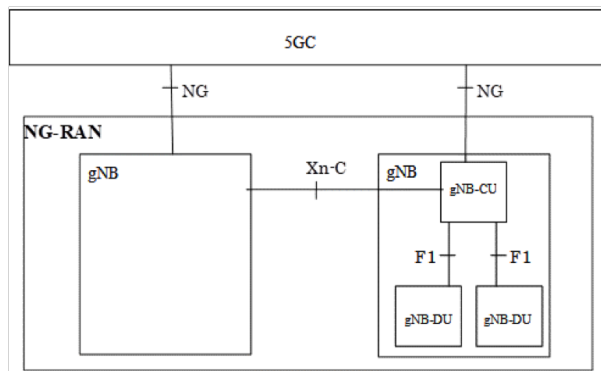


Figure 2.4: NG RAN gNB Architecture [13]

### 2.1.3 New study item for 3GPP Release 15/16 revisiting relay nodes

The 3GPP has agreed recently on a new study item defined as Integrated Access and Backhaul (IAB) in Release 15. It focuses on the investigation of the introduction of fixed relay nodes (RN)s to the NG RAN in future releases, since RNs are not being considered in the most recent Release 15 [12]. The study focuses on Layer 2 and 3 relays, enabling enhanced functionalities at the RN, further described in Section 2.2 of this Thesis. The 3GPP have agreed to consider the future RN as a DU interconnected via F1 to a CU. Among several agreements defined in [5], the study item on IAB will also focus on the important impact of signalling load as an important KPI due to the wireless backhaul connection for fair comparison of IAB node designs. Moreover, it has been agreed to study the impact of the radio resource scheduler, which is the focus of this Thesis, as well. The

outcome of the research presented in this Thesis could contribute to the defined study item, providing deeper understanding of the RRM aspects in the RN-extended networks and revealing detailed insights on possible affordable non-prohibitive signalling requirements on the wireless backhaul. Because of that, the hybrid RRM scheme that will be presented in this Thesis has been designed to have low complexity and small signalling overhead. The necessary low amount of additional signalling traffic for the proposed hybrid scheme is described in detail in Section 4.5.

## 2.2 Relay types in 3GPP

In this section the focus lies on the outcome of 3GPPs work done for the specification of RNs in LTE-A Release 10. As already mentioned, small cells in general are considered as one means to increase capacity and coverage. Besides the possibility to densify the conventional homogeneous Macro Base Station (MBS) network, the introduction of small cells aims to reuse the spectrum most efficiently. To further densify the macro cell network, has critical drawbacks for an operator due to high OPEX and CAPEX as well as practical implications due to very few possible additional accessible site locations [2]. There are different types of small cells introduced to the mobile network. Small cells - pico cells, femto cells and Relay Nodes (RN) - are node types which typically transmit with lower amount of power compared to an MBS [1, 14, 15]. The main target to use such types of nodes is to overcome large path losses which imply low spectrum efficiency usage. Thus, decreasing the path loss by shifting the serving node nearer to terminals enables reusing the system bandwidth with high efficiency gains.

As a major difference compared to pico and femto cells, an RN is attached to the network via a wireless backhaul link provided by the donor MBS (dMBS), while pico or femto cells are wireline connected [3, 4, 16]. An overview of an enhanced cellular network by different small cell node types, further defined as a Heterogeneous Network (HetNet), is illustrated in Figure 2.5. The solid black lines mark the operator controlled wireline backhaul connections of pico and macro cells. The solid blue line shows the user controlled wireline connection of femto cells, while the yellow lightning sign represents the operator controlled wireless connection of the RN.

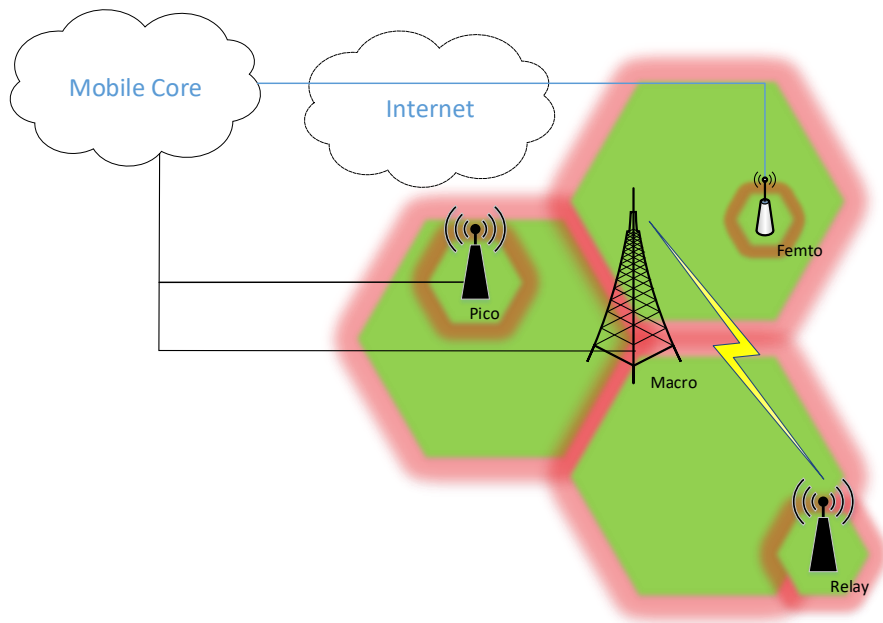


Figure 2.5: A heterogeneous network consists of wireline backhauled macro, pico, femto, cells and wireless backhauled RN

To enable a communication between the dMBS and the corresponding RNs, Figure 2.6 shows the interfaces defined by the 3GPP to connect an RN as well as an User Equipment (UE), further referred to as a Mobile Station (MS). The Uu interface connects the MS to the RN via the Access Link (AL), while the Un interface is dedicated to the Backhaul Link (Backhaul Link (BL)) interconnecting the RN with the dMBS.

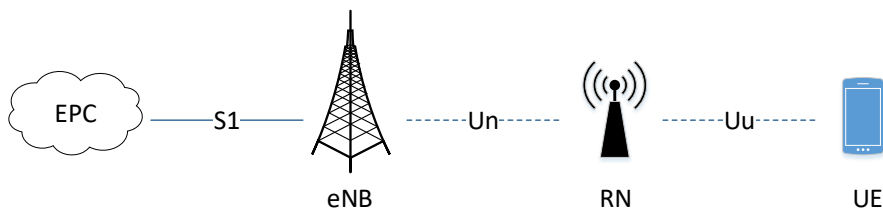


Figure 2.6: Defined interfaces for RN extended mobile networks by the 3GPP

For further clarification, different RN types exist, with different supported functionalities and operating modes. The 3GPP has defined three RN types for LTE-A, mainly distinguished based on the transmitted sublayers of the radio protocol stack and thus the supported signal processing of the considered RN type including different functionality.

The simplest RN realisation is a layer 1 RN type, which is also known as the Amplify and Forward (AF) repeater. It amplifies the total received signal by an analogue Power Amplifier (PA) without any enhanced signal processing and thus amplifies also the receiver's noise level as well as the existing inter cell interference. The corresponding protocol stack data flow is depicted in Figure 2.7. Such an RN type is mainly used as a

means to extend the coverage at low cost, while accepting spectral efficiency losses due to no additional signal processing.

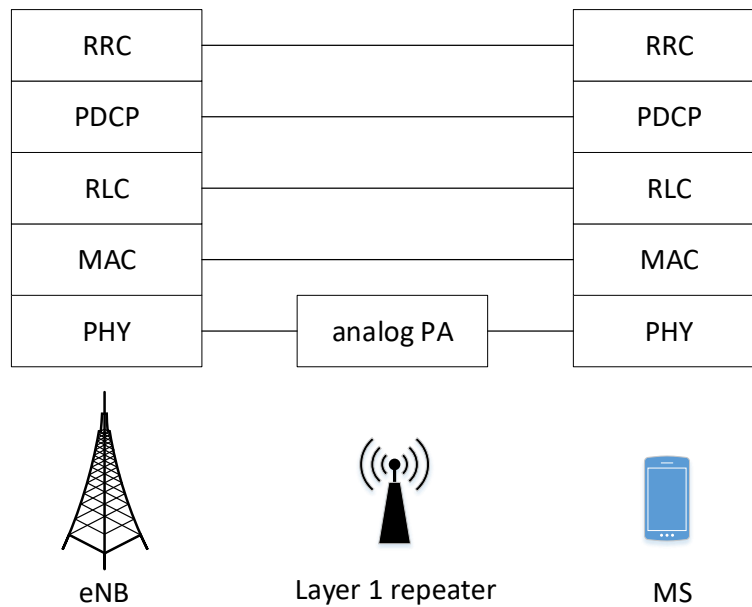


Figure 2.7: Layer 1 RN Protocol Stack

In the contrast to the amplify and forward RN type, a Layer 2 RN is able to demodulate and decode the received signal and then re-encode and modulate again with an adapted Modulation and Coding Scheme (MCS) according to the MS's Signal to Interference plus Noise Ratio (SINR) and the desired target Block Error Rate (BLER). This prevents the noise and interference amplification and reduces the possible error rates by supporting retransmission schemes based on Hybrid Automatic Repeat Request (HARQ) functionality and independent radio resource scheduling. The related protocol stack architecture is shown in Figure 2.8.

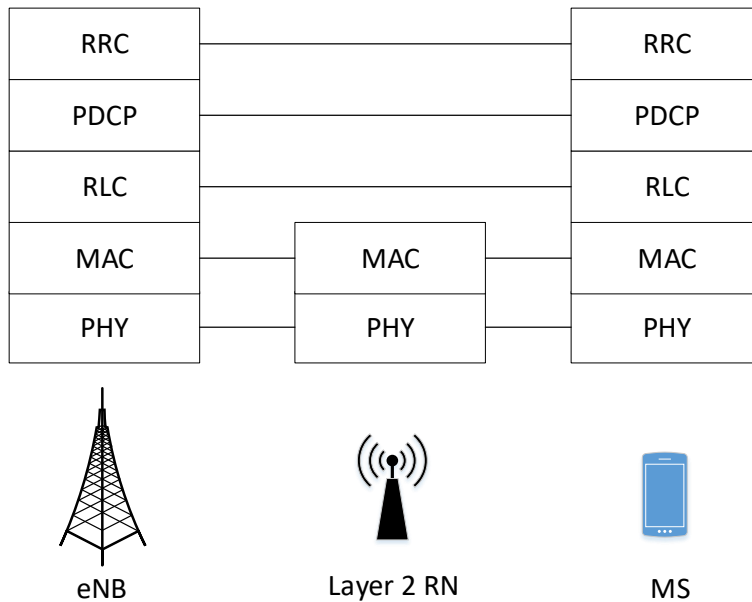


Figure 2.8: Layer 2 RN Protocol Stack

A Layer 3 RN, also known as self backhauling RN, can be considered as a separate base station (BS). In addition to the independent Admission Control (AC) and the mobility management functionality, it also performs decentralized radio resource scheduling, including re-encoding and modulation, HARQ, as well as choosing the MS specific transmission mode, such as beamforming or spatial multiplexing, and other radio functions, such as ciphering, MS data concatenation/segmentation, etc. It performs the complete signal processing as a separate BS. The radio protocol stack is depicted in Figure 2.9 and is in focus of the work presented in this Thesis. For additional detailed information about the functionalities of the RAN protocol stack the reader is referred to [9, 12, 17].

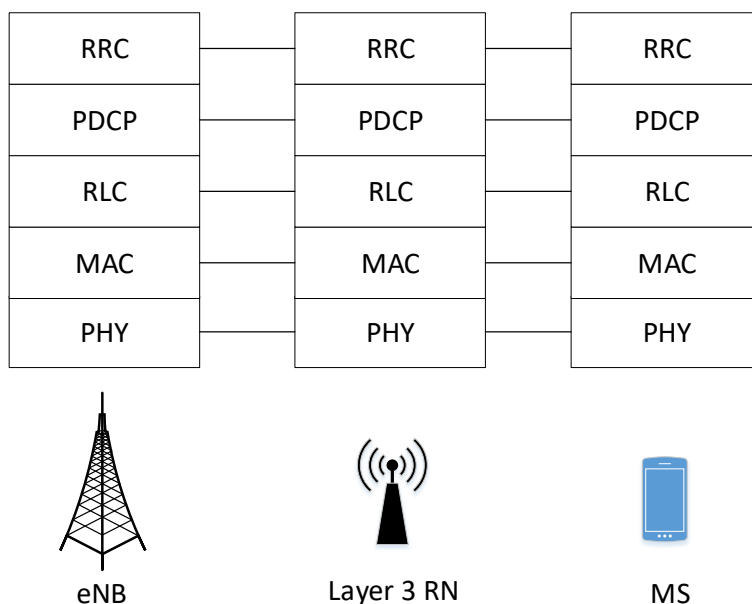


Figure 2.9: Layer 3 RN Protocol Stack

The summary of the main advantages and disadvantages of the introduced RN types is given in Table 2.1.

Table 2.1: Summary of further RN type attributes

<b>RN node type</b>	<b>Advantages</b>	<b>Disadvantages</b>
Layer 1 RN	<ul style="list-style-type: none"> <li>- Low additional processing delay</li> <li>- Lower cost due to simple functionality</li> <li>- Low impact on standardization</li> </ul>	<ul style="list-style-type: none"> <li>- Noise and interference amplified with desired signal</li> <li>- Decreased spectral efficiency</li> </ul>
Layer 2 RN	<ul style="list-style-type: none"> <li>- No noise and interference amplification due to the decoding functionality</li> <li>- Error rate improvement due to HARQ support</li> <li>- Support of resource and network cooperation</li> </ul>	<ul style="list-style-type: none"> <li>- Processing delay</li> <li>- dMBS to RN consumes radio resources</li> <li>- Major standardization impact (L2 radio protocols needed)</li> <li>- High additional amount of signalling</li> </ul>
Layer 3 RN	<ul style="list-style-type: none"> <li>- No noise and interference amplification due to decoding</li> <li>- Small standardization impact (reuse of existing MBS protocols)</li> <li>- Error rate improvement due to HARQ support</li> <li>- Support of resource and network cooperation</li> </ul>	<ul style="list-style-type: none"> <li>- Highest processing delay</li> <li>- dMBS to RN consumes radio resources</li> </ul>

Besides the existing RN types defined by the 3GPP, there is a need to further differentiate between RNs regarding the mode of operation. In the following an introduction to the most relevant functionalities is given. Further details on possible RRM schemes and their practical implications, such as additional necessary signalling overhead and the assumed level of centralization can be found in Section 2.3.

1. The wireless backhaul link operates either in-band or out-of-band: The wireless backhaul link operates in the same frequency band as the access link or in a separated band.
2. Half or full duplex mode: While in the Half Duplex (HD) mode the RN is not able to transmit and receive at the same time, radio resources need to be allocated with a Time Division Multiplexing (TDM) based scheme. In the Full Duplex (FD) mode advanced interference cancellation techniques or sufficient receive and transmit isolation have to be considered, due to the creation of self interference at the RN
3. Transparent or non-transparent mode: The RN either appears as a separated cell or it

is part of the dMBS. Therefore the 3GPP differentiates between type 1 RNs as non-transparent and type 2 RNs as transparent RNs. Based on that, further clarification is needed with respect to the level of centralization of the designed RRM scheme.

4. Network-centralized, macro cell-centralized or RN specific decentralized RRM approaches: One of the most critical challenges and often overseen is the assumed available Channel State Information (CSI) feedback. A lot of the proposed RRM schemes rely on impractical amount of CSI [18] which will be further discussed in Section 2.3. For instance, sophisticated network-centralized Coordinated Multi Point (CoMP) schemes, which typically require quantized explicit feedback with tight delay requirements [19, 20], seem to be impractical in combination with RNs due to additional necessary feedback of the RN access link, which needs to be forwarded to the dMBS in a first step and then gathered at a central controller. On the one hand scarce radio resources need to be used carefully and cannot be allocated with an exceeding amount of overhead, while on the other hand additional delays due to the introduced two-hop connections need to be taken into account regarding coherent channel states over time. Especially, this is already an critical issue in conventional networks for FDD downlink transmissions.

Furthermore, in the existing literature it is often not obvious, which type of RN is considered. Moreover, It is often unclear which additional functionalities are supported at the RN based on the proposed methods. Furthermore, necessary considerations of the feedback delays and the caused feedback overhead by the algorithm is often left open. The existing solutions are further discussed in Section 2.3.

### **2.2.1 Enabling Time Division Multiplexing (TDM) for half duplex RNs in 3GPP**

The 3GPP defines the Multicast Broadcast Single Frequency Network (MBSFN) subframe, which is used to enable the wireless backhaul reception at the RN [21] when in-band operation mode is applied, as illustrated in Figure 2.10. While an MBSFN subframe is used at the RN, it is able to receive control and user data served by the dMBS. Before the RN can switch to reception mode it is necessary to transmit expected control information to the MSs served by the RN, depicted as the dashed red arrows. In another subframe next the RN switches back to sending mode by using a conventional subframe format in

which control and user data is transmitted.

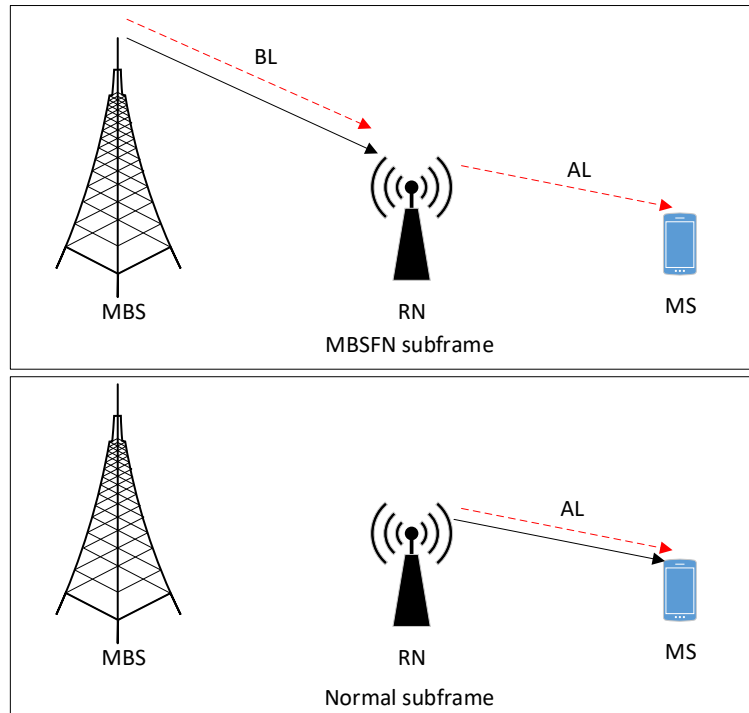


Figure 2.10: Downlink half duplex RN radio link operation

Further details of the applied TDM scheme in LTE Release 10 are illustrated in Figure 2.11. The MBSFN subframe gives the opportunity to transmit at first the Physical Downlink Control Channel (PDCCH), presented as the brown control data region. This information is expected by each MS within every subframe. After the system relevant control channel transmission the RN switches to reception mode within one Orthogonal Frequency Division Multiplexing (OFDM) symbol, shown as the grey area on the left. The RN is now able to receive control (shown as the dark green area) as well as user data from the dMBS (light green data region). During that time the MSs attached to the RNs are not served with data. At the end of an MBSFN subframe the RN again switches back to sending mode within one OFDM symbol, illustrated as the grey area on the right.

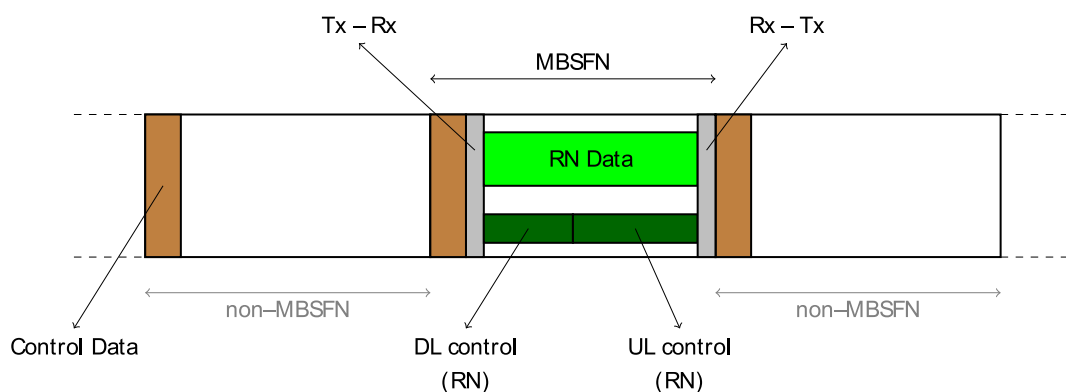


Figure 2.11: Use of MBSFN subframe structure to receive data at the RN

Moreover, there exist some additional constraints which are summarized as follows.

In the LTE FDD downlink frame structure several subframes are not configurable as MBSFN subframes since they transport system relevant information such as the Physical Broadcast Channel (PBCH) (1st subframe) or the Primary and Secondary Synchronisation Signal (P/S-SS) (5th, 6th and 10th subframe). In addition, the MBSFN subframe has a periodicity of 8 milliseconds (ms) while the LTE frame structure is defined with a periodicity of 10ms. In principle, each RN could be configured in the sending or the receiving modes at different times. However, this might introduce critical unwanted RN to RN interference. The used number of MBSFN subframes can be updated every 40ms via the PBCH to react on, e.g. a changing traffic demand of the RN (see also [3]). This results in a higher dynamic of interference than in a system without RN extension and introduces additional challenges to cope with, such as the aforementioned faster outdated channel feedback information in FDD downlink [22]. The limitations and additional overhead assumptions are carefully taken into account in this Thesis and further described in Section 3.5.

## **2.2.2 Full duplex and Half duplex relay operation mode**

Compared to half duplex (HD) RNs, which are in focus of the work presented in this Thesis, another RN type is currently being considered by the academia and the industry. The full duplex (FD) RNs, are RN types which have the ability to transmit and receive simultaneously in the same band. Compared to the HD RN, the FD RN clearly should improve the spectral efficiency by avoiding the utilization of two independent radio channels for the end-to-end transmission. The basic differences of HD and FD RN types are illustrated in Figure 2.12. The major challenge when it comes to the practical implementation is to handle the extremely unbalanced power levels of transmit and receive signals at the RN. Self interference cancellation techniques with extreme requirements regarding the affordable processing time have to be considered. Current research results show that it is for further study to which extent FD RN can be useful in real networks [23–26].

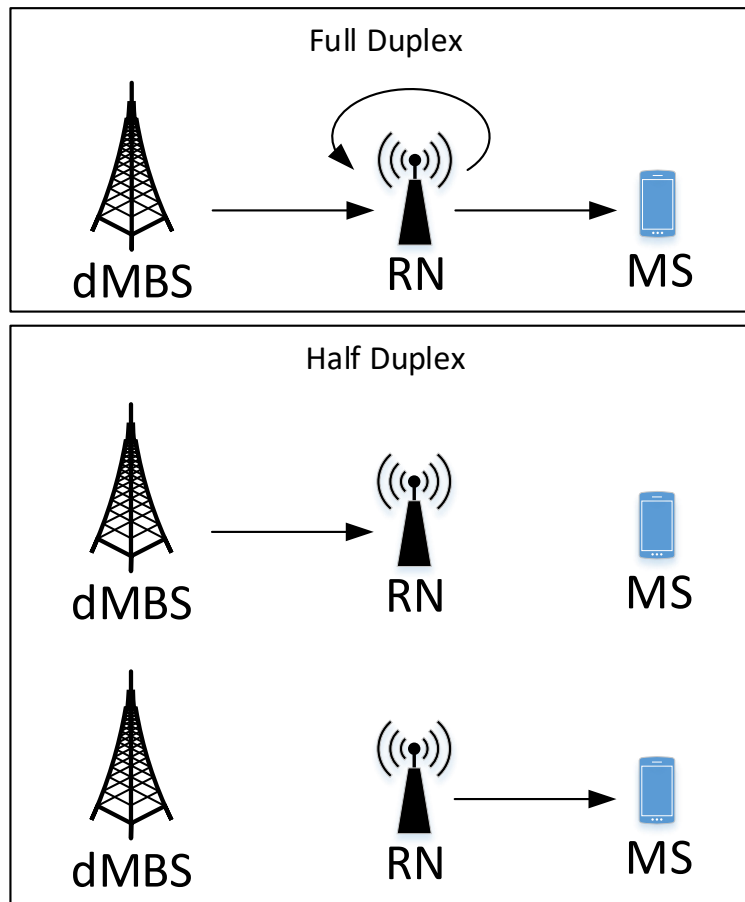


Figure 2.12: Full Duplex vs. Half Duplex transmission

### 2.2.3 Radio channel feedback

Different channel adaptive techniques, such as Frequency Selective Scheduling (FSS), dynamic Link Adaptation (LA) or transmission scheme selection are applied in mobile networks today to support a better utilization of the radio resources. This implies the requirement to have accurate channel knowledge at the serving cell in both transmission directions, the uplink and the downlink. In the Time Division Duplex (TDD) systems, where the same frequency band is used in downlink and uplink, the channel information requirement can be met, since channel reciprocity is exploited and radio channel properties can be estimated based on the measurements performed directly at the serving cell, based on the uplink transmissions. In the Frequency Division Duplex (FDD) systems, where a dedicated frequency band for uplink and downlink is used, channel reciprocity does not hold true, since the separation ends in uncorrelated radio channels. Therefore, typically appropriate feedback signalling from the MS to its serving cell is necessary to obtain downlink channel conditions. In the RN-extended systems not only the channel information feedback of the access link (AL) needs to be provided the downlink trans-

mission at the MBS, but also channel information about the backhaul link (BL) as well as for the second hop is required. Therefore, additional signalling feedback needs to be provided from RN to its dMBS to derive which radio resources the RN gets allocated in an appropriate manner. Further details on the proposed two-hop frequency selective scheduling approach in this Thesis and the implication on necessary feedback can be found in Section 4.4 and 4.5. The considered scheme aims to minimize the necessary additional feedback. On the one hand there is a need to reduce the necessary measurements at the MSs and on the other hand it is necessary not to overload the wireless backhaul of the considered non-transparent type 1 RNs with signalling traffic. Some further insights on possible feedback types and the implication on the additional amount of overhead introduced by those are discussed in the following.

There are two different feedback types possible. The first type, often referred as the Channel Quality Information (CQI) feedback, and further referred as implicit feedback, typically sends back indications of the channel conditions, e.g. as indicators of the recommended MCSs to use in multiple subbands. Such type of feedback is introduced to LTE in Release 8 and further enhanced until the latest Release 15 in [27]. The second type is known as explicit CSI feedback. While the CQI feedback is a means to find a trade-off between the information accuracy and the resource efficiency, the quantized explicit CSI feedback introduces higher signalling overhead. The quantized impulse responses provide greater detailed information about the radio links. To support advanced coordinated multipoint CoMP schemes or precoder designs, explicit information is required for instance to support downlink joint transmission in FDD systems [28].

In the research presented in this Thesis a solution with the constraint of limited additional feedback is considered, to prevent unwanted high signalling effort on the wireless backhaul of the RN and additional complexity at the MS side, generating explicit CSI feedback in the FDD system. Moreover, as stated before due to the introduced two-hop connections additional feedback delay needs to be considered, which is critical in terms of the coherence time of the radio channel. Since the necessary additional feedback in RN extended mobile networks is required and cannot be fully prevented, the work in this Thesis aims to improve the capacity of the system under constraints of limited implicit feedback for downlink FDD half-duplex RN extended systems. As later described in Chapter 4, the proposed scheme takes into account only CQI feedback as well as rarely used feedback on the average received power based on Reference Signal Received Power (RSRP) measurements. No explicit CSI feedback is used and the additional necessary

feedback from RN to dMBS is carefully limited. The additional feedback delay is considered as well and described in Section 3.5.4.

## 2.2.4 Fixed relay deployment scenarios and commercial aspects

Potential deployment scenarios of fixed half duplex RNs have been widely discussed [1]. While scenarios to extend or expand the coverage of the RAN are quite obvious, potentially useful scenarios to increase the capacity are less known. Due to the limitation of the wireless backhaul link the loss in the transmission time and the introduction of additional interference, especially when half duplex inband RNs are considered, it is quite challenging to increase the RAN capacity. However, in a scenario where an MS hotspot is detected and a relatively high amount of users are in the vicinity of an RN it might be possible to improve the capacity, as well [29]. Figure 2.13 shows three RNs deployed in different scenarios. While the upper relay provides coverage extension and the lower RN fills a coverage hole (e.g. shadowed areas by buildings or a poor indoor coverage), an RN might be deployed at an MS hotspot to improve the capacity of the network. In an MS hotspot area, many users at once might profit from a high channel quality of the access and backhaul links. Based on that the possible two-hop connection could outperform the direct links to the MBS.

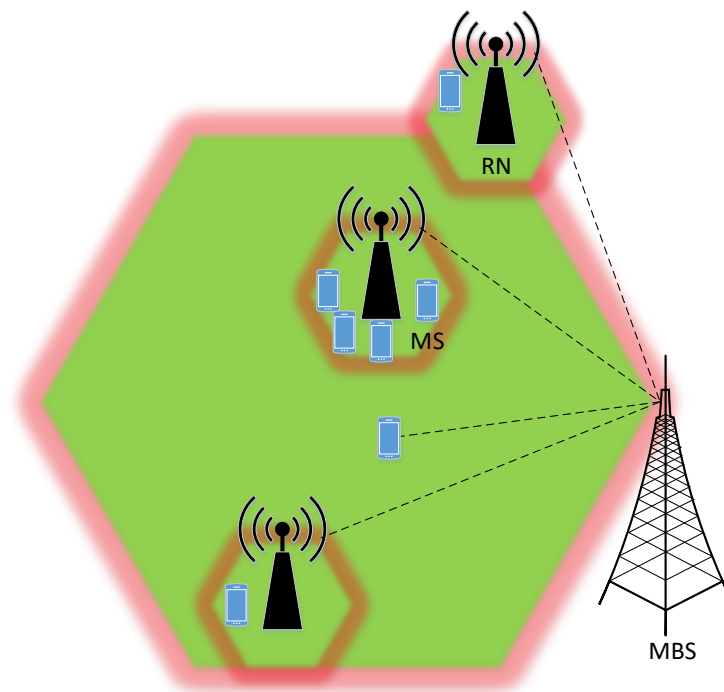


Figure 2.13: Fixed RN Deployment Scenarios

Typically RN deployments bring certain practical advantages compared to the wireline deployed small cells. The operator has to cope with a limited amount of locations where wired backhaul connection can be provided. In addition, the wireline connection in the case of pico cells generates rather high costs in terms of OPEX and CAPEX [16, 30, 31]. When considering femto cells an unwanted unplanned interference situations might appear in the network due to the loss of the control of the appearance of femto cells, which might influence the user experience in an unforeseen chaotic manner. Therefore, the relay nodes can be seen as an alternative useful means in scenarios where fixed line backhauled small cells are difficult to deploy [32]. Furthermore, additional potential cost savings are identified, when the considered RN type and the potentially applied RRM scheme does not necessarily need a Line of Sight (LoS) conditioned ideal wireless backhaul. This reduces planning effort and moreover, potential cost savings appear if no additionally deployed directed receive antenna would be deployed at the RN, which might not make sense anyway in a urban or sub-urban environment to improve the backhaul link [33]. However, all these potential cost savers makes it even more challenging to increase the capacity by means of introducing RNs.

Throughout this Thesis worst case assumptions for the wireless inband backhaul are considered, which makes the solution attractive to save costs. The backhaul link does not necessarily have LoS conditions which reduces planning effort and increases the amount of available potential sites. No additional antenna gains are assumed in the sending and the receiving direction, which makes it unnecessary to equip the RNs with additional antennas. The considered scenario consists of RNs deployed in the vicinity of randomly placed user hot spots within the umbrella macro base stations. Comparable reference results are gathered and comprehensively described in [29].

## **2.3 Radio resource management in RN extended heterogeneous mobile networks**

In the following section an overview of the solutions which has been found in the existing literature for radio resource management schemes in RN-extended heterogeneous mobile networks are summarized. It is necessary to keep in mind the importance to distinguish between the different operating modes of RNs and the underlying network assumptions identified in Section 2.2, to design an RRM algorithm. Before the existing solutions are

discussed, an introduction how to calculate the capacity in a mobile network is given, followed by the general problem formulation. Based on the defined theoretical problem statement the solution of this Thesis decomposes the problem in three sub-problems with different centralization levels later on in Chapter 4, as the work of this Thesis aims to improve the overall network capacity by the design of an hybrid RRM scheme.

### 2.3.1 Capacity of mobile networks

As previously discussed in Section 2.2.4 RNs should either be deployed to improve the coverage or the capacity. Coverage can be achieved by providing the smallest required received power of the desired signal (in uplink at the BS and in downlink at the MS). In principle, coverage can already be provided with a rather low amount of BS located at high altitude on a low carrier frequency, as e.g. often deployed in rural areas.

The network capacity refers to the maximum amount of data the system is able to transmit on the air interface in a fraction of time (Mbps). To estimate the overall reachable capacity of a large scale system (e.g. by means of simulations used in this work), a full load situation needs to be considered, where all BSs transmit on all resources as much data as possible [34, 35]. Further information about the used simulator in this Thesis can be found in Chapter 3. The possible supported rate  $R$  of a single wireless link  $n$  can be estimated based on the Shannon-Hartley theorem, as defined in Equation 2.1, where  $B$  is defined as the system bandwidth and  $S/N$  as the Signal to Noise Ratio (SNR) of the considered wireless link. High SNR enables the possibility to transmit with higher MCS to improve the capacity.

$$R_n = B \cdot \log_2 \left( 1 + \frac{S}{N} \right) \quad (2.1)$$

The theorem only holds true for additive white Gaussian noise (AWGN) channels. When it comes to a multicell scenario, the introduced inter cell interference may be considered as additional added noise. This is only correct if the interference power is Gaussian distributed as well. This is not necessarily the case in practically deployed systems. Further to this the full channel capacity is also limited due to the practical implementation issues, such as channel estimation errors or delayed channel feedback. Therefore, the theorem cannot be used to calculate the exact performance of the system from an information theoretical perspective. However, it is widely used to estimate the upper bound capacity

under the assumption that the appearing interference is Gaussian distributed. In Equation 2.2, the total capacity of a single base station  $C_{BS}$  is defined as the sum of the rates of the existing  $n$  wireless links.

$$C_{BS} = \sum_{n=1}^N R_n \quad (2.2)$$

Equation 2.3 represents the total capacity of the network  $C_{Net}$  in which the capacities of the considered BSs are summed up.

$$C_{Net} = \sum_{i=1}^I C_{BS_i} \quad (2.3)$$

Basically, four options are available to increase the network capacity. The first, the easiest but probably the most expensive option is to linearly increase the system bandwidth  $B$  by using larger amount of spectrum. The second option would be to increase the number of sending and transmitting antennas to send multiple data streams using Space Division Multiple Access (SDMA) [36], based on using Multiple Input Multiple Output (MIMO) channels. As already discussed in Section 2.2, the third option to increase the capacity is to deploy additional BSs and therefore to reduce the path loss between the sender and the receiver (further referred as network densification). This results in an improved quality of the serving signal  $S$ , when shifting the sender nearer to the receiving node and thus improving path loss gains. The major drawback of this option, is the additional interference, which is introduced to neighbouring cells limiting the possible capacity gain. Therefore, the forth option are possible interference mitigation techniques to again increase the network capacity by reducing the interference. The work of this Thesis focuses on the network densification and the interference mitigation option.

### 2.3.1.1 Capacity in half duplex non-transparent relay extended networks

The use of the Relay Nodes (RN)s introduces an additional problem when estimating the possible overall capacity of the network. As already mentioned, when in-band half duplex RNs are considered, the system bandwidth is also used to serve the RNs, while the RNs cannot transmit and receive at the same time.

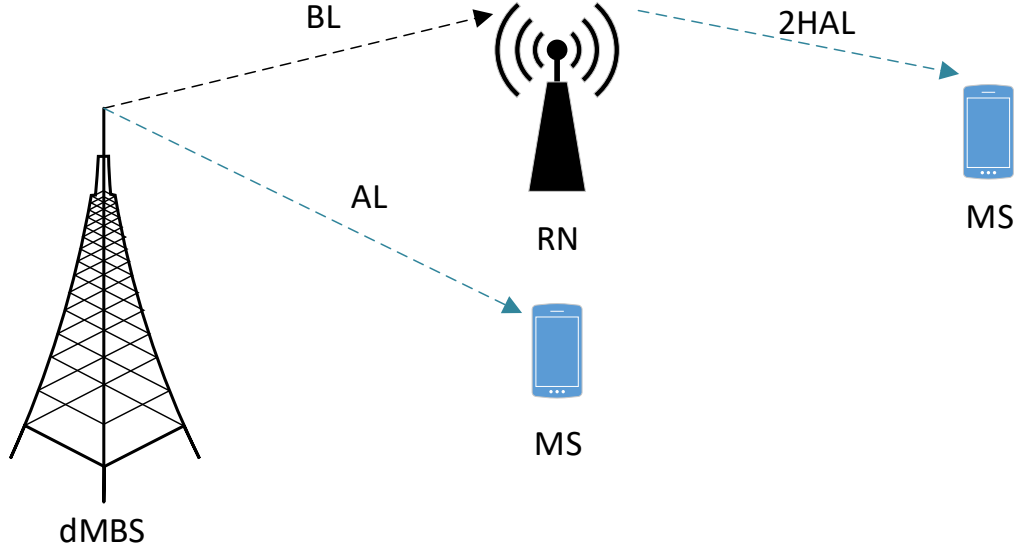


Figure 2.14: Link types for an RN-extended Network

Throughout the Thesis, the direct access link (AL) is denoted as the wireless link which serves the directly attached MSs at the MBSs. The wireless backhaul link of the RNs is defined as backhaul link (BH), while the serving link between RNs and MSs attached at the RNs is noted as two-hop access link 2HALs. For further clarification Figure 2.14 shows the existing links in an RN-extended network.

Equation 2.4 gives the expression for the capacity for a single macro BS in an RN-extended network when the RNs are in receiving mode. The capacity is the sum of the rates of the ALs  $M$  and BLs  $J$ .

$$C_{BS} = \sum_{m=1}^M R_m + \sum_{j=1}^J R_j \quad (2.4)$$

Equation 2.5 defines the possible capacity of a single RN limited by the rate of the wireless BL  $j$  of the considered RN, when the RN is in sending mode.

$$C_{RN} = \sum_{m=1}^M R_m, \quad (2.5)$$

with  $C_{RN} \leq R_j$

Finally, Equation 2.6 represents the total capacity of the RN extended network with  $J$  considered RNs. It has to be mentioned that the backhaul data rates needs to be subtracted

as the rates only forward the data to the RNs.

$$C_{Net} = \sum_{i=1}^I C_{BS_i} - \sum_{j=1}^J R_j + \sum_{j=1}^J C_{RN_j}, \quad (2.6)$$

with  $C_{RN_j} \leq R_j$

A large network capacity is most relevant for the downlink transmission as this is the dominant amount of traffic in large scale communication systems [37, 38]. Based on that, this work focuses on the downlink. In the following Section 2.3.2 the research problem is defined under several constraints for the considered system in more detail.

### 2.3.2 Problem formulation

The theoretical optimization problem formulation to maximize the overall system capacity is defined as Equation 2.7- 2.12. The considered sum-rate maximization depends on the aforementioned possible rates of the different link types in the Equations 2.4 - 2.6 [22, 39, 40].

$$\max(C_{Network}) = \max_{k,p,t} \sum_{m=1}^M \sum_{j=1}^J \sum_{n=1}^N R_{m,j,n} \quad (2.7)$$

$$\text{subject to } \sum_{n \in N} \sum_{k \in K} t_{n,k,l} \cdot p_{n,k,l} \leq P_{max,m,j}, \quad (2.8)$$

$$j = \begin{cases} 0, & l = 1 \\ j \in \{1, 2, \dots, J\}, & l = 2 \end{cases} \quad (2.9)$$

$$m = \{m \in \{1, 2, \dots, M\} \mid l = 1\} \quad (2.10)$$

$$\sum_{n \in N} t_{n,k,l} \leq 1, \quad n \in N \quad (2.11)$$

$$R_n = R(t_{n,k,l}^{0,i}, p_{n,k,l}^{0,i}, \beta) \quad (2.12)$$

The rate of a single link is derived from the allocated radio subchannel which consists of multiple radio resources. Typically, a single radio resource consists of an OFDM frequency subcarrier  $k$  transmitted with a power  $p$  in a time fraction  $t$ , e.g. for the  $n^{th}$  user attached to the MBS  $m$  or the  $j_{th}$  RN, as defined in Equation 2.7. Each possible data rate is limited by a maximum allocated power to a specific subchannel as well as the time

allocated for transmission, as defined in Equation 2.8. A specific subchannel consists of a number of allocated subcarriers  $k$  to the considered radio link/channel. Dependent on the supportable MCS, which is dependent on the corresponding effective SINR on the allocated subcarriers and the total number of the allocated subcarriers the throughput of either a AL, BH or a 2hAL can be determined. It is obvious that, the better the effective SINR a higher MCS can be used and thus, an increased spectral efficiency can be expected on the allocated subcarriers. Finally, this results in a higher capacity of the total system. It needs to be further distinguished between time slots  $l$  for receiving (1) and sending (2) mode for a relay node  $j$ , while the possible served MBS MS can receive data during both time slots. The MS receives data exclusively on the allocated resources from the cell where it is attached. Further, the serving link is denoted as 0 and interfering links  $i$ , respectively in Equation 2.12. The possible RN transmission rate is limited by the half duplex mode of the considered RN type. This means the MS attached to the RN cannot receive more data, than buffered at the serving RN, denoted as buffered data  $\beta$ , considered in Equation 2.12 as well. In summary that means, the data rate of an MS  $n$  is dependent on the allocated time, power, subcarriers as well as the existing interference in a multi cell environment.

While the sum-rate maximization will result in a maximized capacity but does not consider a fair resource distribution among the individual MSs, fairness constraints need to be taken into account in addition, which is explained in more detail in Section 2.3.7. As is can be seen from Equation 2.12 the maximization of the system capacity will be a multi objective optimization problem, which is typically unsolvable and declared as a non-deterministic polynomial (NP)-hard problem. Such optimization problems are often divided in sub-problems to find at least a solution which still improves the system capacity rather than finding the theoretical optimal solution.

Already in conventional networks, it is a challenge to optimally allocate the available resources, due to the dynamic channel variations, the channel estimation errors, the limited total transmit power, processing time and the channel feedback. Not every subcarrier can be dynamically modulated and encoded in every OFDM symbol [41–45]. Due to complexity reasons a grouping of the available resources is necessary [46].

For instance, Figure 2.15 shows a defined Physical Resource Block (PRB) in LTE. The smallest schedulable entity is defined in [47] as two PRBs which consist of 14 OFDM symbols (2 time slots) with 12 times 15 kHz subcarriers. This results in a Time Transmission Interval (Time Transmission Interval (TTI)) of 1ms with 180 kHz PRBs.

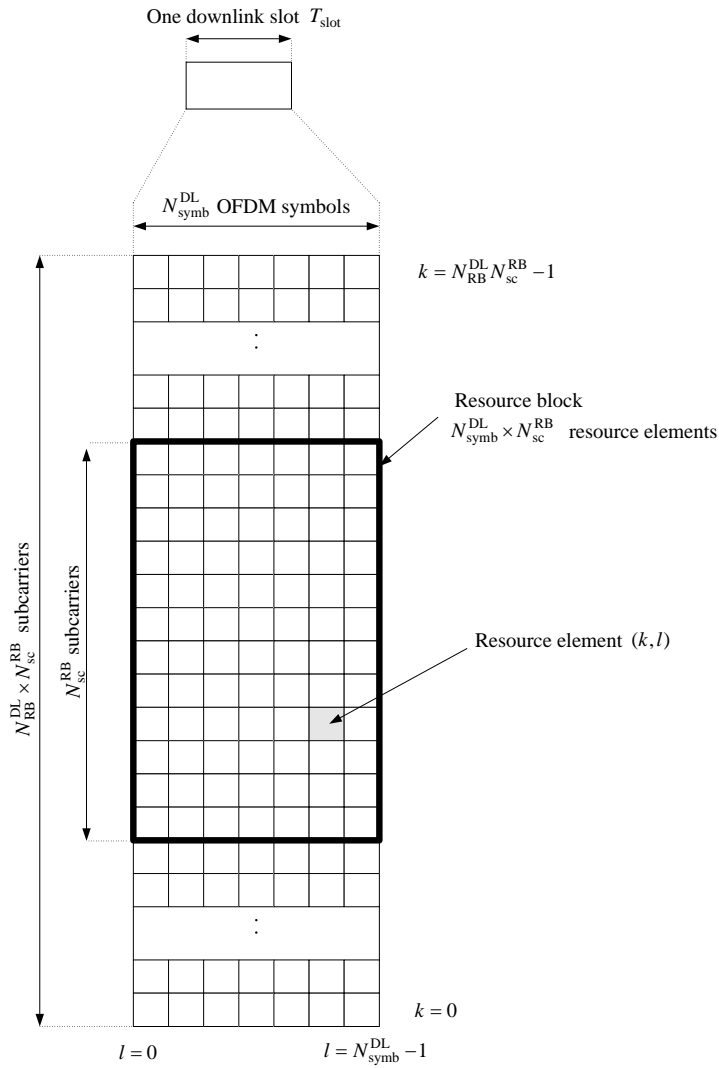


Figure 2.15: Downlink resource grid in LTE [47]

Further, if multiple PRBs are scheduled to a specific MS, the Transport Block Size (TBS) (bits per TTI per MS) needs to be modulated and encoded with a single MCS. Due to that, a link adaptation (LA) algorithm needs to derive the used MCS for transmission [48–52]. Moreover a limiting factor for optimal resource allocation of the PRBs is the accuracy and granulation of the assumed channel feedback. For instance, if in an LTE network frequency selective scheduling is applied, it would be of great advantage to have knowledge of the channel states of each PRB in each TTI to perform an ideal LA to get the best performance. However, this would increase the measurement requirements of the MSs and increases the signalling overhead a lot. To this end, it is finally necessary to find a good practical trade-off between, the signalling overhead, the maximum system capacity and fairness among the MSs [53, 54]. Detailed information on the system model used in this work, which assumes such a trade off, can be found in Section 3.

In this Thesis the considered research problem is decomposed in three sub-problems

to find a practical solution to improve the system capacity. In the upcoming section an overview on existing designed RRM schemes for relay extended networks is summarized, which try to improve the system capacity. Different important works from the industry and academia are identified and evaluated in the context of the necessary feedback overhead, the additional complexity and the assumed level of centralization.

### **2.3.3 Level of centralization and signalling overhead for RRM schemes**

To fairly compare proposed RRM algorithms two aspects are mainly relevant here:

1. It is necessary to consider the introduced channel feedback overhead as input information for the RRM scheme and thus the type of feedback (implicit feedback or explicit feedback, as described in Section 2.2.3).
2. It is important to distinguish among the levels of the centralization and whether the required feedback information arrives with a delay. Typically, three levels of centralization are considered:
  - A network-centralized RRM scheme, where it is required to gather global knowledge about channel states to handle the resource allocation for the entire network.
  - A cell-centralized scheme considers the resource allocation of the dMBS and of the RNs located in its coverage area.
  - A completely decentralized scheme does the resource allocation only based on local channel information of available information between the serving cell and the MSs.

The Figures 2.16 and 2.17 shows the basic differentiation between network-centralized, macro cell-centralized and decentralized schemes in combination with the required feedback in either FDD (Figure 2.16) or TDD (Figure 2.17) mode. While in the FDD RN extended networks the required feedback needs to overcome three hops for a network centralized approach (MS to RN to dMBS to CU), in the TDD mode the situation is a bit more relaxed when only two hops have to be taken into account - RN to dMBS to centralized unit (CU) - illustrated in Figure 2.16 and 2.17. However, even in TDD systems and the possibility of non-ideal wireline backhaul to attach the cells to the centralized unit, the situation might be critical for the correct assessment and thus, the benefit of the designed RRM approach.

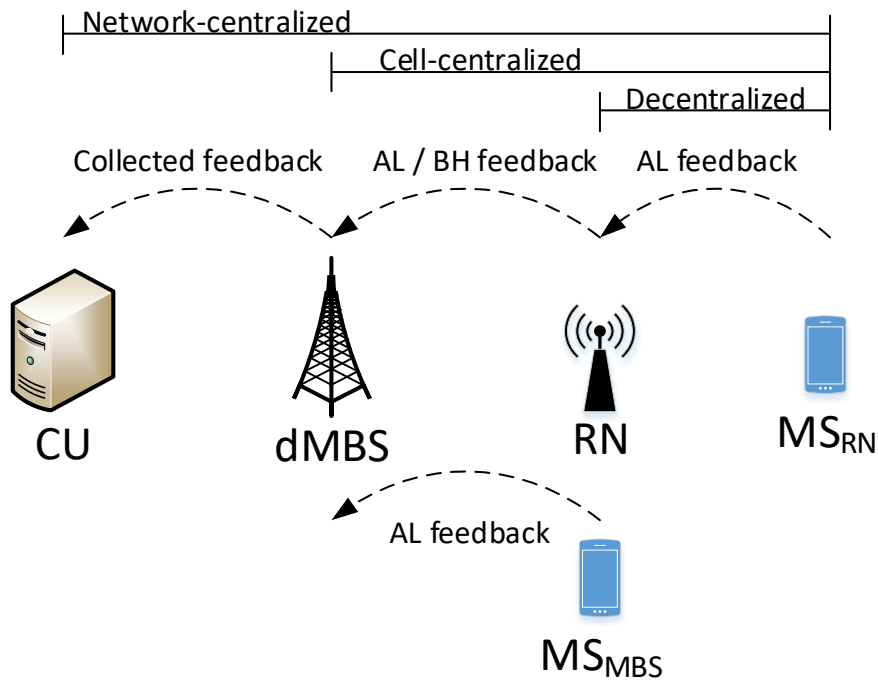


Figure 2.16: Level of RRM centralization and corresponding feedback requirement for FDD downlink

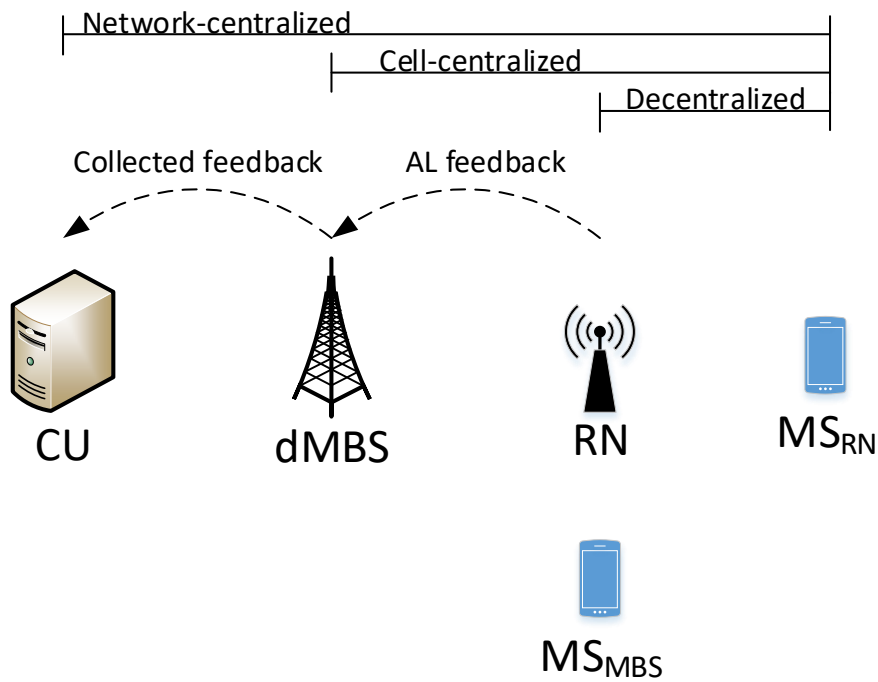


Figure 2.17: Level of RRM centralization and corresponding feedback requirement for TDD

Upper bound calculations can be found in the literature for different types of simplified RN extended systems with different levels of centralization. Typically, the perfect channel knowledge on a subcarrier level is assumed and a pool of a total system transmission power which can be distributed among the appearing links on a subcarrier level.

For instance, Li et al. present in [55] a theoretical upper bound calculation with fairness constraints for a cooperative transparent relay network with centralized RRM, considering multiple two hop connection to a single receiving node. They conclude, that in practical RN systems, such a centralized approach will introduce prohibitive signalling overhead and recommend to focus on distributed RRM schemes in the future.

In [39] two different cell-centralized RRM schemes for a single MBS aided with a single non-transparent RN environment are considered and compared with a network centralized approach. Perfect knowledge about the explicit CSI is assumed on each sub-carrier and no inter cell interference is considered. A substitute information of the RN to MS links is reported back to the dMBS. The information consists of a channel matrix (number of MSs times the number of subcarriers), gathered and fed back by the RN. It is assumed that for each time slot such information is available at the MBS to perform the resource allocation. Even with the already relaxed feedback information, in a multicell environment with inter cell interference a very short feedback periodicity would be necessary, which is impractical due to the very high amount of overhead and the additional measurements, which would still occur.

Moreover, for a single cell environment with a single transparent RN theoretical upper bound capacity calculations are performed, assuming a MIMO channel in [56]. Under the assumption of the perfect explicit channel knowledge, the authors derive an optimal relay precoding matrix to separate the relay MIMO channel into multiple parallel Single Input Single Output (SISO) sub-channels, to result in the maximum capacity of the RN supported MIMO link.

In [57], the authors aim to maximize the sum of the MS data rates based on a macro cell-centralized approach, for a TDD network which consists of a single MBS, six RNs and multiple MSs. Perfect explicit channel knowledge of each subcarrier is assumed. First, they describe the theoretical problem formulation for optimal resource allocation taking into account a constraint of the overall limited transmission power. An additional constraint imposes the restriction that each subcarrier can only be assigned to one link in a specific time slot. Still the optimization problem is declared as an unsolvable NP-hard combinatorial problem with non-linear constraints decomposed into two sub problems. First, they assign subcarriers to the links with high channel gains to maximize the overall capacity. Based on that, they reassign the resources in an iterative process, when the channel quality is unbalanced between backhaul and access link of a single two-hop link, since no buffer at the RN is assumed (for further information the reader is referred to

Section 2.3.5). A heuristic algorithm is applied, adapting the assignment in such a way that the system capacity is improved under consideration of the quality imbalance of the two hops. Once the algorithm has found an improved resource assignment, the decision is taken as granted and a power allocation algorithm is performed, which distributes the total available power among multiple two hops, based on a water filling approach.

The authors in [58] propose a cell centralized algorithm to balance the resource allocation between a single dMBS and six RNs placed in its coverage area. They aim to maximize the system throughput under fairness consideration using a game theoretical approach. It is not clearly stated if the authors consider an FDD or TDD system. However, the algorithm needs to be aware of the actual SINR values of MSs and RNs at a central point to allocate the resources. Having in mind the necessary distinction depicted in Figure 2.16 and 2.17 the cell centralized approach would need a lot of forwarded channel information of the MSs served by the RN, even in TDD mode, to gather the necessary amount of SINR values to gain from the scheme.

Also RRM schemes for large scale networks have been considered under the assumption of perfect explicit and implicit channel knowledge.

For instance, the authors in [40] consider a joint backhaul and access optimization problem for a network-centralized radio access network (C-RAN) TDD system. They assume to have network wide explicit channel knowledge at the central C-RAN control entity and ideal backhaul conditions. Therefore, the MBSs need to send a very large amount of collected CSI information to the C-RAN central entity. Besides that it is assumed in that the MBS only serves RNs, while no MBS-MS connections are considered in the network. The scheme cannot be applied to FDD systems due to the very challenging feedback requirement.

In [59] the authors formulate a joint subband, power, rate allocation problem, decomposing the NP-hard optimization problem in three sub-problems. In the first sub-problem they allocate the resources at the dMBS. Based on that, subproblem two is allocating resources at the RNs. While no buffer at the RN is assumed the resources are reallocated to reduce the difference between the scheduled data rate for a particular MS in sub-problem 3. The authors consider a TDD system, with imperfect explicit channel knowledge due to estimation errors based on additional noise on the uplink pilots and duplexing delay, which means the channel difference between uplink and downlink is varying over time. However, the assumed feedback type is assumed as perfect channel knowledge (explicit feedback with no delay), which still introduces a very large amount of overhead. Even for

the TDD in downlink transmission, the overhead due to the feedback of CSI from MSs to their central controllers grows linearly with the number of MSs. Therefore, they propose to reduce the overhead, by introducing a feedback threshold broadcasted by the central controller. Only if a certain user has the potential to gain based on exceeding the threshold the channel information is updated. The central controller collects new data from the MBSs and RNs which have measured the new CSI. However, in FDD the MSs and RNs would need to report a lot of feedback at first with additional delay to the serving cells, before it could be collected by the controller. Moreover, a rather optimistic assumption is used when assuming an directional receive antenna at the RN with 20dBi antenna gain. LoS conditions are assumed as well for the backhaul connection. These assumptions makes it easy to outperform direct links and can be seen as too optimistic.

In [60], a cell-centralized scheme is proposed to maximize the data rate of an two hop MS by adjusting the time ratio between backhaul and access links to counteract on the different channel states of both as no buffers are assumed at the RNs. The scheme is shown to improve fairness and system throughput. Perfect explicit channel knowledge is assumed and no further information is given on the influence of additional feedback delay of the second hops. They consider only one macro cell and thus they do not take into account the inter MBS interference. The authors assume full flexibility of switching between transmit and receive time slots which is impractical in large scale networks due to the interference uncertainties when neighboring cells have relays which receive and transmit in different time instances. The channel information would be outdated very fast and result in a higher error rate probability.

Jeon et al. in [61] propose a cell centralized approach where the MBS tries to maximize the direct MSs while guaranteeing a minimum rate requirement for the two-hop MSs. First they decompose the research problem in two sub-problems. In the first step they allocate the resources under the assumption of the equal power distribution among them. Once the scheduling decision is done the power allocation optimization based on a water filling approach is only done at the RNs. The MBS uses only the resources which are unallocated by the RNs in sending mode. This implies additional feedback in every TTI about the scheduling decision at the RNs and reduces the available amount of resources at the MBS. Based on a game theoretical algorithm and additional feedback about SINR values of the two-hop users they try to transmit the second hop as efficient as possible to fulfil a minimum data rate and to allocate as much resources as possible to the users served by the MBSs. Based on that, fairness has not been considered. No

information about feedback delays could be found and no further information about the assumptions of the wireless backhaul are given. Based on the discussed schemes and the underlying assumptions regarding the feedback and the level of the centralization the main advantages and disadvantages for the different levels of centralization are summarized in Table 2.2.

Table 2.2: Advantages and Disadvantages of the RRM centralization level

<b>RRM Centralization Level</b>	<b>Advantages</b>	<b>Disadvantages</b>
Network centralized	<ul style="list-style-type: none"> <li>- Global feedback knowledge enables highest possible gains</li> </ul>	<ul style="list-style-type: none"> <li>- Dependent on the required feedback type, possibly prohibitive huge overhead</li> <li>- Additional backhaul delay for the second hop has to be considered</li> <li>- Possible outdated feedback in a real environment which makes network centralized schemes less attractable for real networks especially for FDD</li> </ul>
Cell centralized	<ul style="list-style-type: none"> <li>- Macro cell wide channel knowledge enables possible gains for RN extended networks</li> </ul>	<ul style="list-style-type: none"> <li>- Additional feedback is required about the second hop at the dMBS.</li> <li>- Additional delay due to feedback forwarding from RN to MBS</li> <li>- The type of feedback needs to be carefully considered. It might be a prohibitive amount of feedback due to the usage of scarce wireless backhaul resources</li> </ul>
Decentralized	<ul style="list-style-type: none"> <li>- Lowest amount of possible additional overhead</li> <li>- The cell selection can be done decentralized</li> </ul>	<ul style="list-style-type: none"> <li>- Only local channel knowledge is considered</li> <li>- Lowest or no gains can be expected due to the loss of the knowledge about the quality of the second link at MBSs</li> </ul>

### 2.3.4 Inter Cell Interference Coordination

In a multi cell environment, the generated interference between the existing cells in the system limits the possible system capacity. Introducing additional RNs in the network increases this challenge by introducing more interfering nodes to neighbouring cells. When

considering half duplex RNs an additional loss in transmission time has to be handled as discussed in the previous sections. Based on that the interference situation appears with higher dynamics over the time due to the half duplex mode. Based on that, inter cell interference coordination (ICIC) schemes are of interest to handle critical interference situations. The ICIC schemes mainly focus on either cancelling, suppressing or mitigating the interference in multi cell environments and thus, to improve the capacity and the coverage. Depending on the assumed channel knowledge level, different schemes with varying level of complexity are designed in the literature. Lee et al. give an overview on RRM and ICIC schemes for HetNets in [18]. After an extensive literature search, they conclude that to date it remains a challenging task to design resource allocation schemes for LTE/LTE-A relay networks with low complexity, while simultaneously excelling in aspects such as interference mitigation, resource utilization and fairness. Furthermore, a comprehensive classification of RRM schemes for RN enhanced networks can be found. The authors give an overview of research problems in heterogeneous networks. Most of the considered schemes come with the burden of heavily increased explicit CSI feedback exchange, which introduces increased control traffic exchange among MBSs and additional signalling on the RN wireless backhaul links for the RNs, as discussed in previous sections. This is especially the case when FDD downlink transmission is considered. Furthermore, the authors identify different kind of heuristics, such as evolutionary and game theoretical approaches as promising techniques to overcome the NP-hard declared optimization problem for practical RRM schemes.

Furthermore, an excellent overview and classification of possible means to handle interference in carrier grade networks can be found in [62]. Boudreau et al. give a comprehensive overview on possible ICIC techniques in general for OFDMA networks. The ICIC schemes with different levels of complexity and depth of understanding are separately listed. As an example, minimal additional complexity comes with the introduction of Fractional Frequency Reuse (FFR) patterns, illustrated in Figure 2.18.

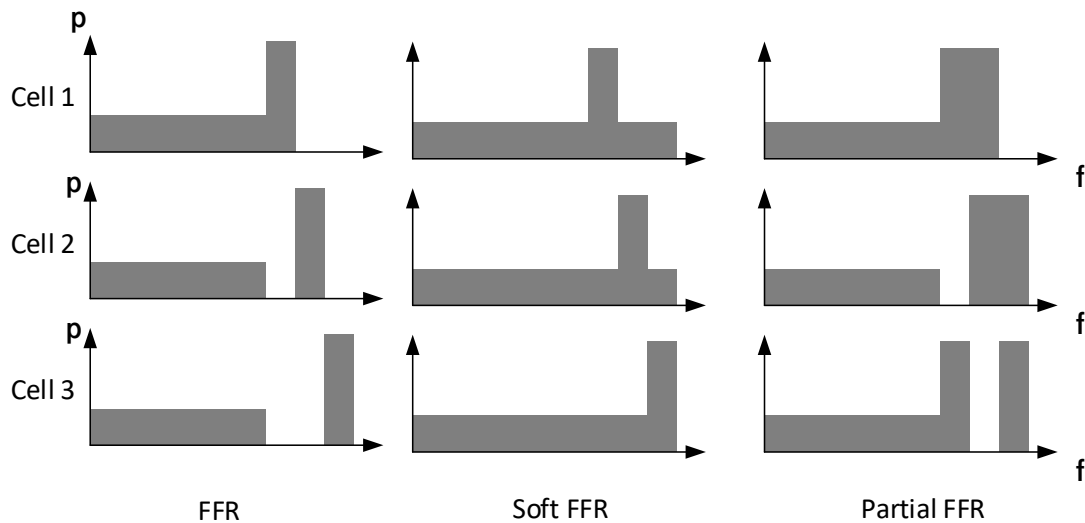


Figure 2.18: Example Fractional Frequency Reuse Patterns

Typically, when FFR strategies are applied the used pattern will be preconfigured on the considered subbands in the network. In a defined subband the transmission power is kept on the default level, to serve cell edge users and prevent a higher outage probability. The shared bandwidth is transmitted with a lower amount of power to prevent a higher overall transmission power. Such techniques are often used to mitigate negative SINR regions and improve the cell edge performance. Traditional frequency reuse schemes often reduce the available amount of resources to relax the interference situation in the neighboring cells. That is why frequency reuse schemes are mainly used to improve the cell edge performance and accept a loss of the overall system capacity [63]. However, in relay extended networks they might also be useful to increase the overall capacity which is proved in [64]. Accordingly to Figure 2.18 the FFR pattern can be organized in three different ways, listed as follows:

- FFR: A part of the system bandwidth is used in all cells with equally reduced power, while the second part is organised, with a reuse higher than one transmitted with full power to create a subband with low inter cell interference. Two subbands remain unused and decrease the available bandwidth in the considered cell.
- Soft FFR: The shared subband is used with static reduced transmission power. Only in a defined frequency band the cell is transmitting with full power. The shared subband experience a lower amount of interference caused by the nearest neighbour cells, while Full bandwidth is available in each cell.
- Partial FFR: A mix of the two previous schemes. A larger subband is used with

full transmission power but only part of it exclusively. Again a defined subband is transmitted with reduced power with a reuse of one, while at least one interfering sector is suppressed by not using a subband, where the other cells are transmitting with full power. One subband remains unused and decrease the available bandwidth in the considered cell.

In principle the soft fractional frequency reuse pattern might result in higher gains in average compared to the other FFR schemes due to the full availability of the system bandwidth at each cell. The cell edge performance improvements will be limited due a lower degree of freedom to improve negative SINR regions. This makes it a promising solution which needs to be adapted for the purpose of this Thesis, further described in Section 4.3.

An adaptive FFR algorithm for RN enhanced networks is proposed in [65]. Here, a dynamic resource allocation algorithm is proposed by applying dynamically FFR and Soft Frequency Reuse (SFR) patterns at MBSs and RNs for half duplex RNs in the FDD downlink transmission. Due to the radio channel dynamics a CQI periodicity of 1ms is assumed to receive accurate implicit channel knowledge to take decisions about the dynamic allocation in the applied reuse patterns. This introduces a very high amount of signalling and seems to be impractical. No further information is given about the quantification of the CQI reports and the additional delay of the forwarded second hop link qualities which need to be gathered at the donor MBS. Further they assume a directed receive antenna at the RNs which requires LoS conditions. A planning gain for the wireless backhaul connection is assumed. As already mentioned, this is an idealized assumption which can be seen critical and will be further discussed in Section 3.5.1.

Adaptive FFR algorithms enhance the technique with higher dynamics and adaptation to occurring interference situations in the system. However, therefore an additional information exchange of implicit CQI information as well as a higher periodicity of the channel feedback are required. The problem here is the dynamic variations of the radio channel and the risk to loose diversity gains when the reconfiguration doesn't follow the channel dynamics. If the adaptation of the FFR shall follow the dynamics of the radio channel again a large amount of CQI information exchange is required. Furthermore, after a successful reconfiguration is done, current information which is available at the radio resource scheduler is outdated and the MS needs to feedback updated channel feedback based on the new interference situation. This influences the link adaptation as only

outdated feedback is available for several scheduling decisions which will result in higher error rates. Furthermore possible ongoing retransmissions are affected negative as well. Therefore an optimized semi-static fractional frequency reuse pattern based on limited feedback is applied in this Thesis and frequency selective scheduling is applied for fast switching channel conditions. It is able to make use of the channel dynamics and requires only intra cell MS feedback and no additional exchange among MBSs. The scheduling decisions gain from higher channel diversity. This is possible when the adapted transmission power over the subband is kept stable over a longer timer period.

Possible FFR schemes as well as other possible ICIC schemes in heterogeneous networks are also considered in [66]. The authors distinguish between global centralized and fully distributed schemes and discuss the aforementioned challenges regarding practical implications and available channel information, for conventional and pico cell extended networks. The paper also recommends to investigate lower complexity heuristics to solve the ICIC problem, since near optimal means can be economically and technically infeasible due to the aforementioned limitations in practical systems.

Moreover, the authors in [67] identified a promising trade-off between complexity requirements and possible gains analysed for conventional macro BS networks. Here, the authors propose a hybrid scheme, where fast time scale scheduling decisions are done in a decentralized way, while FFR patterns are centralized dynamically adapted on a PRB level with very high amount of implicit feedback. However, the general idea of such a hybrid RRM scheme is focus of this work in combination with the introduction of the RNs to the network.

### **2.3.5 Buffer aided RN**

The use of the data buffer at RNs is an additional design criteria for resource management algorithms. The RN is able to keep received data and transmit it over multiple TTIs which introduces a higher degree of freedom scheduling data on the access link. If no buffer is applied the total amount of data needs to be forwarded in the next TTI after switching from the receiving to the sending mode. This implies less flexibility to react on an imbalanced link quality between the backhaul and the access link. It is then necessary to consider equal data rates on both links which limits the overall data rate of the two hop connection and thus the overall capacity of the system [68]. For instance, in [69] a low complexity resource partitioning scheme with two-hop proportional fairness is considered. The re-

sults show improved RN MS cell edge performance as well as increased average MBS MS performance with improvement in fairness. No additional buffers at the RNs are assumed and the designed algorithm needs to consider equal data rates for the BL and the AL at the RNs. Moreover, only the average MBS user throughput is presented, without information about the Cumulative Distribution Function (CDF) of the macro MSs. It is not clear if the overall macro MS throughput is influenced in a negative way. Furthermore, no adapted power allocation pattern is applied to reduce the interference or further balance the backhaul and access link data rate imbalance. In other words, if data buffers are not used at the RNs traffic congestion can occur due to the imbalanced channel qualities of the backhaul and access links.

Figure 2.19 shows the principle idea of a data buffer at the RN. The backhaul link between the dMBS and the RN is used to transmit one large transport block (TB) with data for all users attached to the RN. The RN needs to decompose the TB and fill MS specific buffers at the RN. For more information of the buffer aided scheduling process in this Thesis the reader is referred to Section 3.5.6.

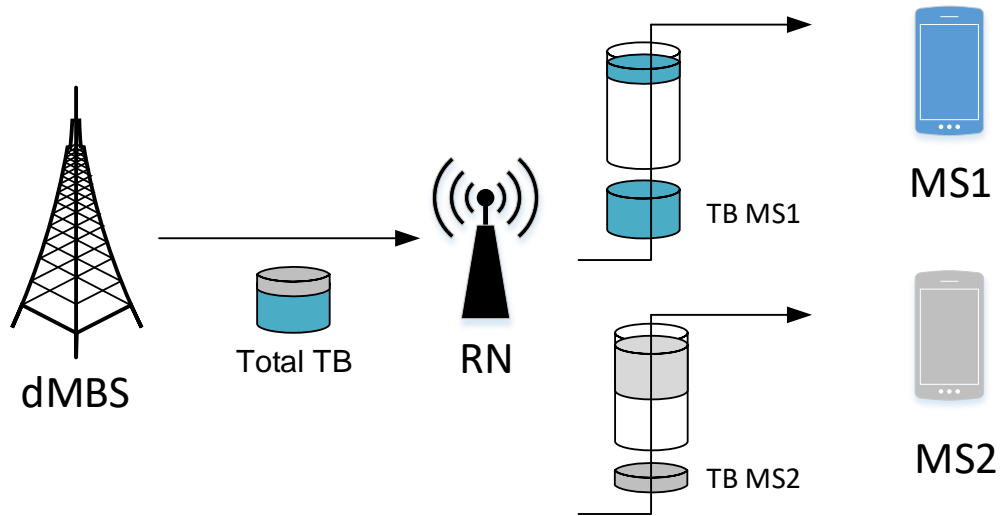


Figure 2.19: MS specific buffer structure at the RN

Wang et al. [70] study fairness and throughput downlink performance based on a designed three step resource allocation scheme when the data buffer is used. In [71] a two-step algorithm is used for the resource allocation considering the buffer status' of the two-hop MSs. Both contributions introduce buffers at the RNs to prevent performance limitations because of the previously mentioned reasons. The authors clearly show an improvement of the overall user throughput and the cell edge throughput. The assumptions regarding the used channel feedback and assumed delays are unclear, though. No additional means to mitigate the interference have been considered in these works.

Based on the existing literature and the previously mentioned reasons it has been decided to use data buffers for the solution of this Thesis. Detailed information can be found in the Sections 3.5.5 and 3.5.6.

### 2.3.6 MS cell selection in RN extended networks

Due to the introduced two hop transmissions in RN extended networks, it is important to consider possible alternatives to existing MS cell selection methods in conventional networks, such as RSRP or wideband SINR based assignment methods used in today's networks [72]. These methods consider only the signal strength or the link quality of the access link while the backhaul quality is not considered here. Depending on the aforementioned RRM schemes it makes sense to adapt the decentralized attachment procedure based on the consideration of the possible two-hop transmissions. Therefore in [73] an end-to-end optimal routing strategy is proposed, which considers the maximum end-to-end data rate of a two-hop link compared to the possible direct links. Equation 2.13 defines the proposed strategy. Each MS  $n$  is attached to the serving node  $s$ , with the maximum data rate in which  $R_{k,n}$  represents the possible supportable rate between RN  $k$  and MS  $n$ ,  $R_{0,k}$  denotes the backhaul rate, while  $R_{0,n}$  stands for the possible rate of the direct link between dMBS and MS.

$$s = \max \left( \bar{R}_{0,n}, \frac{\bar{R}_{0,k} \cdot \bar{R}_{k,n}}{\bar{R}_{0,k} + \bar{R}_{k,n}} \right), \quad (2.13)$$

where  $k \in K_{RN}$  and  $n \in N_{MS}$

An extension to the existing assignment procedure often used in previous works was developed throughout this Thesis. A detailed description can be found in Section 4.2 and the corresponding simulation analysis in Section 5.2.1.

### 2.3.7 Radio resource scheduler

As already mentioned before, the radio resource scheduler is in charge of allocating the radio resources in a mobile communication system on a TTI level. It has to find a trade-off between a fair resource distribution among MSs on the one hand and the most efficient transmission on the other hand. In addition, if relay nodes (RN)s are used the scheduler

needs to allocate the wireless backhaul resources to the RNs at the considered donor macro base station (dMBS), which may need to serve multiple attached RNs, besides the direct MSs. The reader has to keep in mind that in this Thesis the non-transparent layer 3 RN is considered which is able to perform the scheduling process for the access link in a decentralized manner, while the resource allocation for the wireless backhaul is done in a macro cell centralized fashion.

In the following, an introduction is given to the basic radio resource scheduling metrics which are used in existing works, while the necessary extensions to the common schedulers in this Thesis for RN enhanced networks are afterwards described in Chapter 4.4. In addition to that, the important co-scheduling functionality which increases the flexibility of the resource allocation is described in Section 2.3.7.6. This feature was decided to be used for the analysis in addition in this Thesis.

### **2.3.7.1 Round-Robin scheduling**

The simplest scheduling strategy is Round Robin (RR), where the MSs are allocated to the radio resources in a periodic manner, without considering the current radio channel conditions. RR scheduling is seen as fair scheduling in terms of equal resource allocation among MSs. A widely known extension would be to reorganize the fairly distributed resources in each TTI based on the current channel state to improve the overall system performance based on frequency selective scheduling. The outcome of the procedure is depicted in Figure 2.20 and performed as follows:

- Each MS gets at first the same amount of resources subsequently (left time-frequency grid in the Figure). As an example three MSs highlighted with blue, green and red are illustrated. The resources are allocated iteratively to the attached MSs without any additional intelligence. For instance each of the coloured MS gets two resource blocks allocated in the first TTI. The MS five and six get their second PRB in the next TTI because no enough resources were available in the first interval.
- After the amount of resources for each MS is defined the scheduler considers received subband specific channel feedback. For that purpose the resources have to be reorganized in each TTI based on better channel qualities.

The MSs will profit from channel diversity gains and thus the overall capacity of the system will be increased. The major drawback of the scheme is, that the system performance

will still suffer from the fair resource allocation. For instance MS1 might have better channel conditions on the allocated resources of MS2 and MS3 in addition.

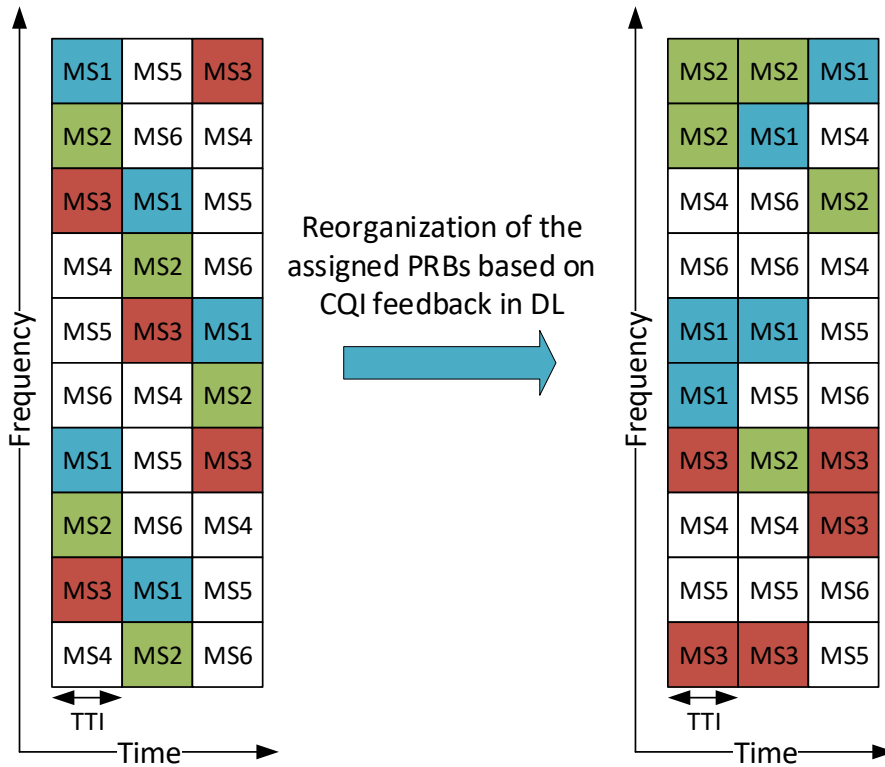


Figure 2.20: Round Robin frequency selective scheduling

As an example, in [74] a simple resource allocation algorithm in relay extended networks is suggested to maximize the average cell throughput and the cell edge performance. The authors propose only a time domain resource allocation split in 3 parts for the backhaul link transmission, the direct link and the access link transmission. A simple RR scheduler is used to assign the resources in time domain within the derived time fractions. No fast fading and therefore perfect channel knowledge has been considered in this work. That is why time domain scheduling is sufficient here. In addition, no feedback delay is assumed. Furthermore, the relays are equipped with a receiving and sending antenna with additional antenna gains for the two-hop transmission.

### 2.3.7.2 Time domain channel selective scheduling

In Figure 2.21 a time selective channel dependent scheduling strategy is presented. Possible channel gains are represented for three MSs marked in color over time on the left side. The dashed black curve represents the hull curve of the MS specific radio channels and illustrates the maximum possible channel gains over time. Due to the time selective scheduling strategy the radio resources are allocated to the MSs with the maximum

channel gains. Since no frequency selective subband channel information is considered, the decision relies on the wideband SINR knowledge. Based on that, the total amount of available resources are allocated to a single MS in frequency domain which limits the flexibility of the scheduler. In this example, all resources from TTI zero onwards to TTI nine would be allocated to MS2 (green coloured in the left and right figure), because of the highest channel gains during that time. In the next 7 TTIs, the MS3 (highlighted in red) would be scheduled, while only 5 TTIs would be allocated to the blue coloured MS1 in the next step and so on. The result improves the overall system capacity due to the most efficient usage of the resources without consideration of any fair resource allocation among MSs. An individual user might suffer from the scheduling strategy, especially cell edge users with worse channel conditions.

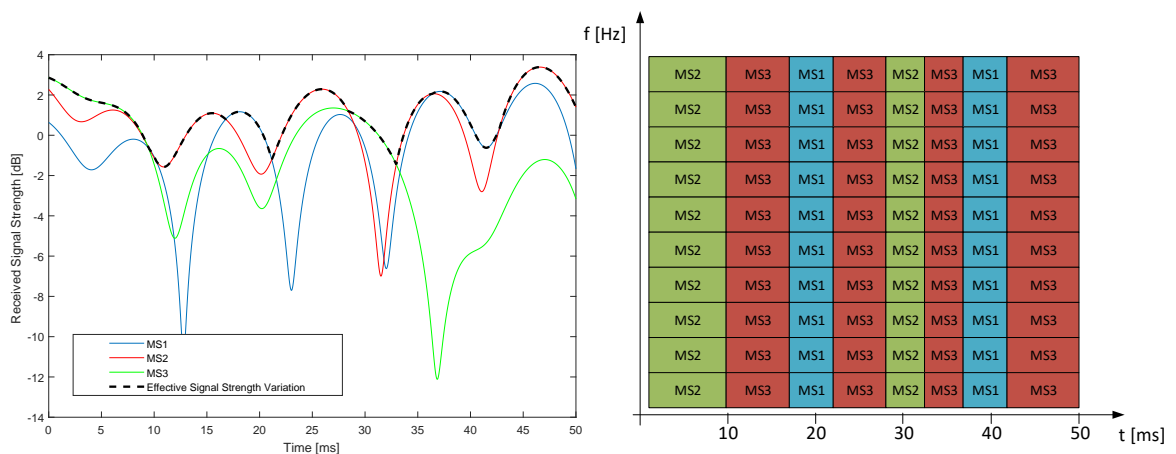


Figure 2.21: Radio channel dependent scheduling

### 2.3.7.3 Time and frequency domain channel selective scheduling

In addition to the previous explained time domain specific scheduling, if subband channel information is available, frequency selective decisions can further improve the system capacity making use of the channel diversity gains not only in time but also in frequency domain. An example situation is shown in Figure 2.22. Here channel dependent scheduling in time and frequency domain is applied, without any fairness consideration. This approach is also known as Max-Min SINR scheduling. Due to that scheduling strategy, a maximized system capacity can be reached because the highest channel gains can be exploited. A single MS, e.g. MS3 marked with red colour in Figure 2.21 will suffer from the approach and gets no resources at all, due to its worse channel conditions compared to other MSs. The result of the scheduling strategy will be a unfair resource distribution and increases the outage probability of the users.

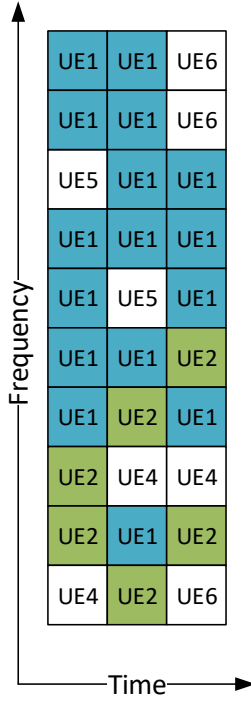


Figure 2.22: Max SINR scheduling

#### 2.3.7.4 Proportional fair scheduling

To provide a trade-off between the RR and the Max-Min scheduling approach and thus a trade-off between fairness and maximum system capacity, a Proportional Fair (PF) metric is proposed in [75]. For conventional networks, the metric is widely used and described as follows.

Equation 2.14 calculates the priority  $P$  for each MS  $k$  on every PRB  $n$  in TTI  $i$ .  $R$  is defined as the frequency selective instantaneous supportable rate, depending on the delayed MS CQI reports on the  $m_{th}$  subband. As already mentioned the subband CQI report on a PRB level would exceed the practical limitation. That is why typically a group of  $n$  PRBs is defined per  $m_{th}$  subband to reduce the feedback traffic. This is another trade-off between channel knowledge and additional overhead. The average throughput  $T$  from the past scheduling decisions is recursively updated. The parameter  $\alpha$  is a MS specific exponential scaling factor, which can be used for user specific prioritization purposes.

$$P_{k,n}(i) = \frac{R_{k,n}(i)}{T_k^\alpha} \quad (2.14)$$

As defined in Equation 2.15,  $T$  of the non-scheduled MSs is multiplied with a forgetting factor  $\beta$ . The scheduled MSs'  $T$  is updated by multiplying with  $\beta$  and adding the instantaneous data rate of the current TTI with a weight of  $1-\beta$ , defining a sliding time window.

Based on the calculated priority matrix  $P$  the PRB allocation is done by taking the MS  $k$  with the maximum priority  $U$  for each individual PRB  $n$ , defined in Equation 2.16.

$$\mathbf{T}_{k,i+1} = \begin{cases} \beta \cdot \mathbf{T}_{k,i} & \text{non-scheduled UE} \\ \beta \cdot \mathbf{T}_{k,i} + (1 - \beta) \cdot \mathbf{R}_{k,i} & \text{scheduled UE} \end{cases} \quad (2.15)$$

$$U_k(n) = \max_k(\mathbf{P}_{k,n}(i)) \quad (2.16)$$

Based on the conventional PF metric, Xiang et al. suggest the following for RN-extended networks [76]. The authors propose to exclusively schedule RN backhaul links (BH) without co-scheduling the direct linked MSs. They derive an access/backhaul partition resource pattern which repeats with a certain period until it is changed by a higher layer configuration. Perfect implicit channel knowledge is assumed for each MS on every PRB and only flat fading for the BL is assumed under LoS conditions. Therefore the SINR is constant over all PRBs. They also relax the research problem and suggest a two step solution, which first partitions resources for the access and backhaul links in time domain. This is kept stable for several seconds, while independent frequency selective PF scheduling at dMBS and RN is applied. Although, ideal BL conditions are assumed, the limited capacity at the RN is taken into account due to possible backhaul data rate limitations. The influence here is unclear. Furthermore, the access link for RN to MS transmission can only use part of a subset of the resources. This introduces possible losses when a fading notch in this resource subset appears. It is also unclear if additional feedback delays are assumed or not.

In [77] the influence on the network performance of the applied RR and PF scheduling metrics is analysed. The authors clearly show that the PF metric outperforms the RR approach in terms of capacity. They assume perfect channel knowledge and no information about additional feedback delays are given. Further, they define a fraction of time for BL transmission and separate the transmissions only in time domain. In addition, no co-scheduling functionality is applied limiting the degree of freedom considering possible frequency selective scheduling decisions at the MBSs.

Different approaches for the RR and the PF metrics for RN-extended networks have been analysed in the course of this Thesis in [78]. It also turned out the better performance of the PF metric with channel dependent scheduling. In the next step the common metric needs to be extended to introduce co-scheduling and thus to further improve the system

capacity by extending the flexibility of the scheduler.

### 2.3.7.5 Two-hop proportional fair metric

For half duplex RN extended networks the possible two-hop links need to be taken into account in the dMBS scheduling metric. Based on [79], a Composite Rate (CR) is defined in Equation 2.17, which is described as the harmonic mean of the instantaneous BL and AL rate  $R_l$ , also defined more general in [80]. This considers the loss in time of the two-hop transmission. For instance, if both BL and AL would have the same link quality the maximum supportable rate of the end-to-end link would be decreased by half.

$$CR_{k,n}(i) = \left( \sum_{l=1}^L \frac{1}{R_{l,k,n}(i)} \right)^{-1} \quad (2.17)$$

Figure 2.23 shows the two-hop proportional fair scheduling principle for one resource block. The depicted relay node is in receiving mode and the donor MBS has to decide which of the attached MSs will be served in the considered time instance. Based on implicit feedback of the RN backhaul link and the access link of the two-hop connection and the feedback of the directly attached MS a decision is taken. For simplicity the history information about previous resource allocations is not considered here. Based on the instantaneous supportable rate of 2 bps/Hz of the direct MS2 and the composite rate based on Equation 2.17 for the two-hop connection of MS1 (1.71 bps/Hz) the scheduler would decide to allocate the considered resource block to MS2. This enables a fair resource distribution between the one and two-hop connections. However, for the transmission itself the BL feedback needs to be taken into account and the resources might be reallocated considering the derived transport block sizes based on the proportional fair resource distribution, further discussed in Section 4.4.

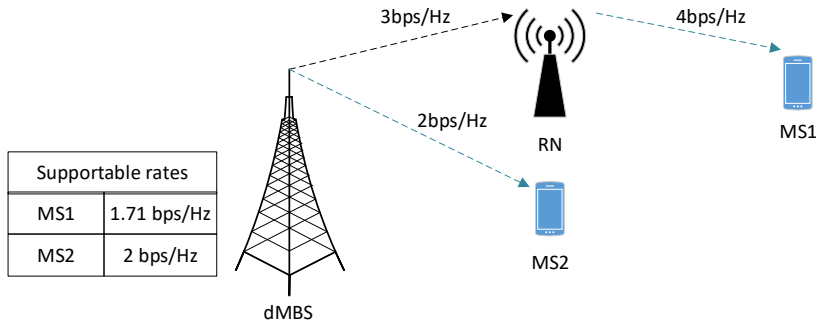


Figure 2.23: Two hop proportional fair scheduling

As an example, in [79] only two hop links are taken into account exclusively without

considering resource allocation for direct linked MSs. The RNs are located at cell edge, while an orthogonal subcarrier set based on reuse 3 for the MS communication in outer macro cell regions is used. A sub-optimal solution is then presented which relaxes again the NP-hard research problem. The resource allocation is done on a subcarrier level, which is impractical as discussed before. Moreover, ideal channel conditions for the BL transmission is assumed with LoS and a SINR of 30 dB.

Liu et al. propose a resource and power allocation optimization for the downlink in [81]. The authors consider two-hop proportional fair scheduling. The optimization problem is decomposed in two sub-problems. They assume, that there is no direct transmission and therefore no co-scheduling is applied between MBS and MSs. For detailed information of the co-scheduling technique the reader is referred to Section 2.3.7.6. Further the authors assume no buffer at the RNs and forward the received data on the same resources as received. Only a single MBS is considered with no inter macro cell interference in the network. In addition they assume only slowly varying radio channels to feed back accurate explicit channel information to be able to calculate a near optimal power and resource allocation for each time slot, which would result in an impractical solution.

For further detailed information about the extended two-hop proportional fair metric in this Thesis the reader is referred to Section 4.4.

#### **2.3.7.6 Co-scheduling between MSs and RNs**

The co-scheduling functionality has been found as an attractive solution improving capacity and the coverage in RN extended networks [82]. While a lot of works assume exclusive time domain based BL scheduling to serve the RNs a higher flexibility especially in real system is provided by that feature to react on channel variations and unbalanced MS assignments among RNs and dMBS. The principle idea is presented in Figure 2.24.

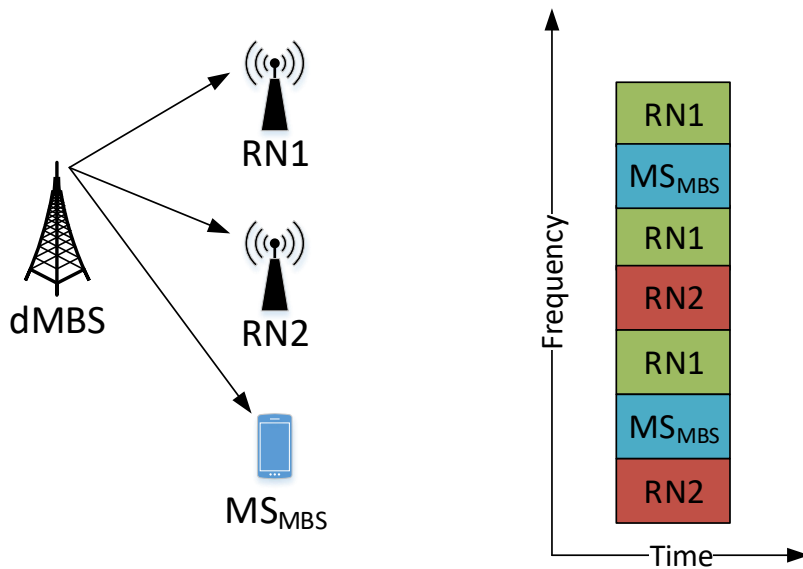


Figure 2.24: Two hop co-scheduling among directly attached UEs and RNs

As shown in Figure 2.24, co-scheduling introduces the possibility to allocate resources for BLs and direct ALs in the same TTI, when RNs are in receiving mode. With this feature it is possible to schedule RNs and MSs in the same TTI in a frequency selective manner.

In [83,84] the authors analyse practical resource allocation strategies for non-transparent inband relays in an FDD system. They use frequency selective scheduling at the MBSs and the RNs. The backhaul links are served with higher priority than the directly served MSs at the MBSs. The MBS is able to serve users and RNs in the same time slots, which means the support of the co-scheduling feature. By varying the number of backhaul subframes, they show the influence on fairness and downlink throughput. However, no additional interference mitigation strategy is applied to further improve the throughput. Also an additional simple planning gain of 5dB for the backhaul link is assumed, which is in contradiction to the often identified bottleneck in realistic RN extended network [33]. Therefore, no further strategy is introduced to improve the backhaul capacity. Also the assumptions for the used feedback type and the feedback delay is unclear. No information is given how the authors derive the transport block size for the backhaul transmission. Finally they conclude to use ICIC schemes in addition in future research contributions as the users directly served by the MBS suffer from the RN enhanced network because of the increased level of interference.

In [85] a single relay link consisting of a source a relay and a destination is considered. Different relay schemes such as AF and DF are dynamically used dependent on the instantaneous radio channel conditions. Two kind of suboptimal solutions for a joint

power and bandwidth allocation are presented. They assume perfect channel knowledge at all nodes and recommend to proof the performance improvement of the sub-optimal solutions under worse accuracy of the channel knowledge. They state, that this work can be used as a baseline for future research in combination with a suitable modelling of the overhead ratio, the interference and channel estimation errors.

In [86] a mobile network consisting of a single donor BS with multiple relays is considered. Each user exclusively communicates over a second hop with the BS. The second hop uses WiFi or Bluetooth for the communication. They assume static channel conditions. Each RN can only serve one UE at most at anytime. The proposed scheme at first searches an optimal relay and terminal matching according to the channel conditions. Then the optimal resource allocation problem is solved by a game theoretical approach. Very high additional amount of overhead is required as the BS collects channel state information in every time slot. Further, all RNs and UEs need to know in each time slot which nodes belong together for the upcoming transmission as it can dynamically change. In addition, user and relay need to exchange additional signalling regarding the game theoretical optimization considering the used resources and the rates, which can be achieved. Note, that the solution would also require non-standardized cross radio protocol information e.g. between IEEE and 3GPP. If a multi cell scenario would be considered the additional overhead might be prohibitive and therefore it is unclear how the scheme would react in a multi cell environment.

The authors in [87] present a cooperative joint power allocation and strategy selection (PASS) for different RN modes. A single cooperative relay link is considered with source destination and a relay. Half-duplex Decode and forward and Compress and forward strategies are considered. The PASS scheme adjusts the power along the time over channel states in an optimal manner, chooses the relay strategy dynamically based on possible channel gains and sets the time division dynamically for the sending and receiving mode at the relay. It is for further discussion how the scheme would react applied in a large-scale network with non-ideal channel information and out of cooperation cluster interference.

In [88] a resource allocation scheme for self-backhauled half-duplex small cells is proposed. The scheme uses only a limited amount of feedback based on a decentralized approach. In a first step they consider a long term resource allocation decision based on long term averaged SINR. No fairness among one and two hop UEs is considered. Furthermore, no adapted power allocation is considered. During the second step the long term allocation is adapted based on wideband SINR values in a time selective manner

between the UEs. Here, no possible frequency selective diversity gains are considered. Finally the results show significant gains in terms of the average UE throughput. However, the CDF shows a crossing point compared to the baseline for the approximately 77 percentile which means that 23 percent of the users might suffer from the scheme.

In [89] several state of the art scheduling approaches are considered with service differentiation (QCI classes) considering adaptive weights based on several thresholds such as delay budget, target data rate and channel conditions when relays are deployed in cell edge areas. It can also be observed that UEs, which are located in the vicinity of the macro BS suffer from the proposed scheme in terms of throughput when relays are deployed.

The authors in [90] analyse in-band self-backhauling relays for multiple virtual service providers, which share a common physical infrastructure. Therefore, the radio resources are abstracted as virtual resources and allocated to the terminals in an optimized way based on channel state information and queue states. The available spectrum is segmented for the number of considered service providers. No power optimization is considered for the backhaul link as well as no detailed information about the considered type of channel information is given. Furthermore, it is assumed that the proportion factor for backhaul and access link transmission is dynamically adjusted which typically results in channel uncertainties and increases the probability of outdated channel feedback. No fairness criterion and no power adaptation for the improvement of the resource allocation decision is considered.

He et al. focus on the combined use of the half-duplex and full-duplex scheme in a coordinated way in [91]. They define three separated regions in the considered frequency band into backhaul-only, access-only and shared resources. The regions are adapted in every time slot and therefore a possible switch between HD and FD mode is assumed in every time slot, which will be far too dynamic in practical systems. Based on perfect channel knowledge and global knowledge of queue states they define the three aforementioned spectrum regions. They assume a joint resource scheduler at a central unit which gathers all the necessary information in an ideal way. Further, they assume the carrier frequency as 28GHz, which eases the interference situation due to high path loss gains and better isolation between neighbouring BSs. In addition, no long-term power adaptation is considered.

A hierarchical RRM scheme is proposed in [92] with a global long-term and a decentralized short-term control part. A heterogeneous network is considered where a number of pico cells are connected via a wired backhaul while another group of pico cells are

connected through a wireless backhaul. All cells are connected via an additional low-cost signalling backhaul to a centralized radio resource management controller, which coordinates the resource allocation among all cells. Furthermore, also multi-hop connections larger than 2 hops are considered. Dynamic muting pattern for pico and macro BS are applied to ease the interference situations as a long term decision over multiple frames summarized as a superframe. Due to the assumed wired signalling backhaul to the central unit no additional feedback delays need to be considered in this work.

## **2.4 Summary**

Based on the previously presented aspects for RN extended networks in the following Table 2.3 the most relevant principles design principles are summarized and used for the development of the hybrid RRM scheme for RN extended OFDMA networks in this Thesis.

Table 2.3: Summary RN RRM design principles

<b>Design Principle</b>	<b>Summary</b>
RN type	Types of RNs based on Table 2.1 in Section 2.2
Non-/ Transparent	The RN is either part of the macro cell or acts as an own cell, which mainly influences the cell selection scheme, adaptive routing and cooperative schemes
Buffer aided RN	Distinguished whether the RN has a data buffer or not. If no buffer is assumed rate match is necessary between backhaul and access link, since the received data needs to be directly forwarded and BL / AL imbalanced data rates are critical
Half-/ Full Duplex	The RN does either receive and transmit at the same time slot or not. Especially full duplex mode introduces higher complexity to the relay due to required self interference cancellation techniques, but does not lose time slots for reception compared to half duplex relays.
In-/ Outband	The wireless BL of the RN operates on the same frequency band as the AL or not. Out of band assumption increases the available system bandwidth and relaxes interference issues. However, it is then assumed that additional highly expensive scarce spectrum is used exclusively for wireless BL transmission.
Non-/ Cooperative	The RN and MBS transmit combined signals based on exchanged explicit channel state information for cooperative mode. Cooperative schemes might benefit from the centralized design, while it comes with the cost of higher CSI feedback overhead. Especially in FDD critical.
TDD/ FDD	RRM design depends on TDD or FDD mode of the system, due to channel reciprocity in TDD systems or additional channel feedback required with less accuracy for FDD downlink. An additional challenge in TDD is the necessary UL / DL transmission pattern among cells to prevent UL / DL interference.
Resource scheduling and reuse schemes	How to schedule the resources for backhaul and access transmission is an important design criteria. In addition it is the question how to reuse the resources within an MBS with several RNs as well as in a multicell scenario. Typically reuse one provides highest degree of freedom and supports higher frequency selective gains, while also a high interference level has to be handled. Frequency selective two-hop proportional fair scheduling with the co-scheduling feature increases the degree of freedom for best scheduling decisions.
Network and Cell De-/ Centralized	The need to differentiate if the RRM is network centralized, which assumes a level of global channel knowledge and usually requires high amount of signalling. If the scheme is designed as cell centralized, the RN needs to feedback a certain amount of channel information to the serving cell, depending on the complexity of the scheme and thus the required type of feedback. If a decentralized approach is assumed no or only very low amount of additional signalling feedback is required, from RN to dMBS and no addition feedback is necessary to the CU (see Table 2.2).

To provide maximum flexibility and to make use of channel diversity gains, and thus to improve the system capacity under fairness constraints throughout this Thesis, the

adapted two-hop proportional fair frequency selective co-scheduling principle and reuse 1 resource partitioning pattern is applied and found as a promising solution for real networks for the cell-centralized part of the proposed solution. For the network-centralized part an optimized semi-static soft FFR pattern is used for the power adaptation on a subband of the system bandwidth to further improve the capacity of the network described in Chapter 4. To remind the reader, within this Thesis an in-band half duplex, non-cooperative, non-transparent, buffer aided, layer 3 relay in FDD mode is considered.

Besides the presented derived principles in Table 2.3, the discussed designed RRM scheme targets on specific KPIs, such as the maximization of the system capacity, fairness, interference mitigation techniques, energy aware, queue aware and QoS aware scheduling, which are classified in [18]. As discussed in this section, the main challenge designing RRM algorithms for RN extended systems is that an optimal solution requires prohibitively exhaustive solution search, with complexity of  $O((MK)^N)$ , where M, K and N represent the number of RNs, BSs, and subchannels, respectively [55,93,94]. Therefore the unsolvable NP-hard problem is often divided in subproblems.

The details of the design of the hybrid RRM scheme and its decomposed sub-problems in this Thesis are described in Chapter 4.

## 2.5 Research problem

The goal of this work is to improve the overall performance of a half duplex relay extended OFDMA network, under consideration of the practical limitations of an downlink FDD network, by improving the RN backhaul capacity while protecting the performance of the MSs, directly served by MBSs. Omni-directional receive antenna at the RN for wireless backhauling with no LoS requirement are taken into account, which makes the relay even more attractive to deploy for an operator, as discussed in Section 2.2.4. The considered relay type is a non-transparent relay in half duplex and non cooperative mode, which makes the RN a separated small cell besides the existing MBS cells in the network. The RN has its own scheduling functionality and appears at the donor MBS as an MS. Furthermore, the RN has the ability to queue received data from its donor MBS. The serving station has suboptimal frequency selective channel knowledge based on user CQI feedback as defined in [95]. A user has exclusively orthogonal access to a subchannel within a cell (MBS/RN), which results in no intra cell interference, while full reuse one among cells is assumed. This introduces inter cell interference but provides full access to

the radio resources for each cell. The target of this contribution is to design a practical low complexity solution which aims to satisfy a combination of several research challenges identified during the past years, revisited in the previous sections. On the one hand in dense RN FDD networks the backhaul link is often identified as the bottleneck for the downlink [96]. Therefore it is investigated if it is possible by an adapted transmission power pattern to improve the backhaul link spectral efficiency without losing macro user performance and introducing additional non-practical high amount of periodic implicit feedback. On the other hand fairness needs to be obtained as well as queue awareness and energy efficiency needs to be considered. Therefore the proposed practical low complexity solution with frequency selective co-scheduling functionality results in the design of an hierarchical RRM scheme, which consists of a decentralized cell selection scheme, an asynchronous network-centralized as well as a synchronous macro cell-centralized part. It aims to reduce the interference and used energy for the transmission in the downlink shared channel, while improving the wireless backhaul capacity under fairness and overhead constraints, and therefore resulting in an improved overall user throughput.

To the best of our knowledge no solution could be found, which combines an improvement of multiple objectives in terms of fairness, increased capacity, less energy consumption as well as interference mitigation under affordable amount of CQI feedback in an efficient manner. Furthermore, practical limitations such as feedback and processing delay, channel estimation errors, limited channel feedback, non-ideal wireless backhaul assumptions are assumed. Therefore, a practical combined solution is investigated in this work based on comprehensive calibrated SLS for large scale OFDMA networks, introduced to the reader in the upcoming Chapter.

# Chapter 3

## Methodology

To evaluate the behaviour and influence of a technology, such as the design of a hybrid radio resource management (RRM) scheme, basically three options are available.

First, a field trial can be carried out, based on prototypical hardware implementation, with predefined test cases to derive the difference between the system with and without the enhanced technology. Second, an analytical model can be mathematically defined and the influence of the novel algorithm can be identified. Third, computer based simulations can be used to evaluate a large scale network. Specially when it comes to considering effects such as inter cell interference system level simulations are an excellent choice to analyse the considered technique in a large scale network with low cost compared to a field trial. Compared to an analytical model, which would be very difficult to apply, considering the total complexity of a full mobile network, system level simulations will be the method of choice in this work due to the excellent trade off between complexity and costs, compared to the other opportunities.

Based on Table 4.1 in [97], useful simulation tools to analyse a mobile communication network are classified in four groups. Depending on the focus of the desired investigation, different models need to be used to find a reasonable trade off between accuracy and computational complexity. Protocol level simulations (Class I) focus on larger time scales (in the order of tens of seconds to minutes) and typically evaluate higher layer protocols (e.g. IP or Transmission Control Protocol (TCP)). Therefore, lower layer aspects are simplified to be able to reach the target result (e.g. frequency flat radio channels). Class II simulation tools are defined as dynamic system level simulators (SLS) and typically focus on mobility procedures, such as hand over techniques. Here, the required real time for accurate evaluation is in the order of seconds. Thus, simplifications are needed on PHY

and MAC layer to simulate the time frames necessary for the mobility procedures. Link Level Simulation (LLS) focus on the precise modelling of the air interface and thus, on one single link, e.g. between a BS and an MS. Here, typically the real time requirement is in the order of several tens to hundreds of milliseconds. Due to the detailed modelling of PHY layer procedures, such as modulation and coding, typically inter cell interference or MAC scheduling aspects are simplified to lower the complexity. To simulate a large scale mobile network with detailed assumptions on the radio channel and MAC scheduling a Class III simulator is used throughout this work. Class III simulations typically use simplifications on link level, e.g. modulation and coding are not simulated but link level results are taken from look up tables. Class III SLS use detailed radio channel and resource allocation models and consider large scale networks with multiple BSs and MSs. The real time requirement typically lies in the range of hundreds of milliseconds to end up in statistically converged results. Further useful information about such types of simulators can be found in [34]. In the following Sections, the computer simulation tool used and extended in this Thesis are described in detail.

The Chapter is organized as follows: First, used models of the DT SLS are described, followed by the defined KPIs to analyse the results. Then, the DT SLS is calibrated to verify it as a comparable tool within the 3GPP simulation framework. Afterwords, the extensions done throughout this Thesis are described and analyzed to introduce layer 3 in-band FDD half-duplex RNs. Based on that, the proposed RRM algorithm is defined and evaluated in Chapters 4 and 5.

### **3.1 System level simulation processing chain**

The simulation tool enhanced throughout this Thesis is a MATLAB based modular designed Class III LTE-A system level simulator, developed at Deutsche Telekom (DT) premises, further referred as Deutsche Telekom System Level Simulator (DT SLS). It follows the agreed SLS assumptions in 3GPP and is therefore calibrated to provide comparable, trustworthy results, as presented in detail in Section 3.6. A block diagram of the main functionalities is depicted in Figure 3.1. Each block can be configured separately with different models, based on the defined objective. For instance, the scheduler update block can be defined as a RR or a PF scheduler. The SINR calculation can be configured based on a simplified wideband AWGN channel based approximation or as a detailed multipath channel model considering subcarrier based calculations for various transmis-

sion modes, such as beamforming or spatial multiplexing. The DT SLS was extended for RN aided LTE-A networks in this work, to implement the RRM scheme. In the upcoming sections, an overview on the program blocks is given, where the most relevant methods are summarized and discussed.

In general, the DT SLS runs through an inner and an outer loop, defined as snapshot and scenario loop, as illustrated in Figure 3.1. In the scenario loop a drop of multiple MSs as well as the network layout is calculated. In principle any network layout can be defined for that purpose. To provide comparable results, typically standardized scenarios are used for e.g. urban, sub-urban or rural scenarios. Based on the chosen network layout and environment, the so called large scale parameters, such as Shadow Fading (SF), LoS probability or path loss are calculated. Once the total environment is determined, the scenario is simulated for several hundreds of milliseconds within the snapshot loop. This represents the real time the considered network is analysed. Within one snapshot loop, e.g. the TTI based scheduling decisions, channel feedback and channel updates are calculated. Due to multiple drops of MSs in the same network layout (scenario) and updated statistically created physical layer properties, such as e.g. the SF of the mobile network, a statistical validity is reached after a certain amount of scenarios and snapshots. The results converge when statistical certainty is provided. Based on Figure 3.1 the modules are described in greater detail in the following.

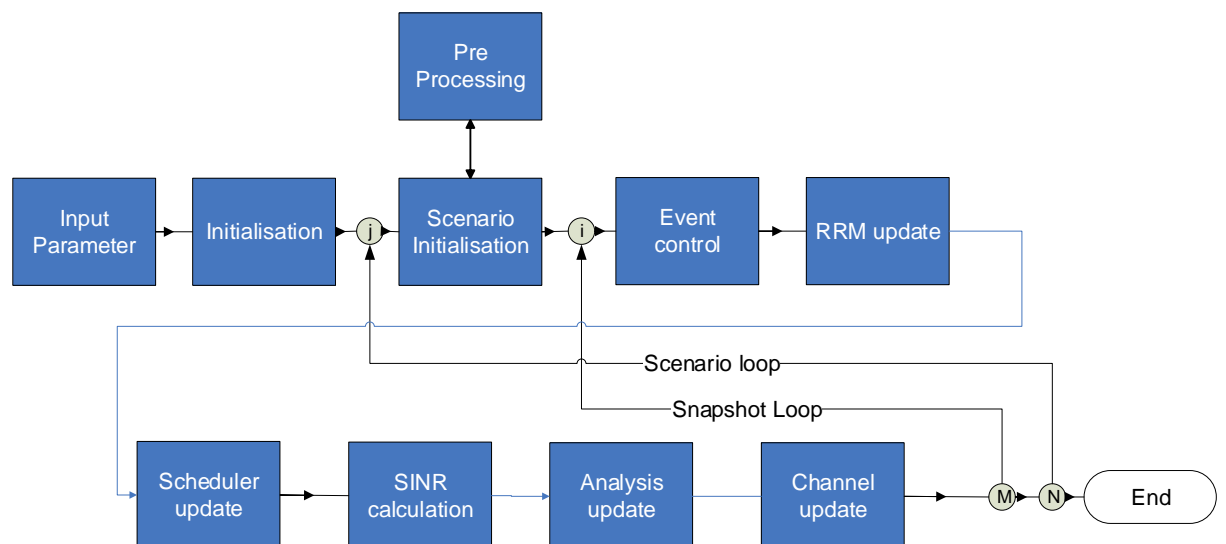


Figure 3.1: DT System Level Simulator Block Diagram

### 3.1.1 Input parameter

Within the input parameter block a large set of necessary default parameters, constants and flags are configured. At first the physical layer values are defined, such as the carrier frequency, the system bandwidth, subcarrier spacing or the number of subcarrier per resource block, to name only a view of them. Then all the relevant parameters for the BS and the MS are set, e.g. the used antenna pattern, the antenna height, the receiver type, etc. In addition all functionalities of the considered modules are defined. As an example, the used RRM method or the used transmission modes are determined.

### 3.1.2 Initialization

During the initialization phase, the defined input parameters, such as procedures, physical parameters and system processes, the chosen network layout, used models and cell types, e.g. MBS and RN are configured. A standardized network layout typically consists of multiple hexagonal cells, usually of two rings, as depicted in Figure 3.2. Here, an urban scenario with a standardized Inter Site Distance (ISD) of 500 m is shown. For instance, the default macro cell configuration assumes three sectors operated per site. The bore-sight angles of the macro cells are fix at  $0^\circ$ ,  $120^\circ$  and  $240^\circ$ . Moreover, in order to simulate realistic interference conditions over the whole network environment, a so called wrap around technique is used to avoid border effects, at the outer ring. Therefore, the total simulation area is mirrored six times around itself to have proper interference conditions at the border, comparable to the centre area of the network layout. An illustration for that is shown in Figure 3.3, where the yellow coloured inner 57 sectors represent the analysed network, while the green cells are the wrapped around mirrored sites.

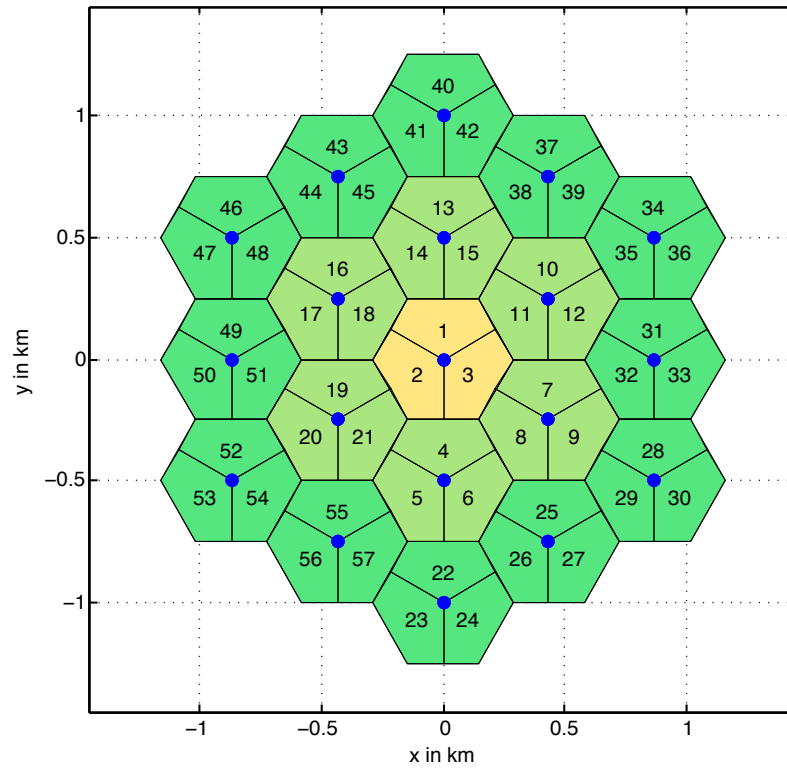


Figure 3.2: Standard network layout with two rings of MBS sites with three sectors

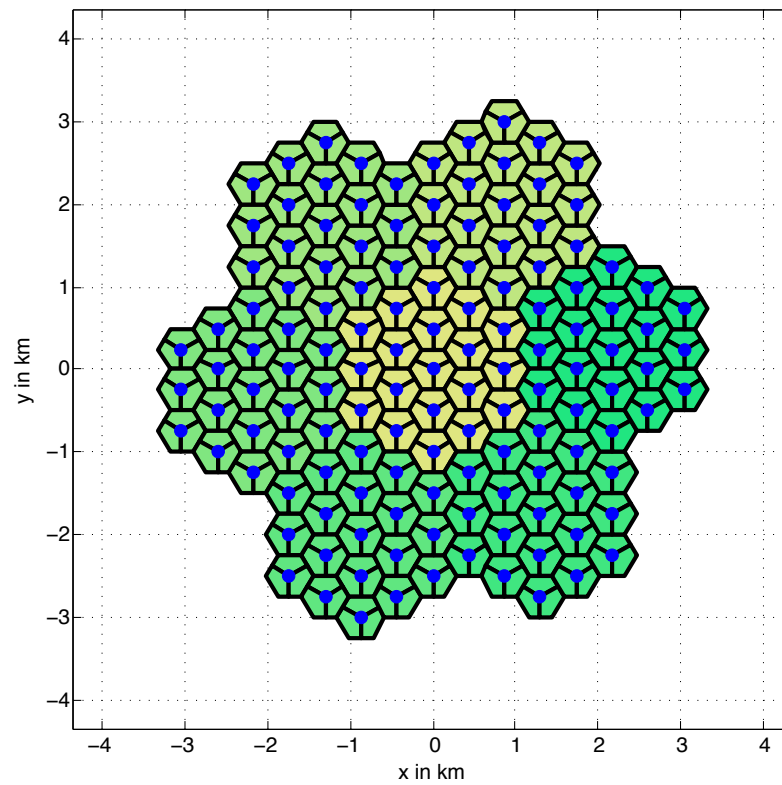


Figure 3.3: Wrap around technique to prevent border effects

This technique gives the advantage to evaluate a larger number of BSs at the same time with realistic interference conditions and thus a faster statistical convergence can be reached due to the higher number of statistical probes within each scenario run.

## **3.2 Scenario loop**

### **3.2.1 Pre-Processing**

The pre-processing module calculates a grid related propagation data set which includes all relevant large scale parameters to calculate the link budget for all link types between the defined network elements. At first, all link types are determined, e.g. macro base station to MS and/or macro base station to relay node and/or relay base station to MS. Then, all distances and angular relationships among each pixel of the grid for the horizontal and vertical dimension are calculated. After the calculation of the total geometrical relationships in the system the Large Scale Parameter (LSP) (SF, Delay Spread (DS), Angle of Arrival's Spread (ASA), Angle of Departure's Spread (ASD), K-factor (K)) based on the Table B.1.2.2.1-4 in [98] are determined. These parameters are then used by the frequency selective channel model which calculates the Impulse Response (IR) for all links, described in Section 3.2.2.5. As an example, the SF matrix is calculated based on a log normal distribution with a standard deviation of 6dB for non Line of Sight (nLoS) and 4dB for LoS, when the WINNER urban macro propagation model is applied. The SF is cross-correlated with the other defined LSP. In addition, it has a correlation distance of 30 meters for LoS and 40 meters for nLoS. Further detailed information can be found in [98,99]. After the propagation data per LSP is calculated the Path Loss (PL) among all pixels for all link types can be calculated.

### **3.2.2 Scenario initialization**

The scenario initialization defines the simulation conditions for at least one user drop (scenario). The initialization procedure takes care of the separated functionalities in the following sub modules.

#### **3.2.2.1 Locations of MSs and RNs**

With this module, small cells, such as RNs and MSs are dropped into the simulation area, based on the model which is used. There are different configurations, which can

be applied. The 3GPP defines typically four scenarios to evaluate small cell enhanced networks [98]. Either a small cell is dropped randomly into an MBS sector or it is located at the cell edges. MSs can either be dropped randomly with an average number per MBS sector or a defined percentage of MSs are dropped into so called user hot zones with a specified radius of 40m. For the latter case, small cells can be dropped either in the vicinity of the hot zones or randomly. Figure 3.4 shows an example scenario where two RNs are dropped randomly into each MBS sector. Figure 3.5 illustrates the MS distribution based on configuration 4b defined in [98]. While in average 30 MS per cell are dropped, 2/3 of them are located in a user hot zone within a radius of 40 meters in an urban environment (500m ISD) The hot zone is correlated to the location of the small cells.

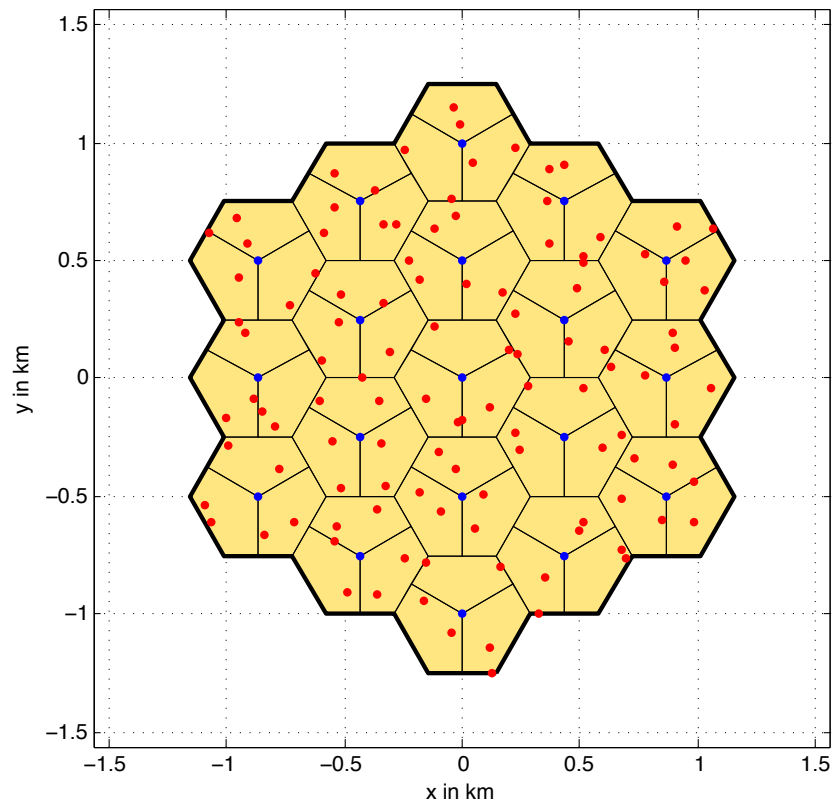


Figure 3.4: Two randomly distributed relays per sector

### 3.2.2.2 MS movement

The MS movement can be defined either as quasi static (static MS position but a certain velocity is assumed to calculate the radio channel variations) or as dynamic for different flavoured e.g. mobility related research topics. Since the focus of this Thesis is to improve the system capacity and thus, detailed modelling of the radio channel is necessary, in the

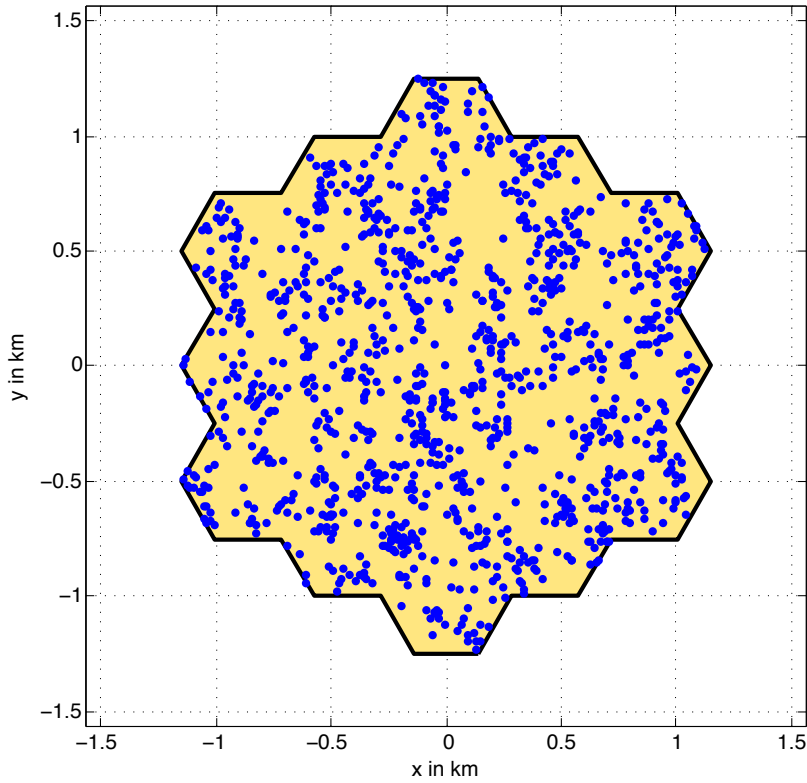


Figure 3.5: 1/3 randomly dropped, 2/3 user hot zone distribution

following a quasi static simulation is assumed, to find a trade-off between complexity and relevant aspects for the investigation.

### 3.2.2.3 Traffic model

The work presented in this Thesis aims to improve the system capacity and thus, the supportable link data rates. This is best evaluated with a fully loaded system, which represents a worst case scenario in a multi cell environment. The used full buffer model assumes an infinite amount of data for MSs coming from the core network. Since all PRBs of the system are always allocated at the MBSs, the total available system bandwidth is always used on the one hand, on the other hand worst case interference situations are considered. It has to be kept in mind, that throughout this work the considered RNs support buffers for the two hop MSs to serve. Therefore, not all PRBs at the RNs might be allocated at all times, dependent on the dBSSs scheduling decisions.

### 3.2.2.4 Radio propagation model

The propagation conditions, which are calculated on a grid raster as explained in Section 3.2.1, are assigned to the existing geometrical links, after the MS drop and the small cell

drop has been done, as described in Section 3.2.2.1. For instance, a macro BS-MS link can have an urban macro propagation condition, while a RN-MS link is influenced by urban micro properties. Here, the distance-dependent pathloss models are used, with a certain LoS probability. Based on the geometrical (distance, heights) relations and the large scale parameters (LSP), such as shadow fading (SF) and path loss (PL), the link budgets and thus, the received powers can be calculated based on Equation 3.1 for different purposes. For instance, it is used for the MS attachment procedure or the amount of power distributed over multiple rays in the radio channel model. The resulting average received power depends on different parameters summarized in Equation 3.1.

$$P_{RX} = P_{TX} + G_{TX} + G_{RX} - L_P - L_{FF} - L_{SF} + L_{TX} + L_{RX}, \text{ where} \quad (3.1)$$

$$P_{RX} = \text{received power [dBm]}$$

$$P_{TX} = \text{transmit power [dBm]}$$

$$G_{TX} = \text{transmitter antenna gain [dBi]}$$

$$G_{RX} = \text{receiver antenna gain [dBi]}$$

$$L_P = \text{path loss [dB]}$$

$$L_{FF} = \text{fast fading margin [dB]}$$

$$L_{SF} = \text{shadow fading loss [dB]}$$

$$L_{TX} = \text{transmitter feeder loss [dB]}$$

$$L_{RX} = \text{receiver feeder loss [dB]}$$

Based on the linear values of the link budgets of all existing links in the network a wide-band SINR, also referred as User Geometry (UG), can be calculated for each MS  $n$  in the considered scenario, based on Equation 3.2. The serving link  $s$  is divided by the sum of the interfering received powers  $i$  plus a typical noise floor  $N$  with the thermal noise density of -174 dBm/Hz.

$$UG(n) = 10 \log_{10} \left( \frac{P_{RX,s}}{\sum_{i=1}^I P_{RX,i} + N} \right) \quad (3.2)$$

Figure 3.6 shows an example of the UG of each pixel for an urban macro BS scenario. The cell edge areas are depicted in green and yellow in a UG region between approximately -5 and 5 dB. Below -5 dB regions turn into red colour, while the best UG conditions around 20 dB can be observed in the main lobes of each sector in purple. This example

also illustrates the possible UGs in a RN extended network, but only during the backhaul transmission times, when the RNs are in receiving mode.

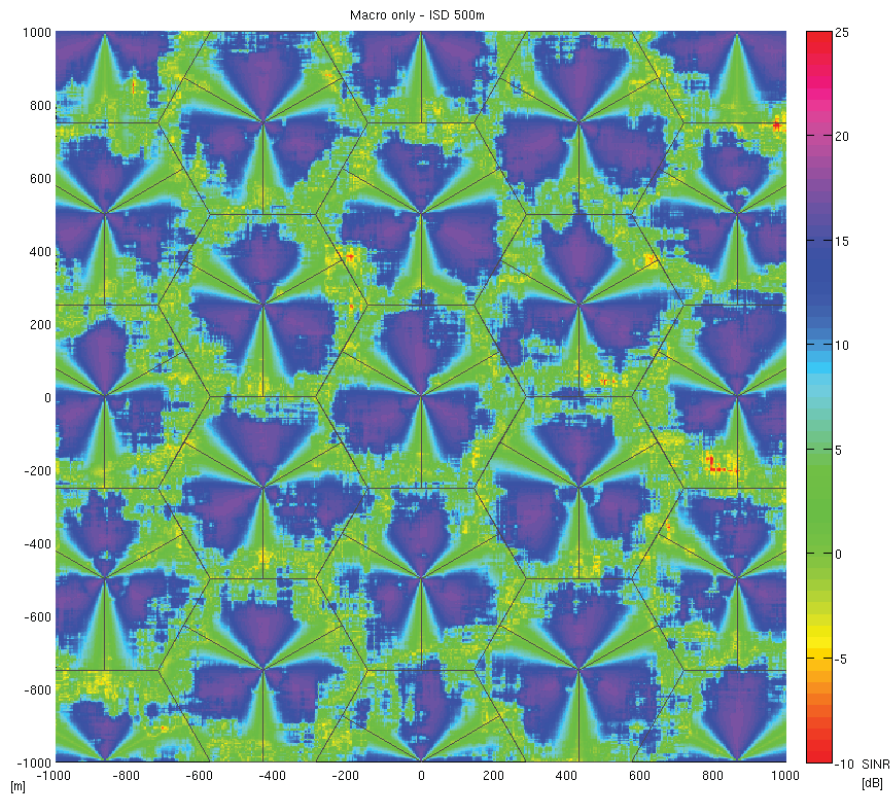


Figure 3.6: User Geometry for an MBS/RN Scenario during RN receiving mode

In Figure 3.7 an example of an access link TTI, where the RNs are in sending mode is illustrated, with one randomly dropped RN per sector. An increased UG can be observed within the vicinity of the RNs (above 20dB). However dependent on the location of the RN, larger cell edge regions can be observed. The figure also explains the challenge introducing inband RNs for capacity improvements. The regions in which the BL quality is the best (blue to purple areas), also interfere the RN access link the most.

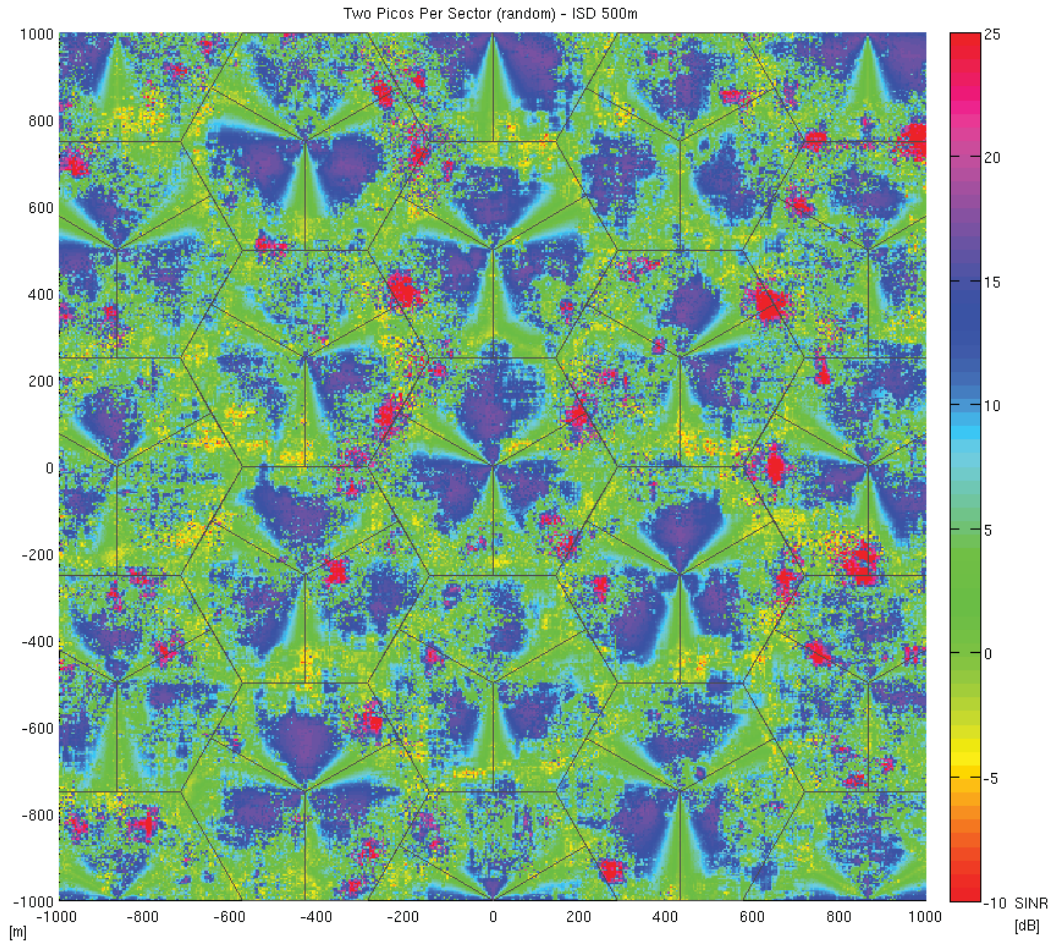


Figure 3.7: User Geometry for a MBS/RN Scenario during RN sending mode

### 3.2.2.5 Radio channel model

The initial impulse responses (IR)s for the fast fading channel realization are calculated based on the recommended statistical multipath frequency selective, time variant channel model in [100] and further specified in [98] and [101]. Basically, the received signal of an MS consists of a defined number of time delayed multipath components plus a possible LoS path. Each path consists of a cluster of subpaths, defined with certain powers and delays, based on a fraction of the average received power and the delay spread of the signal. For this purpose the Small Scale Parameter (SSP) of the channel are determined using the pre-processing outcome. After the initialization is done a parameter set with the channel coefficients is calculated based on the agreed statistical assumptions, e.g. the Angle of Arrival (AoA)s, and thus the delays of subpaths. The sum of all rays at the destination builds the IR. After the IR is successfully calculated for all possible links the channel transfer function is determined by an Fast Fourier Transformation (FFT) of each link. To provide a good balance between accuracy and computational complexity,

typically not all subcarriers are calculated within one PRB.

### **3.3 Snapshot loop**

In the next step the snapshot loop is started after the scenario is finalized, as illustrated in Figure 3.1. Typically, a snapshot represents one TTI. During a snapshot, the final outcome of one iteration is the transmission of a transport block size of each scheduled MS or RN based on the best useful transmission scheme derived from the received CQI feedback. If the transmission is not successful the HARQ retransmission procedure gets active for upcoming snapshots. A detailed description can be found in Section 3.5.4.

#### **3.3.1 Event control**

Within this block any event can be triggered in a specific time instant if necessary. In this Thesis the event update block has been used to trigger the network-centralized subband power allocation calculation, further described in detail in Section 4.3.

#### **3.3.2 RRM update**

This block is subdivided in two main functionalities of the RRM. The first part is responsible for the control of the applied reuse scheme. In the default configuration all BSs in the system have access to all PRBs which is known as a frequency reuse of one. In the case of a network design where frequency reuse of e.g. three is used the neighbouring BSs will only use a subset of the available PRBs.

The second part controls the admission of MSs which send a registration request to a specific BS. Every MS has a prioritization list of BSs which is derived from e.g. the link budget calculation, explained before. If there is no specific rule defined, all requests are accepted by each BS. After the process is finalized the state information of each MS is updated. The state can be either inactive, admission request or active. The implemented alternative attachment procedures for RN extended networks as proposed in this Thesis can be used here, further described in Section 4.2.

#### **3.3.3 Scheduler update**

The scheduler block handles the adaptive resource allocation for each MS, RN assigned to a dMBS and RN, respectively.

HARQ feedback handling: In the beginning of the process it has to be determined if any new HARQ feedback is available for any MS at the current BS. Therefore, the current HARQ processes have to be checked (a maximum of eight parallel processes for one MS) whether there is a feedback received or not. Based on the information of the retransmission feedback (Acknowledgement (ACK) or Negative Acknowledgement (NACK)), the scheduler is able to occupy the needed PRBs for all retransmissions which have to be done in the current TTI.

CQI feedback handling: After updating the HARQ processes at the BS the next step is to check, if new CQI feedback of any MS, RN is available. Basically, the report consists of multiple subband reports, including three indices. An index for the recommended MCS, a Precoding Matrix Indicator (PMI) (codebook based precoding index to either amplify the serving signal or suppress the interference) and a Rank Indicator (RI) (number of useful data streams) is given. The definition of the CSI and CQI feedback is described more precisely in Section 3.3.4.2. In case of the CSI feedback information the BS receives quantized channel transfer functions of the serving and the interfering links. Since, one of the major targets of the Thesis is to design a low complexity RRM scheme, the CSI feedback is out of scope in this work, which is typically used for more complex schemes such as CoMP [19], as also explained in Section 2.2.3.

Resource Allocation: After updating the HARQ processes and the channel feedback information the actual resource assignment process can be done based on the assumed metric. Considering the newest available CQI feedback a supportable rate for all assigned MSs on the left PRBs can be determined in a frequency selective manner. Once the scheduler has decided which PRBs belongs to the MSs, the transmission parameters need to be determined. Therefore the Mutual Information Effective SINR Mapping (MIESM) link adaptation interface is used to determine a single MCS for an MS specific transmission, based on [99] and also explained in the Section 3.3.4.1.

A detailed description of the necessary enhancements for RN extended networks is described in Section 3.5.

### **3.3.4 SINR calculation**

In the beginning, a sample rate is defined for how many sub-carriers the SINR value per scheduled PRB should be calculated. Based on these values an effective SINR is determined for the transmission. The samples are used to reduce the computation effort to

derive the effective SINR for all users on each PRB but still to model frequency selectivity within a single PRB. At first, the total received power is equally distributed among the number of sub-carriers of a PRB. Then the channel transfer functions are calculated by an FFT for the serving link and the interfering links. Based on the calculated channel transfer functions and the percentage of the total power of the scheduled PRBs an effective channel data matrix is calculated where the normalized channel data is weighted with the distributed powers. By using this effective channel data matrix, inter cell interference covariance matrices are calculated including the channel coefficients for a defined number of dominant interfering BSs on all antenna ports for each and every link. To reduce the computational effort, typically only for the most dominant interferers the multipath fast fading is taken into account. The non-dominant interferers are assumed as spatially white and only their average interfering power per PRB is considered. To complete the calculation of the SINR the current pre-coder which is used based on the given feedback information considered by the scheduler, has to be taken into account. Finally an additional degradation of the calculated SINR is done due to represent a channel estimation error and the receiver noise floor. The degradation is derived out of LLS results.

Based on the calculated SINR values of the sampled subcarriers for the MS specific PRBs it has to be determined whether the transmission has been successful or not. Therefore an error probability is derived, with the MIESM interface explained in the following.

#### **3.3.4.1 Link to system mapping**

The MIESM interface is used to determine an effective SINR which is calculated based on the multiple SINR values per scheduled PRB per user, as well as the Block Error Rate (BLER) probability of the transmission. It is also used to define the used MCS for transmission at the scheduler. In principle, it finds a trade-off between BLER probability and transmission efficiency. At first based on the multiple SINR values the corresponding mutual informations are determined weighted and averaged. With the weighted average value and the known MCS which is used during the transmission, the BLER probability can be obtained from LLS results used as look-up tables. After the BLER probability is determined it can be calculated whether the transmission was successful or not. Therefore a random value between 0 and 1 is set. If the random value is greater than the BLER probability the transmission of the transport block size of the MS is declared as successful. With this information, the HARQ status can be updated and the HARQ feedback can be

either set to ACK or NACK.

#### **3.3.4.2 CQI feedback generation**

In the next step the CQI feedbacks for the configured sub bands are generated. Therefore, a brute force calculation is performed where all the possible combinations regarding the available transmission schemes are calculated based on maximum SINR per subband. If this is done the MCS with the maximum reachable throughput for each MS is chosen to generate the feedback. To determine the maximum available throughput an exhaustive search is done which decides on the MCS to use. All available pre-coding matrices have to be iteratively tested for each transmission scheme. In summary a comparison is done between all available pre-coders for each transmission scheme, on each possible stream for all BSs and the corresponding MSs. After this complex process the best possible CQI report is created and a First Input First Output (FIFO) feedback buffer is updated. In addition a feedback activation time is set including a defined offset, which represents the feedback and processing delay. The default value is set to 5 ms. Out of that, the CQI feedback update module, which is performed by the scheduler at the BSs, can use the newly created feedback five ms later.

Again, for the RN-extended networks it is necessary to update the module to react on the flavour of the half duplex transmission. Details are explained in Section 3.5.

#### **3.3.5 Analysis update**

This module records statistics of the KPIs and other interesting parameters during the simulation run. This needs to be done for different user groups, e.g. the MSs attached to the RNs.

#### **3.3.6 Channel update**

This module updates the radio channel transfer functions by considering the assumed velocity of the MSs. Within the considered scenarios typically a speed of 3 kmph is assumed, since pedestrian or nomadic user are considered.

### 3.4 Definition of the key performance indicators

To evaluate the behaviour of the simulation procedure different KPIs are defined by the 3GPP, where each of them represent a part of the simulation chain. Since a large set of parameters influence the simulation results, the described indicators show on the one hand the influence of the configured modules, such as the used scheduler, the SINR calculation or the link to system mapping, etc. On the other hand the influence of the applied models, e.g. antenna diagrams, propagation properties, fast fading channel models, etc. can be analyzed and compared for calibration purposes. Most of the results are presented as CDFs. A CDF represents the cumulative occurrence probability of a value for a specific KPI. In other words, it describes if a certain value of the abscissa has an occurrence probability of the corresponding value on the ordinate or less. For instance, in Figure 3.8 an example MS throughput simulation result is illustrated. Typically, the 5 percentile, the 50 percentile, the 95 percentile and the average value, which is approximately in the region of the 60 percentile, are used to evaluate the result. Usually, the 5 percentile represents the cell edge user performance, while the 95 percentile shows users with excellent conditions.

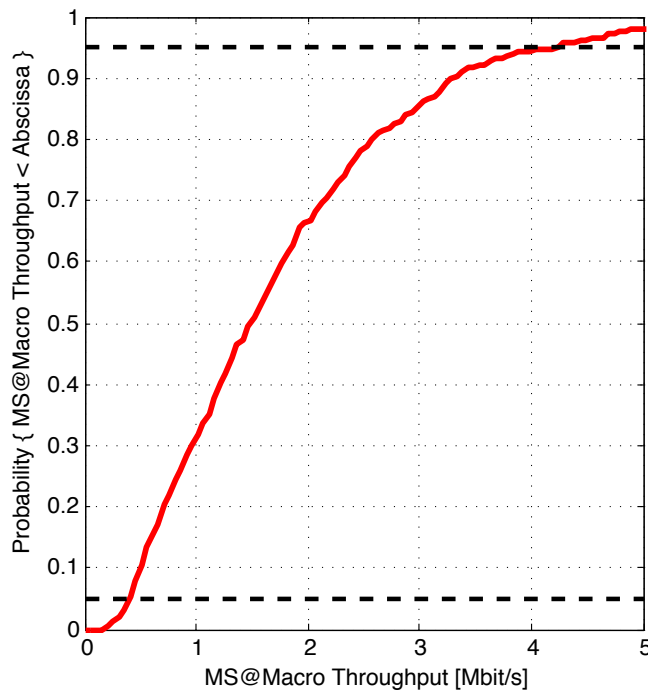


Figure 3.8: Exemplary CDF of the user throughput assigned to MBSs

### 3.4.1 User Geometry (wideband SINR)

As already explained, the UG is defined as the average wideband SINR based on the average received power levels for every MS in the system, as already defined in Equation 3.2. This parameter helps to understand the relations in the scenario, based on the LSP and without influence of the scheduler or the channel model. It represents the influence of all parameters which are used to calculate the link budget as well as geometrical relationships, such as transmission powers, propagation and antenna models, etc. The RN and user distribution influences the result of the UG, since statistical probes are collected based on the positions.

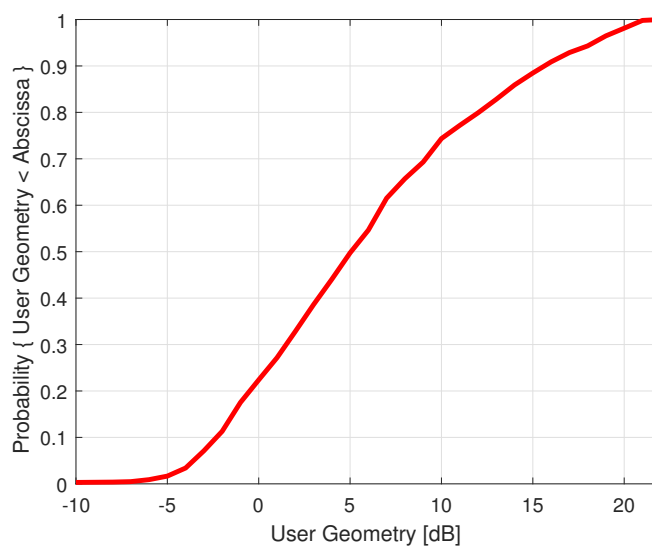


Figure 3.9: Example CDF of the UG assigned to MBSs

### 3.4.2 SINR calculation

The SINR CDF is calculated based on the distribution function of all subcarrier based SINR values that are calculated during the whole simulation run. It gives additional information about the interference behaviour including the influence of the scheduler, the multipath channel model as well as the used transmission schemes and receivers.

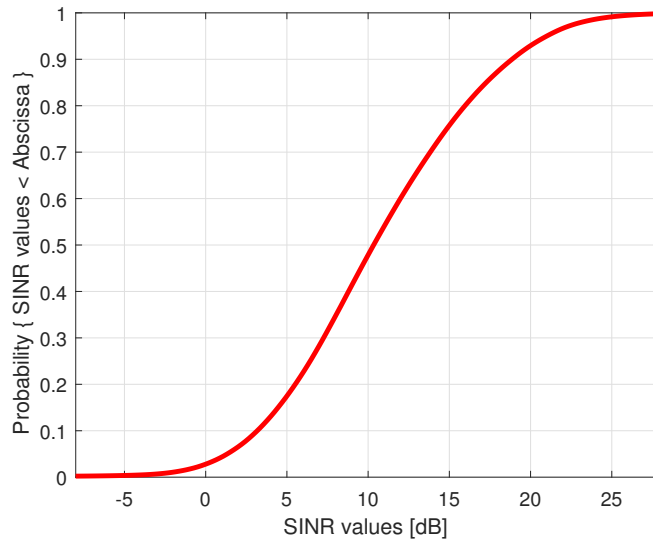


Figure 3.10: Example CDF of the SINR assigned to MBSs

### 3.4.3 Fairness (Normalized user throughput)

The fairness behaviour of schedulers can be monitored by plotting the user throughput CDF as a function of the user throughput normalized to the average. According to the fairness criteria in [102] the dashed blue line in Figure 3.11 defines the level of fairness which has to be fulfilled. It sets the boundary line between the allowed and the not allowed region of the fairness diagram. The boundary line can be read as the following. With a probability of 100% a user in the system will get the average user throughput or less. At least, with a probability of 50% it will get half of the average throughput or less, and so on. In addition the result (black line) of the normalized users throughput is shown. The CDF has to be on the right of the dashed blue line in every case in order to fulfil the fairness criteria. In the example the scheduler works in a fair manner. The result can be interpreted as the following. For instance, with approximately 62% probability a user gets the average throughput of the system or less. In theory a step function would be the fairest case since all appearing users would experience the same throughput. However, as explained in Section 2.3.7 a feasible result should be always a trade-off between fairness and maximum resource utilization.

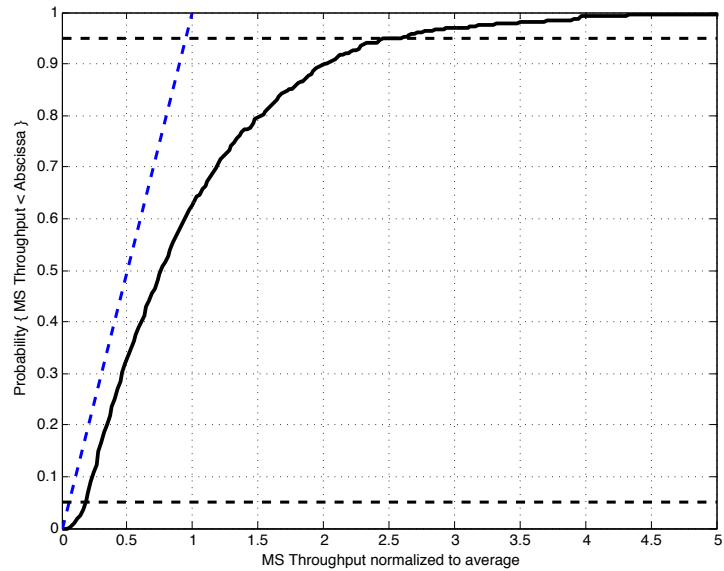


Figure 3.11: Example CDF for the normalized MS throughput representing fairness of the network

### 3.4.4 User throughput

The user throughput CDF of all MSs located in the network is presented here. It includes all processes in the simulation chain and thus, it is the major KPI giving the information about the final performance of the system. For the RN extended networks it is interesting to separate between different user groups, such as macro and relay users or a relay as receiver for the presented KPIs. An example for the relevant user groups is given in Figure 3.12. While the blue curve represents the overall user throughput, the green curve illustrates the performance of the MSs attached to the RNs. The red curve shows the throughput for the MSs attached to the MBSs, while the black curve shows the data rates reached by the wireless backhaul transmission. In this example the MBS MSs experience much higher throughputs than the two-hop MSs. The overall blue curve is basically the weight sum of the green and red curves. For the further detailed analysis of the results presented in this work, the reader is referred to Section 5.

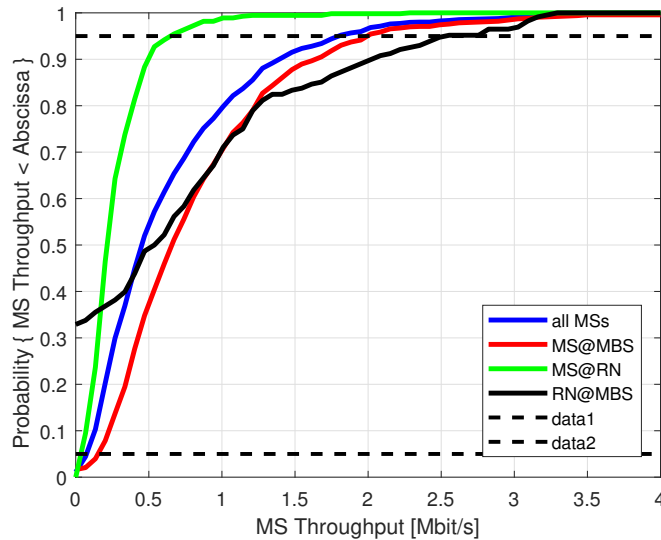


Figure 3.12: Example CDF for the MS / RN throughput separated in different user groups

### 3.5 Implementation of relay nodes

To enable the simulation of a relay extended network additional implementations were necessary, which are summarized as follows. An excellent summary of related simulation results and updated channel and propagation models which are implemented and used throughout this work can be found in [29].

#### 3.5.1 Site planning approach

Based on [98], a simplified abstraction is implemented to encourage the advantage of a possible site planning of the RNs. There are two ways to consider a site planning gain within the SLS. The first rather simple approach is just to add an additional gain of 5dB on the link budget of each dropped RN to its serving dMBS. The second alternative makes use of the possibility to define five randomly chosen additional virtual positions in the surrounding area of the physical location. Then the possible locations are compared with each other and the location with the best wideband SINR is chosen as the final position during the simulation. This improves the link budget to the serving dMBS and decreases the possibility of a nLoS connection. The virtual positioning approach can be seen in Figure 3.13. The results of a comparison of both approaches are summarized in Table 3.1.

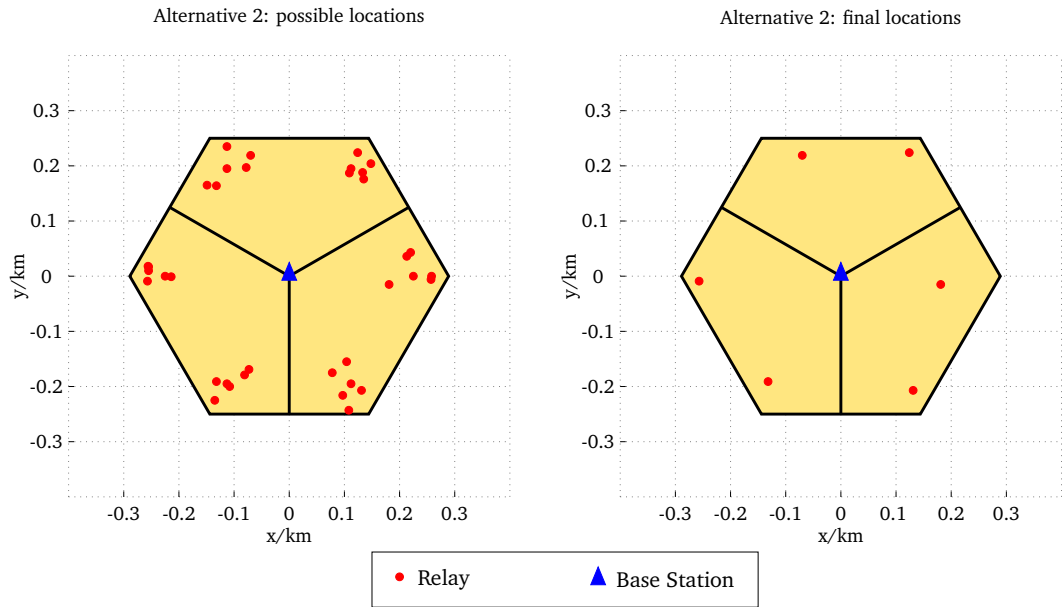


Figure 3.13: Virtual Positioning of RNs

	average wideband SINR [dB]					
	RN1	RN2	RN3	RN4	RN5	RN6
Alternative 1	14.34	14.70	14.92	14.92	14.70	14.34
Alternative 2	16.01	14.70	15.46	15.46	15.62	14.99

Table 3.1: Relay planning gain: A comparison of two alternatives

As can be observed the alternative 2 results in a more optimistic wideband SINR for the backhaul than alternative 1.

However, it turned out to disable the proposed planning gain methods for this work because of the reasons, discussed in Section 2.2.4. The reader has to keep in mind potential cost savings and a higher degree of freedom choosing the site of a single RN in a real network, when worst case situations for the wireless backhaul are assumed. Finally, the quality of the backhaul link is improved based on the hybrid RRM scheme proposed in this Thesis.

### 3.5.2 Different link types

According to [103], where the propagation and channel model parameters are defined for different simulation environments, an extension was done to introduce multiple link types within one simulation. As previously presented in Figure 2.14, in RN-extended networks three different link types are considered. The first is the common MBS to MS (AL) link which uses, e.g. the urban macro propagation model and the corresponding channel model parameters. The second link type is the MBS to RN backhaul link (BL),

which may use an adapted urban macro propagation model with a higher LoS probability and adapted channel model parameters. The third link type is the one between the RN and the MS (AL). This is defined as an urban micro characterized link.

### 3.5.3 MBSFN subframe configuration

As previously discussed in Section 2.2.1 the 3GPP has defined in [21] the usage of the MBSFN subframe for RN reception in the downlink to avoid self interference problems at the RN. As discussed, the principle design of such an MBSFN subframe is shown in Figure 2.11. The MBSFN subframe cannot be used in subframe 0, 4, 5 and 9 of a transmission frame, since system relevant information is broadcasted within these subframes. The used MBSFN subframe pattern can be updated with a periodicity of 40ms defined by the PBCH. In general, for each RN the defined number of used MBSFN subframes can be different based on the actual data which have to be forwarded to the served MSs. Figure 3.2 gives an example of a pattern with the maximum usable MBSFN subframe configuration. In Table 3.3 an example use of possible MBSFN subframe patterns is shown. In the example RN1 is switching into reception mode in two MBSFN patterns (a and b) and a second RN2 is using the pattern (e and g). It has to be mentioned that the dynamic of the interference scenario which will occur in the simulation is heavily dependent on the number of used MBSFN subframes and whether they are used in asynchronous or in synchronous mode within the system.

Frame/Subframe	0	1	2	3	4	5	6	7	8	9
1	X	a	b	c	X	X	d	e	f	X
2	X	c	g	h	X	X	f	a	b	X
3	X	h	d	e	X	X	b	c	g	X
4	X	e	f	a	X	X	g	h	d	X
5	X	a	b	c	X	X	d	e	f	X
6	X		g	h	X	X				X

Table 3.2: MBSFN subframe patterns (from a to h) and their periodicity

### 3.5.4 Channel feedback delay and HARQ timing

Typically, in a conventional macro BS network, periodic CQI feedback is assumed with a widely used assumption of the 5ms periodicity. This is an acceptable trade-off between feedback overhead and accurate channel information. In addition, it is necessary to consider a certain feedback delay, which consists of the feedback transmission time  $d_f$  as well

Frame/Subframe	0	1	2	3	4	5	6	7	8	9
1	X	R1	R1		X	X		R2		X
2	X		R2		X	X		R1	R1	X
3	X			R2	X	X	R1		R2	X
4	X	R2		R1	X	X	R2			X
5	X	R1	R1		X	X		R2	R2	X
6	X			R2	X	X	R2	R1	R1	X

Table 3.3: An example of an MBSFN assignment for 2 RNs

as the processing time  $d_p$  at the BS until the feedback information is ready to be used by the scheduler. Typically, an overall feedback delay of 6ms is assumed. Figure 3.14 shows both periodicities. While the red arrows indicate the periodic transmission of the report itself, the black arrows show the assumed feedback delay. In general the feedback delay consists of the delay to measure, transmit and process the information at the BS. Feedback delays are often assumed to be in the range of 5 - 10ms [20]. Here, a widely used value is 6ms. Figure 3.14 shows the feedback transmission for the RN wireless backhaul link. It can only be transmitted when the RN is in the sending mode. In this example the maximum number of MBSFN subframes (6 per frame) is assumed. It can be concluded that no changes have to be made to model the wireless backhaul feedback transmission.

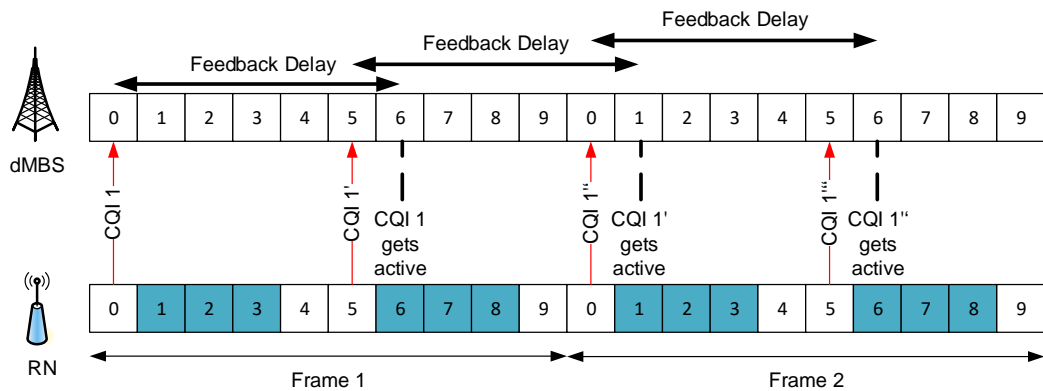


Figure 3.14: CQI Feedback for wireless backhaul

Figure 3.15 shows a necessary SLS extension to support frequency selective two hop proportional fair scheduling at the dMBS.

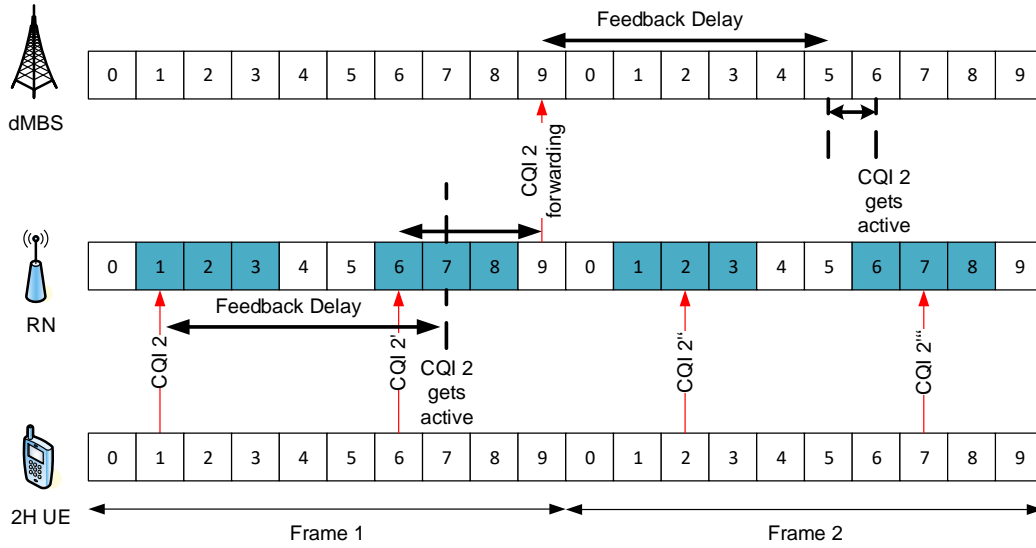


Figure 3.15: Additional Delay caused by CQI Feedback Forwarding for the RN Access Link

As illustrated, the two hop MS reports the information during RN receiving TTIs, again with a periodicity of 5ms and a delay of 6ms. When the feedback is ready to be applied the RN is still in the receiving mode and is not able to forward the AL report to the corresponding dMBS. It has to wait until it is again in sending mode, e.g. in TTI 9 within the first depicted frame. This means it has to wait  $M$  TTIs of upcoming MBSFN subframes until the information can be forwarded. In the example, this effect causes an additional delay  $d_{mbsfn,RN}$  of 2ms. Furthermore, the feedback delay of the forwarding process has to be taken into account as well. When the report is ready to be applied at the dMBS, the RN is in sending mode and cannot be scheduled. Therefore, it needs to be waited until the RN switches again to reception mode, which means the number of TTIs  $N$  until the next MBSFN subframe occurs. Based on that an additional delay  $d_{mbsfn,dMBS}$  of 1ms has to be taken into account in the example. Equation 3.3 defines the new delay budget model considering the necessary changes, which are applied in the simulations for this work.

$$d_{2H,cqi} = d_{f,RN} + d_{p,RN} + M \cdot d_{mbsfn,RN} + d_{f,dMBS} + d_{p,dMBS} + N \cdot d_{mbsfn,dMBS} \text{ in } [ms] \quad (3.3)$$

Furthermore, Figure 3.16 shows the necessary extension for MSs served by the dMBS. Since, the RNs in the network introduce additional interference in their sending TTIs, as also considered in Figure 4.1 and 4.2 the MSs served by the MBSs need to double the feedback generation (CQI1 and CQI2) to give the dMBS accurate information about the

different interference levels and thus, about the higher variations of occurring SINR in the network.

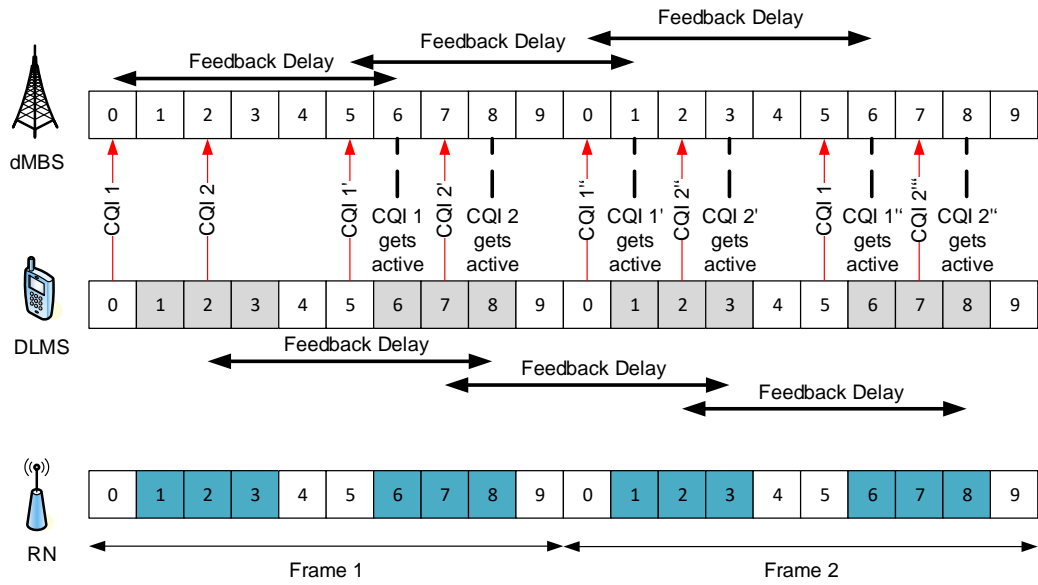


Figure 3.16: Additional CQI Feedback for DL MS

Considering the HARQ feedback delay it turned out that no adaptation of the commonly assumed feedback delay of 7ms is necessary, until the MBS and the RN can receive the ACK / NACK information. Due to the structure of the MBSFN subframe, which is used to set the RN to the reception mode, it is possible to send the HARQ feedback during the first OFDM symbol. An example is given in Figure 3.17. In the first step data is transmitted from the dMBS to the RN. 7ms later the RN is able to send the HARQ feedback, although an MBSFN subframe is configured and the RN therefore switches to the receiving mode. For the two hop MS, data is sent in subframe 4 and the feedback is reported when the RN is in the receiving mode.

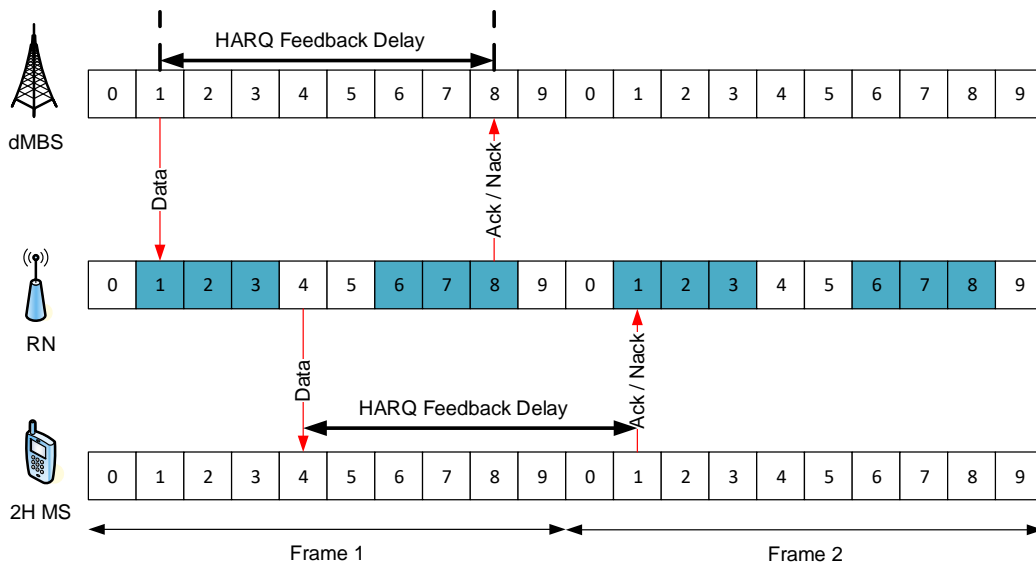


Figure 3.17: No adaptation of HARQ feedback delay necessary

### 3.5.5 Buffer structure for the two-hop transmission

Up to now a simplified traffic model is used where all users have the same demand level which is defined as infinite. This assumption leads to a full load situation at the BS because all resources are used in every TTI. Now, the RN has user specific finite buffers which keep the received data. The received data can then be distributed in different ways, such as in a round robin, fair or in a proportional fair fashion. For the considered RN type in this work, it is necessary to implement a user specific buffer structure at the RN, as depicted in Figure 2.19 in Section 2.3.5. Keep in mind that the dMBS co-schedules directly attached MSs and RNs in the RN backhaul TTIs. When the RN receives data from its dMBS, typically one large transport block will be used for transmission, since the RN appears as a MS. After the transport block is received, the RN needs to fill the MS specific buffers with the corresponding part of the received information.

As an example, Figure 3.18 gives an impression of the buffer extended RN system level simulation, which is implemented in this Thesis. The Figure shows 3 two hop MSs which have MS specific buffers at the RNs. If the data is received by the RN for the MS data is buffered until the RN switches to sending mode. During the sending mode of the relay nodes the buffer status is taken into account in the scheduling process. The RN transmission is limited by the amount of data which is buffered for the two hop MSs.

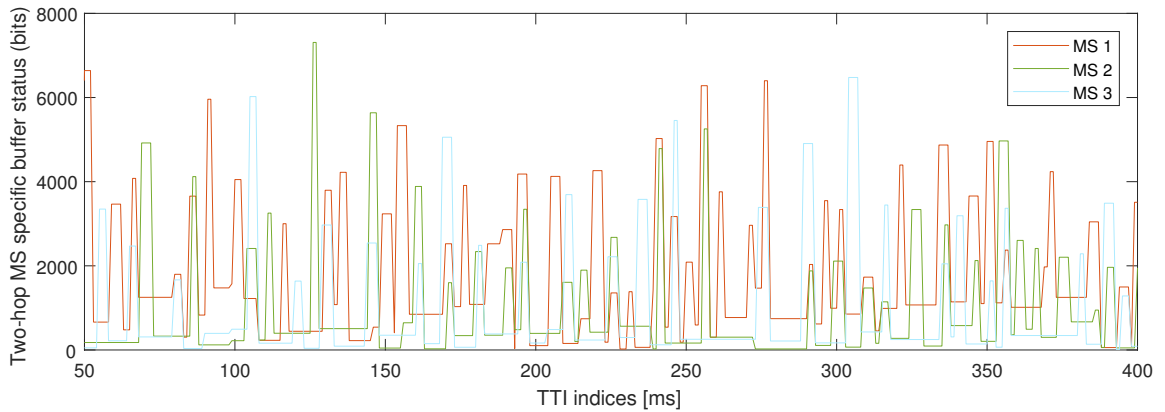


Figure 3.18: Principle two-hop MS specific buffer status

### 3.5.6 Scheduler for relay enhanced networks

Basically, the scheduler is extended to support the RN backhaul transmission and backhaul link co-scheduling functionality. In a first step the scheduler has to check whether the present TTI is an MBSFN subframe or not and has to proceed according to the current situation. The principle steps, how the scheduler works is summarized in the following. Further information can be found in Section 2.3.7 and 4.4.

#### 1. Principle scheduling procedure at the MBS.

- Select the MBS which executes the scheduler
- Update HARQ information
- Update CQI information (CQI and forwarded second hop CQI)
- Identify the MSs and RNs which are assigned to the considered dMBS
- Check whether the current TTI is defined as an MBSFN subframe for the RNs.
  - If yes, the RNs are in receiving mode and need to be considered as schedulable nodes.
  - If no, RNs are able to transmit data and the users attached to the MBS are scheduled exclusively
- Allocate resources for retransmissions
- Calculation of the current subband specific supportable rates based on available CQI information of one and two-hop MSs
- Calculation of the metric for each user on every PRB based on the used scheduler (e.g. two-hop proportional fair)

- Calculation of the TBS of each user, RN respectively
- Derive overall TBS for transmission to RNs
- Re-allocate available resources at the dMBS based on direct links and back-haul links CQI information under consideration of derived TBSs in the previous step (for further information the reader is referred to Section 4.4)
- Iterate for all dMBS

## 2. Principle procedure to schedule the two-hop users at the RN

- Update HARQ information
- Update CQI information
- Update user specific buffer
- Select the users with buffered data
- Allocate resources for retransmissions
- Calculation of the supportable rate based on AL CQI reports
- Calculation of the scheduling metric for each user
- Calculation of the TBS of each user under consideration of transmittable data limited by the buffer status
- Allocate resources
- Iterate for each RN

## 3.6 Calibration

The 3GPP provides a Simulation Framework for calibration purposes to make results comparable and trustworthy. Based on the assumptions, which are agreed and defined in [98] the Deutsche Telekom (DT) SLS has been calibrated as well. In the following, a comparison between the outcome of the DT SLS and results of the partner simulators, participated in the calibration activity is explained. The results of the 3GPP calibration activity can be found in [104].

Before the partners were able to compare the results, a general agreement has been taken on commonly used assumptions and settings. For instance, they agreed on propagation and channel models, common network layouts, as well as principle scheduling

strategies, physical layer parameters and so on. In Figure 3.19 the comparison of the user geometry of the different partners is illustrated. The maximum deviation does not exceed one dB which is a very good result.

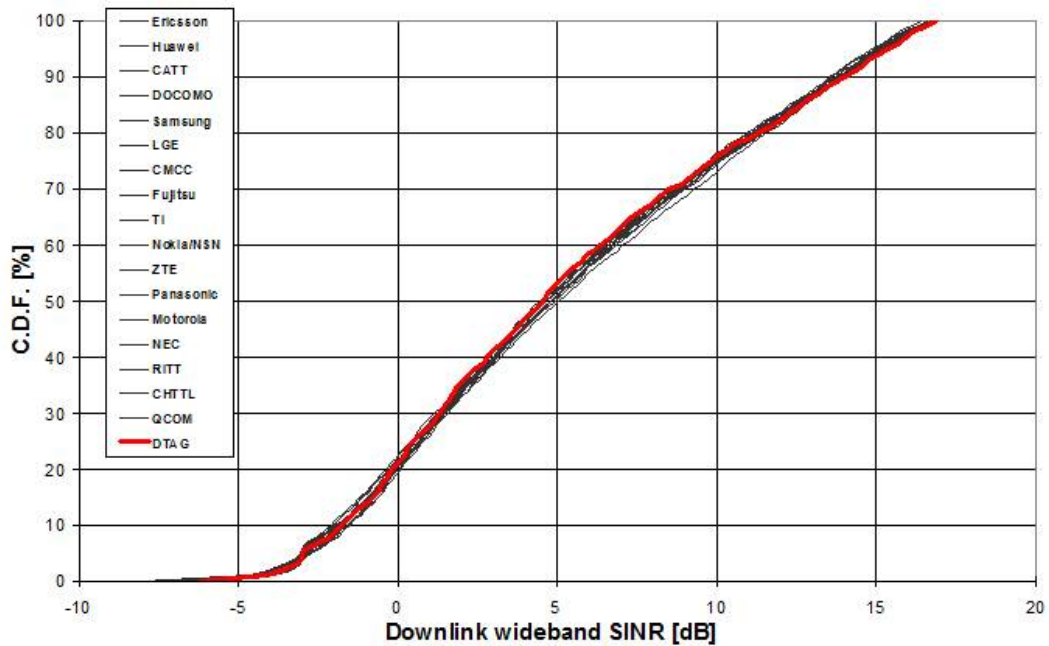


Figure 3.19: 3GPP calibration results for the User Geometry

In Figure 3.20 the comparison of the user throughput normalized to the system bandwidth is illustrated. This terminology of the 3GPP calibration activity should not be confused with the considered KPI considering the fairness criterion, which is described in Section 3.4. The depicted values can be interpreted as the following. For a network with 10 MHz system bandwidth 50% of the MSs achieve a throughput of more than 0.6 to 1 Mbps. To be comparable, a rather simple round robin scheduler was used here. It can be observed that the results have a relatively high deviation, which shows the difficulty to compare such a complex calculation process. The deviation might be derived by the fact, that the scheduler's design are heavily vendor dependent, which represents a unique selling point for them. They are not interested in being comparable in this point. However, the different results at least follow the same trend.

Moreover, the results of the average SINR per user differ from each partner shown in Figure 3.21. For instance, the average value (in the range of the 60 percentile) differs from approximately 7 to 11.5 dB. This might come from the differences in implementation of channel models, receiver models, link adaptation and link-to-system interfaces, since they are not fully standardized in detail. However, the Deutsche Telekom simulation results represent the same tendencies as the other results, depicted as the red curve.

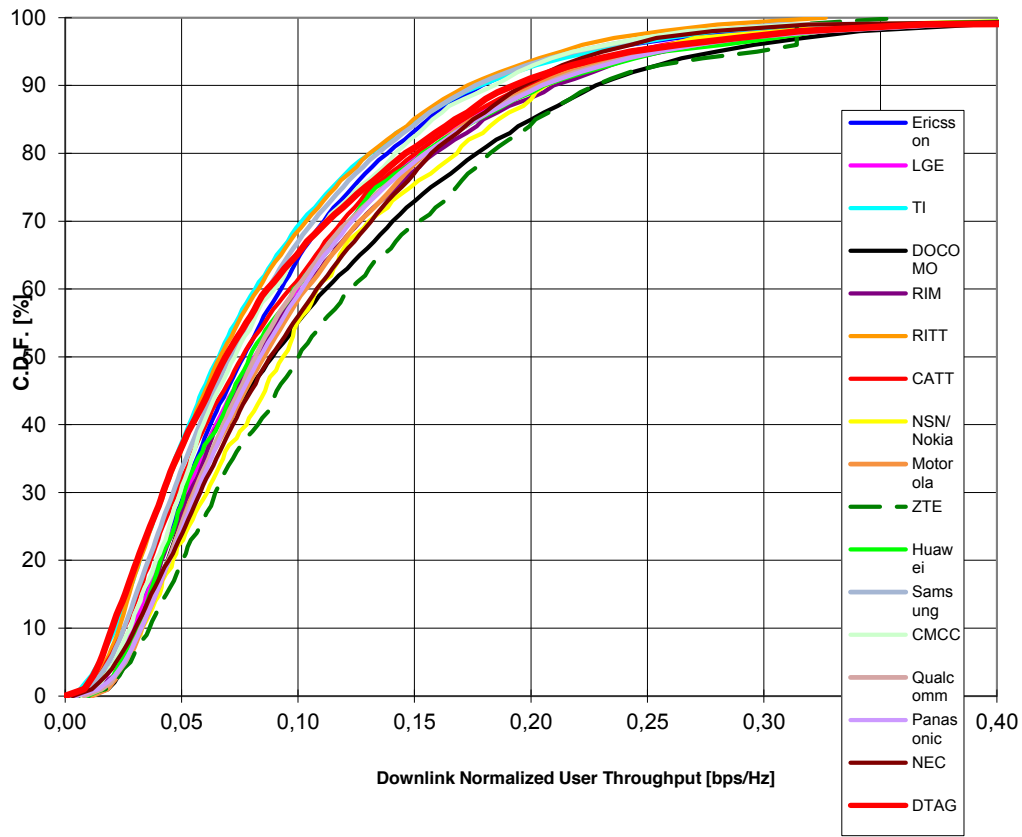


Figure 3.20: 3GPP calibration results for the DL normalized user throughput

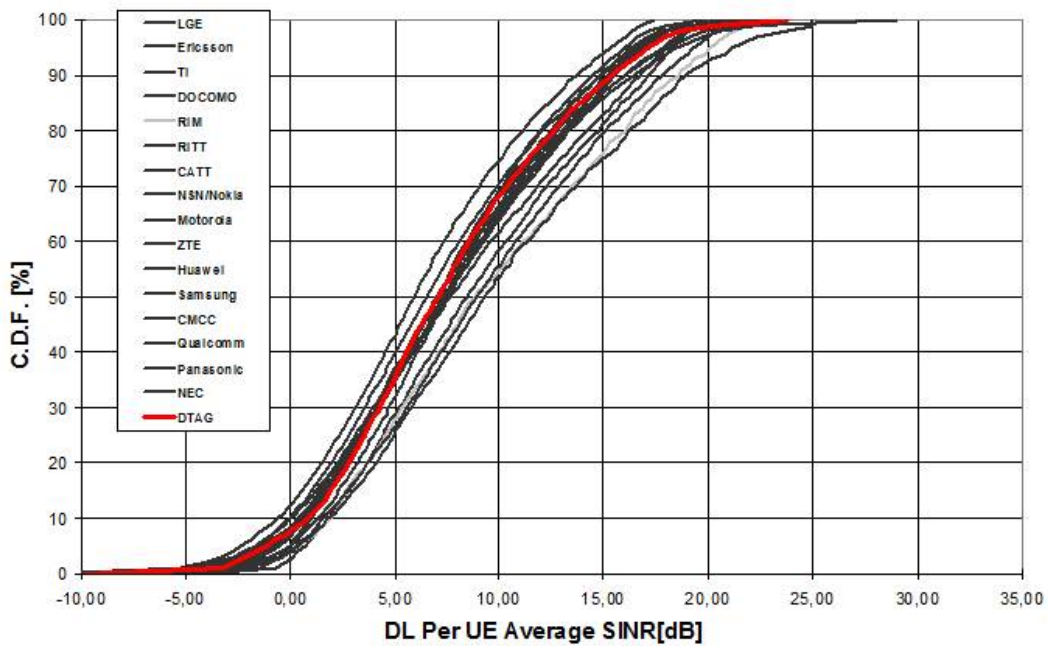


Figure 3.21: 3GPP calibration results for the average SINR per UE

In Figure 3.22 the final performance results in terms of cell average and cell edge spectral efficiency are depicted. The cell average spectral efficiency ( $SE_{cell}$ ) is defined as the average user throughput ( $\bar{r}$ ) divided by the assumed system bandwidth (BW) as shown in Equation 3.4.

$$SE_{cell} = \frac{\bar{r}}{BW} \text{ [bps/Hz]} \quad (3.4)$$

There are two y-axes presented. The left one is related to the average value (blue bars), while the right one refers to the 5 percentile (red bars). The DTAG results seem to be a bit more pessimistic in comparison to other partners. However, the conclusion of the comparison among DT SLS results and 3GPP's calibration activity is that the simulator produces reliable results and lies in range of other simulation implementations. Therefore, the simulation tool can be seen as calibrated.

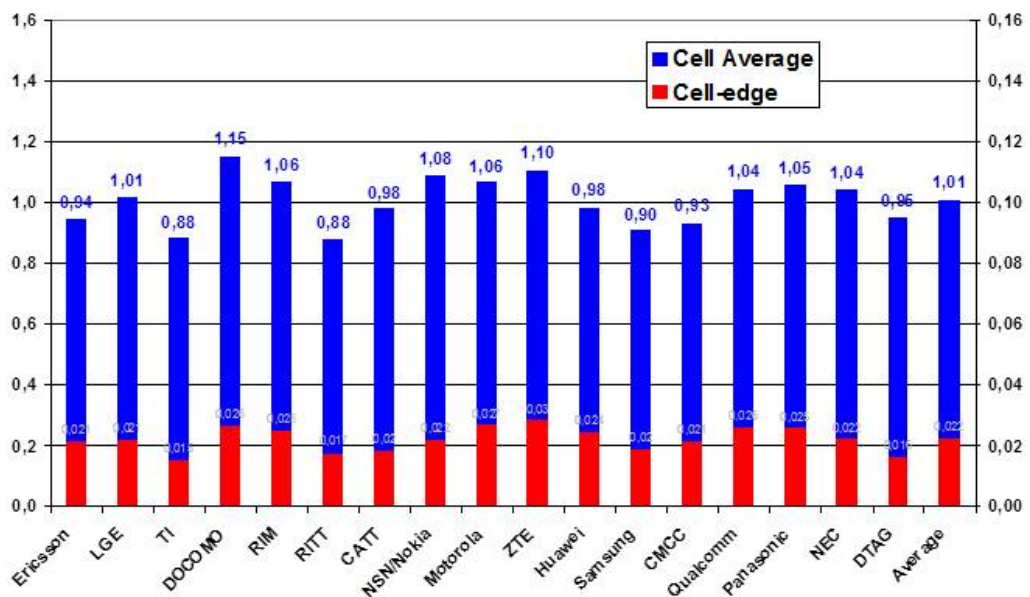


Figure 3.22: 3GPP calibration results for the cell average and the cell edge SE

### 3.7 Summary

This Chapter has explained the potential methods suitable to investigate the research problem and derives why SLSs are a suitable methodology to explore it. The used software, the DT SLS and necessary extensions to simulate RN-extended networks, were described in detail. In addition, calibration results based on the 3GPP simulation framework are

presented and compared with results from other partners. In the following Table 3.4 the necessary requirements are summarized to be able to investigate the research problem.

Table 3.4: Requirements for investigations of RN extended large scale network performance

<b>Requirement</b>	<b>Addressed by</b>
An OFDMA multi-carrier system	Part of the DT SLS.
A frequency selective radio channel	Part of the DT SLS.
A large number of MS and MBS	Part of the DT SLS.
Sending and receiving subframes for RNs	Implemented based on [21] explained in 3.5.
CQI feedback	Inherent part of the DT SLS. However, additional CQI feedback for Downlink (DL), BL and AL subframes is required as well as information of the AL which needs to be forwarded from RN to MBS. This requires an adapted feedback structure with different delays and timing patterns which has been implemented throughout this Thesis, explained in Section 3.5.
RN Buffer Structure	The DT SLS was extended as explained in Section 3.5.
Asynchronous Power Adaptation for Inter Cell Interference Coordination	The required algorithm is a major contribution of the Thesis explained in Section 4.3.
Synchronous Frequency selective time variant radio resource scheduling	Supported by the DT SLS. However the scheduling process in case of RN extended networks with possible two-hop connections has to be extended (Section 4.4). Major contribution of the Thesis.
Cell selection method	Basic MBS and pico cells selection method based on RSRP and Cell Range Expansion (CRE) offset as described in [105] is supported. However, an adapted attachment method for RN extended networks as described in Section 4.2 is a major contribution of this Thesis.

Based on the discussion in Chapter 2 and the necessary implementations summarized in Table 3.4 the reader has to keep in mind that the results in this Thesis are carried out with the following major features for RN-extended networks:

- Subband CQI based frequency selective scheduling.
- Adapted Two-hop proportional fair scheduling.
- Frequency selective correct decisions for the backhaul link transmissions based on Figure 4.18 under fairness constraints.

- Minimized feedback for the second hop forwarded from RN to MBS.
- Co-scheduling functionality for MBSs.
- MS specific buffer aided relays.
- Realistic feedback delay model.
- Adapted cell selection model.
- Adapted subband specific transmission power pattern.

In the following Chapter 4 the major contributions of this Thesis are explained in detail and evaluated in Chapter 5 based on simulation results.

# Chapter 4

## Design of the effective hybrid RRM scheme

In this section the proposed hybrid RRM approach for the half duplex RN-extended networks is presented in which the theoretical problem formulation defined in Section 2.3.2 is decomposed into three sub-problems for large scale realistic networks, listed in the following.

1. The decentralized MS cell selection procedure is adapted for RN extended networks based on the proposed method in Section 4.2.
2. The proposed asynchronous network-centralized scheme is based on a meta-heuristic to sub-optimally adapt the transmission power on a derived part of the system bandwidth and thus to reduce inter-cell interference and power consumption with very low amount of additional feedback overhead. In addition it shall increase the capacity of the non-optimal wireless backhaul link, as discussed in Section 2.2.4 for RNs with non-LoS conditions and unplanned positioning. The approach is described in Section 4.3. Previous tests in the course of this Thesis have shown that an appropriate adaptation of the transmission power is necessary while more aggressive schemes result in performance losses as can be seen in [106].
3. The synchronous TTI based resource scheduling is done in a cell-centralized and decentralized manner, as described in Section 3.5.6 and adapted in Section 4.4 based on defined rules. While the MBSs serve relays and users in a macro cell-centralized manner the relays themselves schedule their users in a decentralized way.

The proposed schemes are the major contributions of the Thesis and defined in Section 4.2 - 4.4. The simulation results for the proposed novelties are discussed in Chapter 5. The following section 4.1 defines the considered scenario and gives important insights regarding the occurring interference situations.

## 4.1 Scenario description

Two different types of time transmission intervals (TTI)s occur in the considered half duplex relay extended networks. The first one, further defined as the Backhaul Subframe (BHSF) serves the RNs, while they are in the receiving mode, and the MSs directly attached to the donor macro basestation (dMBS). Within this TTI the interference is caused only by the MBSs. The possible radio link types which occur in a BHSF are illustrated in Figure 4.1.

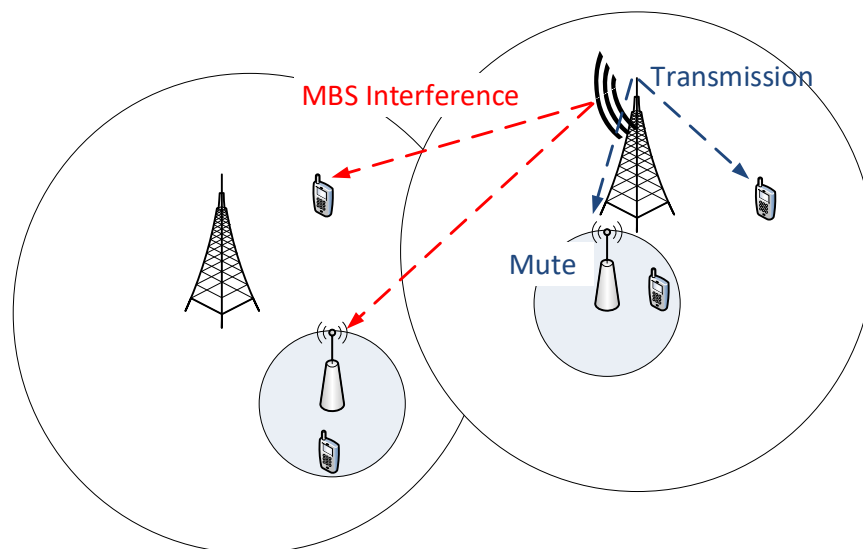


Figure 4.1: Possible serving and interfering links during backhaul transmission time

The second subframe, further declared as Access Link Subframe (ALSF), serves the directly attached MBS MSs, as well as the two-hop MSs assigned to the RNs, while the RNs are in the sending mode. Here, RN interference occurs in addition. Possible link types within a ALSF are depicted in Figure 4.2.

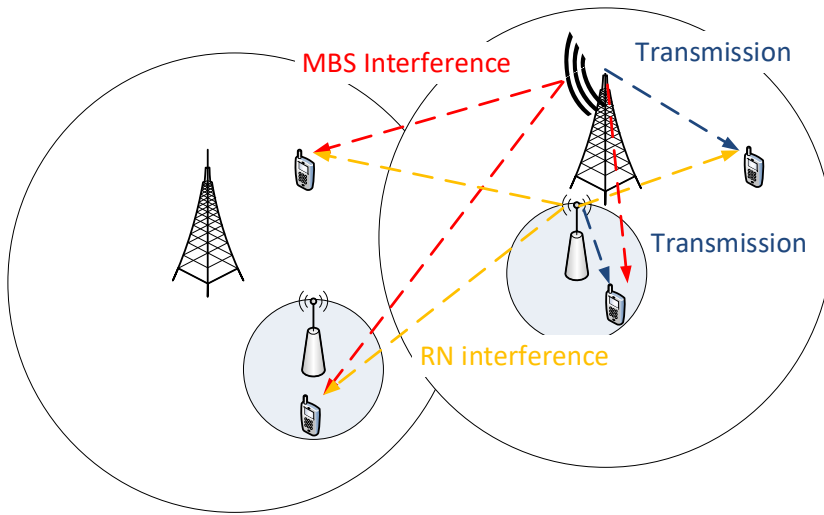


Figure 4.2: Possible serving and interfering links during RN access transmission time

The intended RRM approach aims to improve the RN backhaul links in the first and the directly attached MSs in the second TTI. The possible throughput of the MSs connected to the RNs will be limited by the backhaul transmission for each RN during the BHSF. The RN MS throughput will only improve if the backhaul links in the first subframe will have increased supportable data rates and more data per RN MS will be transmitted and buffered at the RN. The major challenge is to improve the RN backhaul links without a loss of the directly attached MSs, which share the capacity of the BHSF with the RNs. The ALSF, which is exclusively used by the directly linked MSs at the MBS is additionally interfered by the RN to MS transmissions, when RNs are in sending mode. Both subframes are interdependent to each other. When the RNs get too much resources the MBS MSs experience a loss in the BHSF in terms of instantaneous throughput. Thus, the resulting loss, needs to be compensated within the BHSF and ALSF by increasing the instantaneous throughput based on the improved spectral efficiency. An excellent result of the proposed RRM scheme would be to keep the overall direct link MS performance stable, while improving the backhaul link quality of the RNs and thus, improve the overall throughput performance of the two hop MSs. To minimize the additional interference in the ALSF, caused by the RN transmission, the quality of the RN access link should be improved as well, to provide a stable MBS MSs link quality. Further, fairness needs still to be guaranteed as well as possible energy savings need to be considered under limited amount of additional signalling overhead, as previously discussed.

As described before, Figure 4.1 and 4.2 illustrate all possible link types which can occur. The depicted links are formulated, as the following: Equation 4.1 describes the link budget to calculate the average received power of the serving signal 0 for the  $n_{th}$  MS.

It is defined by the transmission power  $P_{tx}$  multiplied by the losses, caused by shadow fading  $P_{sf}$ , penetration  $P_{sf}$  and  $P_{cable}$  cable losses. Further, antenna gains of sender  $G_{bs, rn}$  and receiver  $G_{rn, ms}$  are considered in addition. Equation 4.2 and 4.3 define the interfering links  $i$  of a MBS  $m$  and a RN  $r$ , respectively. Furthermore, the influence of the varying radio channel  $H$  needs to be taken into account. In principle, the powers of all paths of the considered link type at the antenna port 0 are summed up and averaged. The calculation of the RSRP values is defined in Equation 8.1 in [107].

$$\bar{s}_0(n) = G_{bs}^{(0)} P_{tx}^{(0)} P_{sf}^{(0)} P_{penet}^{(0)} P_{cable}^{(0)} G_{ue}^{(0)} H^{(0)}(n) \quad (4.1)$$

$$\bar{i}_m(n) = G_{bs}^{(m)} P_{tx}^{(m)} P_{sf}^{(m)} P_{penet}^{(m)} P_{cable}^{(m)} G_{ue}^{(m)} H^{(0)}(n) \quad (4.2)$$

$$\bar{i}_r(n) = G_r^{(r)} P_{tx}^{(r)} P_{sf}^{(r)} P_{penet}^{(r)} P_{cable}^{(r)} G_{ue}^{(r)} H^{(0)}(n) \quad (4.3)$$

The proposed RRM scheme which aims to improve the system capacity is separated into three parts: The initial step is an adapted cell selection procedure compared to end-to-end optimal routing strategy proposed in Section 2.3.6.

The second step is based on a network centralized asynchronous approach, which aims to adapt the transmission powers of all serving stations, MBS as well as RNs, in the network. Both types of TTIs are taken into account, while interdependencies are considered. The average received powers of serving and interfering links need to be measured by the MSs and RNs and fed back to a central optimization entity. As an additional required information, the optimizer needs to know in which subframe type the measurement was carried out. Once the network-centralized unit has collected all feedbacks, the optimization can be initiated. The final outcome of this asynchronous procedure consists of a transmission power adaptation for each serving station as well as the total number of PRBs, where the adapted transmission power patterns will be applied. The process might be repeated in a larger time scale (e.g. hundreds of ms) to prevent additional feedback overhead, caused by the necessary MS measurement reports for the calculation. Once the improved power pattern is derived, no further action is needed by the network-centralized entity. It is obvious that this might result in a suboptimal solution

due to the nature of the channel variations. However, it can be easily applied in real networks due to its low amount of feedback.

The third part of the process is based on the synchronous adapted scheduling procedure, where in each TTI the available PRBs are allocated to MSs and RNs to serve. This is done based on an adapted two-hop proportional fair metric, which takes into account CQI reporting of RN and MSs, past decisions as well as resource allocation control rules, how to use the optimized subbands. Besides subband CQI reporting which needs to be forwarded by the RN to its donor MBS for all served MSs, also relaxed different type of reports are considered to ease the amount of signalling overhead, further explained in Section 4.4.

## 4.2 Adapted decentralized MS cell selection procedure

As found in Section 2.3.6 the cell selection in relay extended networks is often done with the composite rate of the two hop links to consider the end-to-end supportable rate of the link to choose the serving cell. There is no consideration regarding the possible unbalanced fraction of time used for transmission and reception of the RN. For the purpose of this Thesis it needs to be considered how the unbalanced amount of time used for backhaul and access link transmission influences the performance. In addition to that the possible direct link rate needs further to be differentiated regarding the sending or receiving mode of the RNs, as they appear as additional interferers. Therefore, parameter  $T_{BH}$  is introduced in Equation 4.4 which represents the fraction of time the RN is in reception mode and in sending mode  $(1 - T_{BH})$ . The differentiated rate  $\bar{R}_{BH}$  and  $\bar{R}_{AL}$  are weighted with the corresponding time and summed up.

$$\bar{R}_{MBS} = T_{BH} \cdot \bar{R}_{BH} + (1 - T_{BH}) \cdot \bar{R}_{AL} \quad (4.4)$$

The composite rate for possible two-hop links needs to be extended as well for the purpose of this Thesis. Since buffer extended relays are considered it is also necessary to consider the amount of time a relay can receive and transmit to estimate which will be the best serving cell to use. Therefore, the composite rate is extended as shown in Equation 4.5. The time fraction is normalized to 0.5 which is the inherently considered fraction of time in the original composite rate calculation.

$$\overline{\text{CR}} = \left( \frac{1}{\frac{T_{BH}}{T_N} \cdot \frac{1}{\overline{R}_{BH}(i)} + \frac{1-T_{BH}}{T_N} \cdot \frac{1}{\overline{R}_{AL}(i)}} \right)^{-1} \quad (4.5)$$

Finally the extended Equation 4.5 results in the following form:

$$\overline{\text{CR}} = \frac{T_N \cdot \overline{R}_{BH} \cdot \overline{R}_{AL}}{T_{BH} \cdot \overline{R}_{AL} + (1 - T_{BH}) \cdot \overline{R}_{BH}} \quad (4.6)$$

As previously explained in this Thesis the worst case scenario for the relay wireless backhaul link is considered which introduces advantages in terms of deployment and cost aspects for an operator (Section 2.2.4). Based on that an additional weight factor is introduced to the cell selection scheme in Equation 4.7 and 4.8 to attach to possible connections with better backhaul conditions.

$$\overline{\text{CR}} = w \cdot \frac{T_N \cdot \overline{R}_{BH} \cdot \overline{R}_{AL}}{T_{BH} \cdot \overline{R}_{AL} + (1 - T_{BH}) \cdot \overline{R}_{BH}} \quad (4.7)$$

$$w = \begin{cases} T_{BH}, & \text{if } T_{BH} \cdot \overline{R}_{BH} < (1 - T_{BH}) \cdot \overline{R}_{AL} \\ 1 + T_{BH}, & \text{if } T_{BH} \cdot \overline{R}_{BH} > (1 - T_{BH}) \cdot \overline{R}_{AL} \\ 1, & \text{if } T_{BH} \cdot \overline{R}_{BH} = (1 - T_{BH}) \cdot \overline{R}_{AL} \end{cases} \quad (4.8)$$

A better backhaul connection counts more than the access link quality, as the data can be buffered and the access link resources will be shared among a lower number of users to be served by a single RN. Furthermore, it can be assumed that it is quite likely that the access link has a better quality due to the user hot spot scenario and the backhaul is the bottleneck of the possible two-hop connections. The results of the analysis for the different cell selection schemes can be found in Section 5.2.1.

### 4.3 Network-centralized asynchronous RRM

For the asynchronous network-centralized scheme in this Thesis it is necessary to take a decision which meta-heuristic scheme fits the best and is recommended from existing literature for such type of optimization problems. Once the decision is taken a proper adaptation of the heuristic to the optimization problem needs to be carried out to result

in attractable performance gains. In the following, the decision is motivated based on the existing literature to apply and specifically adapt a Genetic Algorithm (GA) as a promising example meta-heuristic, to reach the target of this Thesis.

### 4.3.1 Simplified numerical example for the centralized optimization process

Before the centralized process is described which will be used for the final simulations the principle idea of the intended optimization is explained. A numerical example is presented with simplified assumptions regarding the optimization scheme and the considered mobile network scenario. The following constellation is assumed:

A simple network illustrated in Figure 4.3 which consists of 2 MBSs, where only one of those serves one directly attached MS and one RN. The second MBS only serves one directly attached MS exclusively.

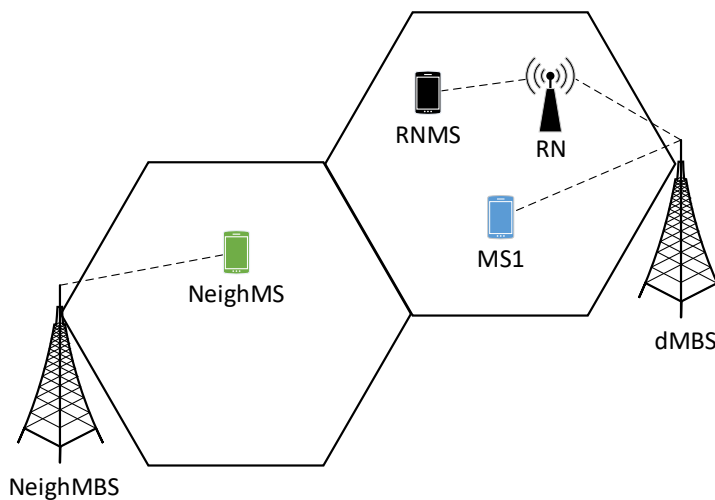


Figure 4.3: Simple network scenario for example optimization approach

Each MS / RN only allocate one PRB for the transmissions, with a MS / RN specific supportable rate dependent on the corresponding PRB specific wideband SINR values. Moreover, only the BHSF is considered when the RN is in receiving mode and the dMBS needs to allocate resources for the backhaul transmission and the directly attached MS1. As assumed in the meta-heuristic, explained in the following Section 4.3, the optimization entity has gathered all RSRP values from MSs, RN, respectively. Once, the values are available the optimization process will start and the process will only be repeated in a longer time frame. Furthermore, a preselected number of possible power reduction values are defined, which can be applied as offset values to artificially decrease the measured

RSRP values. Here for simplification the applied subset of power reduction values are chosen just randomly in each optimization step, without considering the performance of past configurations. The values are defined as a set of quantized dB values. No local intensification and global diversification functions are applied in this simple example, as it will be discussed in Section 4.3.2. Only the very best found configuration is saved from previous calculations and compared. First the effective SINR values are calculated and second the corresponding possible supportable rates are derived based on the Equations 4.13-14. Afterwards, the overall total sum rate is calculated. To prevent an increased outage probability an additional constraint has to be considered. None of the individual supportable rates are allowed to result in 0, which ensures a reasonable outage probability but also fairness. This defines the quality of service criterion for the example. If the outcome of the considered optimization step outperforms the previous best configuration it is set as the new best found solution. For simplification in this example the optimization procedure has a fixed number of iterations without considering the convergence of the result. A flow chart for the described simplified approach is presented in Figure 4.4.

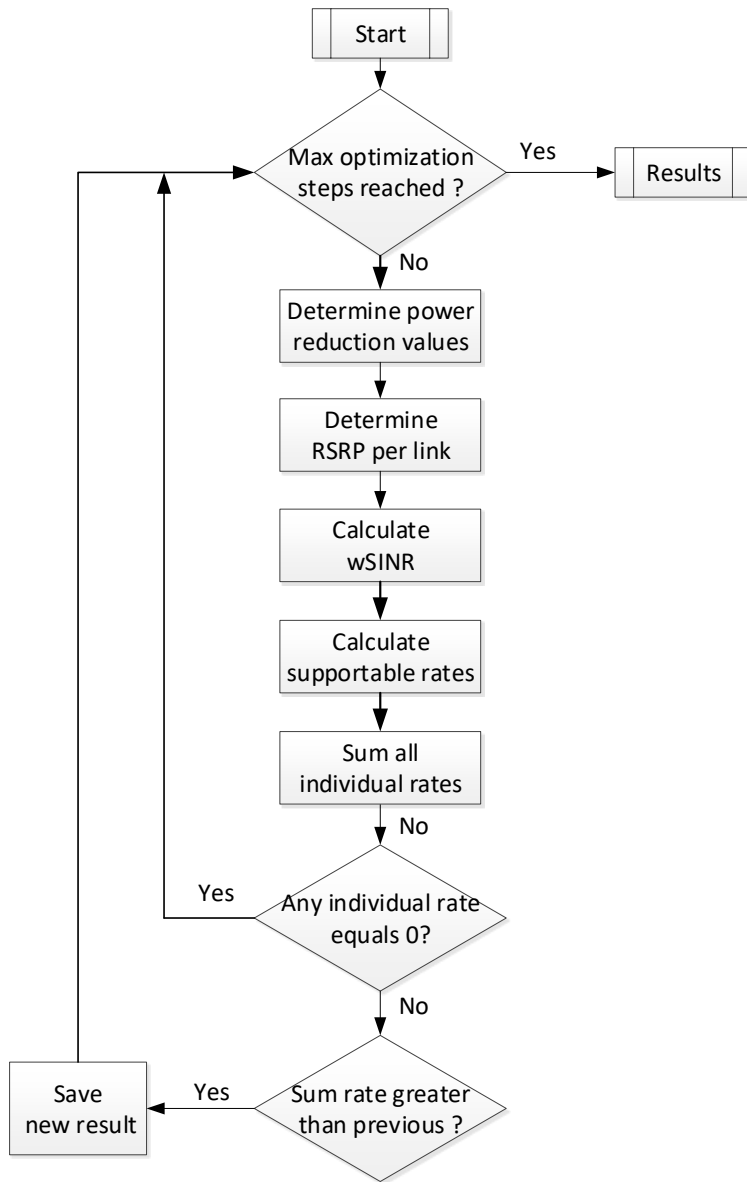


Figure 4.4: Flow chart for simplified example optimization approach

Figure 4.5 shows the behaviour of the numerical example. In the upper subplot the power reduction values are depicted for each of the serving nodes in the network (dMBS, RN and neighbour MBS). In the middle subplot the MS specific data rates are presented, where the two hop MS is black coloured and relies on the two hop supportable rate dependent on the BL and AL quality, defined in Equation 2.17. Finally, in the lower subplot the total sum rate which consists of the MS specific rates is illustrated as the black dashed curve. It can be observed, that the optimization process increased the overall sum rate from approximately 6.2 bps/Hz to 9.1 bps/Hz after the 26th optimization step, while no individual MS is in outage (no MS specific data rate equals 0).

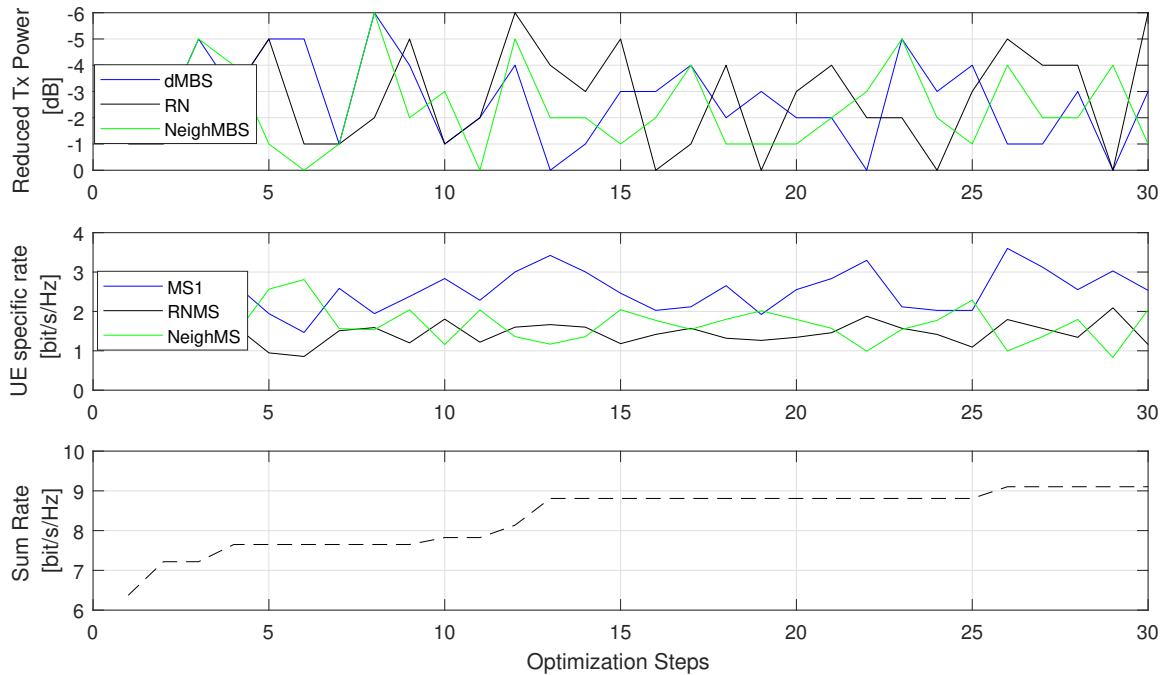


Figure 4.5: Numerical example for simplified optimization approach

After the process the centralized optimizer would now send the power reduction values to the corresponding MBSs, RNs respectively. Based on the found configuration the RN needs to reduce the transmission power by 5 dB, while the dMBS and neighbour MBS needs to reduce by 1, 4 dB respectively (upper plot in step 26). For clarification it has to be kept in mind, that the suggested network-centralized approach discussed in this section follows the design principle to introduce a minimum amount of additional overhead. Therefore, it relies on long term values such as the average received power (RSRP), which does not prevent losses based on short term effects, such as fast fading. The cell-centralized part of the proposed RRM scheme takes care of synchronous effects. Furthermore, it is quite unlikely that in a large scale scenario with a lot of MSs a configuration can be found where all MSs will profit from the optimization. To this end, the optimization result will only be applied on a subset of resource blocks of the total system bandwidth, further explained in the upcoming section. Moreover, it has to be considered that the access link subframes (ALSF) need to be optimized as well, which is not considered in this example. Just to give an idea about the solution search space of the considered problem. Already in the simplified scenario  $(7 \cdot 2)^3$  which equals 2744 possible combinations would be necessary to be evaluated by an exhaustive search approach finding the optimal solution (7 power reduction values, 2 subframes, 3 serving nodes as explained in Section 2.4). In the following section the final network-centralized part of the proposed

hybrid RRM scheme of this Thesis is described in detail. The mainly relevant large scale system level simulation assumptions can be found in the tables 5.1 and 5.2.

### 4.3.2 Heuristic approach

Various types of meta-heuristics are widely used in mobile communications for different optimization cases. Applying meta-heuristics to complex optimization problems, which are identified as NP-hard is a well known method to find a non-optimal but proper solution with reasonable effort [108]. Basically, all designed approaches rely on two main concepts to guide the search process for an acceptable solution. Figure 4.6 shows the principle idea.

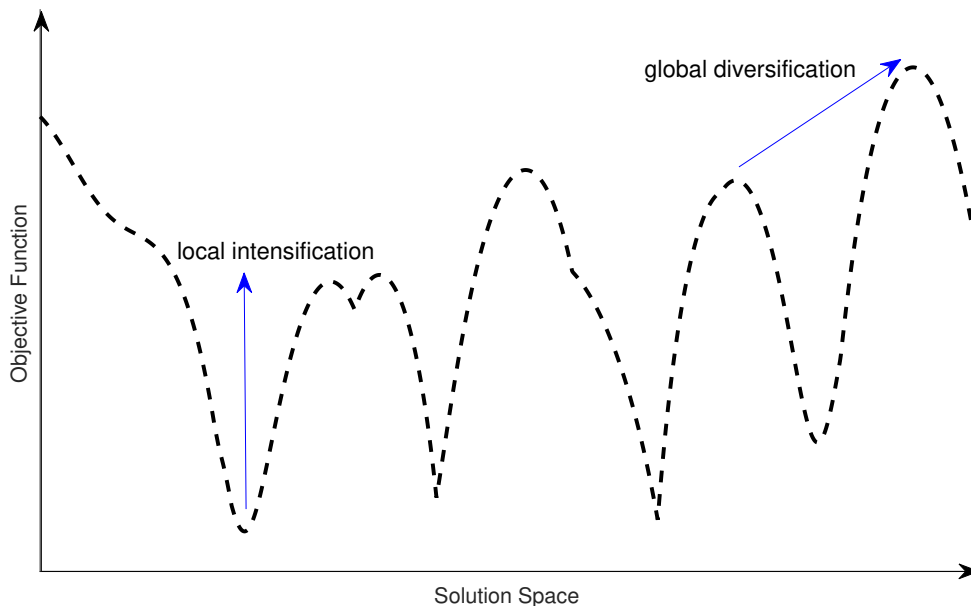


Figure 4.6: Basic idea of a meta heuristic to find a near optimal solution

A defined objective function which consists of the optimization target and the possible constraints, evaluates promising solutions explored in the overall solution space. The meta-heuristic needs to support two functionalities to result in an acceptable improved solution. The first functionality needs to take care of the so called local intensification process to find better solutions in the local search space, while the second functionality needs to provide the so called global diversification, to not stuck in a local optimum. In literature it is often differentiated between the population based methods (Genetic Algorithms (GA), Partical Swarm Optimization (PSO)) and the trajectory based methods, such as Simulated Annealing (SA) or Tabu Search (TS) to name only a view of them [108–110]. While the population based approaches start the evaluation process with multiple possi-

ble solutions, the trajectory heuristics typically start the optimization process based on a single solution. Therefore population based meta-heuristics are more attractive for huge solution spaces because they typically converge in a shorter amount of time. Moreover, they are inherently parallelizable and therefore more interesting for real implementations due to faster computation times. A further classification of different approaches can be found in [111]. A comparison between GA and PSO approaches are presented based on different benchmark tests presented in [112]. The authors show high quality results for both population based approaches and nearly the same computational effort for constrained non-linear optimization problems, as it is considered in this Thesis. In [113] a comprehensive study on existing approaches using GAs in wireless networks for different optimization problems is provided. The authors conclude, that GAs are identified as most tractable meta-heuristics for wireless communication systems. Moreover, they state that GAs are most attractive for centralized optimization purposes in mobile cellular networks considering general capacity improvements or energy-efficient transmission schemes, as for instance in [114, 115] and in this Thesis.

As already discussed, it would be quite challenging to find the theoretically optimal power distribution pattern, due to the huge number of existing combinations in large scale relay extended networks. The combinatorial problem cannot be optimally solved during runtime of the system, even if only average received power values are considered, such as the RSRP values. As already described in the numerical example in the previous section it is necessary to reduce the number of combinations by a limited subset of transmission power reduction values, which will be applied for the access link (AL) and backhaul link (BH) subframes. If for instance a set of 10 possible power reduction values are assumed, it already results in a large number of possible combinations. In a large scale network consisting of 57 MBS and 228 RNs as it is considered in this Thesis it results in an impractical solution space which is NP hard to solve. An optimal result also cannot be found by an exhaustive search (deterministic approach) in a proper amount of computation time.

Finally in the work of this Thesis, the principles of the GA based meta-heuristic are used and specifically adjusted for the network-centralized asynchronous part of the hybrid RRM approach. The target is to adapt the transmission power of MBSs and RNs in both appearing subframes either if the RNs are in transmission or reception mode. This is done for a subband of the available system bandwidth to be still able to serve users which do not gain from the approach. Again, the intention is to improve the non-ideal wireless backhaul

link of the RNs without decreasing the throughput of the MSs which are attached directly to the MBSs. In Figure 4.7 the flow chart of the GA is shown.

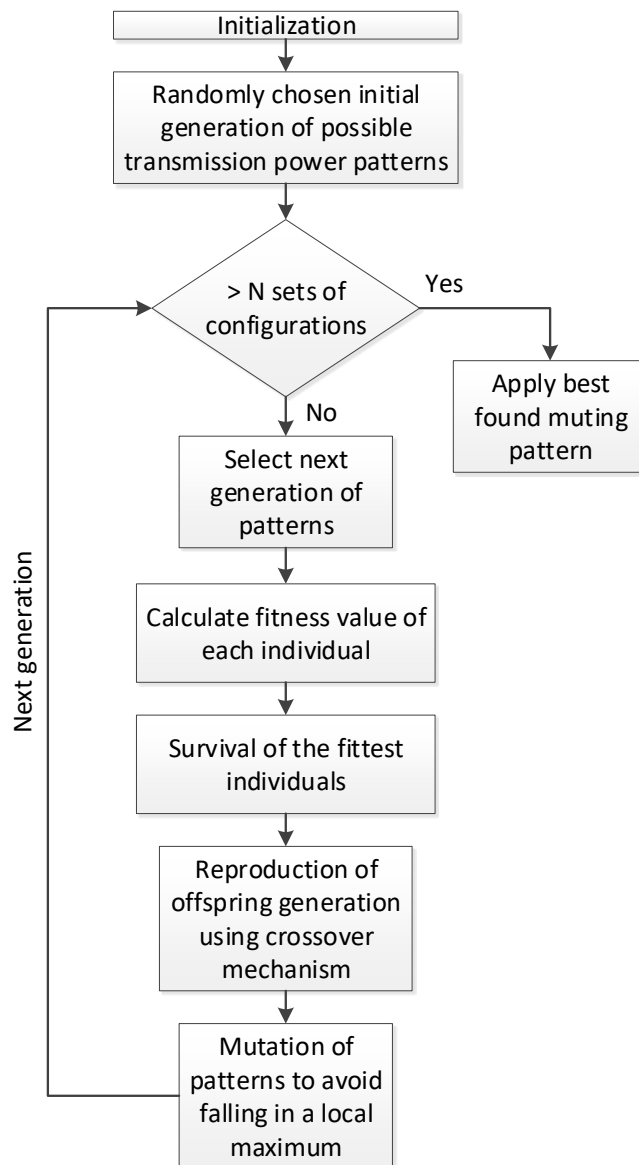


Figure 4.7: Flow Chart of the applied genetic algorithm

The procedure first starts with the initialization of the algorithm. Several functionalities, such as the choice of the objective function further referred as the fitness function, the mutation rate which is responsible for the global diversification, the crossover mechanism which is responsible for the local intensification, the number of generations (optimization steps), etc. are defined. As an example, a parameter set applied for the conducted simulations can be found in Table 5.2 in Section 5.1. After the initialization is done, a randomly chosen first generation is defined. This generation includes a number of individuals which consists of a set of possible transmission Power Adaptation Value (PAV)s for each MBS in the BHSE and the ALSF. In addition a set of PAVs for each RN in the

ALSF is chosen. In the next step the fitness values for all individuals are calculated, based on the measurement reports received from RNs and MSs.

#### 4.3.2.1 Calculation of serving and interfering links with power adaptation values

Equation 4.9 defines the adapted received average power of the serving signal  $\bar{P}_{rx}$  of the MS  $n$  for the individual  $i$  in the subframe type  $s$ , based on the Equation 4.1. The  $\theta$  is defined as the MBS  $m$  or the RN  $r$  specific PAV, as a scalar of the vector  $P_{pav}$ , which consists of the defined possible PAVs. Accordingly, Equation 4.10 and 4.11 define the sum of the total number of interfering links, based on Equation 4.2 and 4.3 either for interfering MBSs  $\bar{i}_{MBS}$  or RNs  $\bar{i}_{RN}$ , respectively, while  $\bar{i}_{RN}$  only needs to be defined for the ALSF, due to reception mode of RNs in the BHSF.

$$\bar{P}_{rx}(n, i, s) = \Theta_{m,i,s} \cdot \bar{s}_0(n, i), \quad (4.9)$$

where  $\Theta_{m,i,s} \in P_{pav}$

$$\bar{I}_{MBS}(n, i, s) = \sum_{m=1}^{M_{BS}} \Theta_{m,i,s} \cdot \bar{i}_{MBS}(n, i), \quad (4.10)$$

where  $\Theta_{m,i,s} \in P_{pav}$

$$\bar{I}_{RN,AL}(n, i) = \sum_{r=1}^{R_{RN}} \Theta_{r,i} \cdot \bar{i}_r(n, i), \quad (4.11)$$

where  $\Theta_{r,i} \in P_{pav}$

#### 4.3.2.2 Calculation of adapted wideband SINR for access and backhaul subframe

The next step to be able to determine the fitness value of each individual  $i$  is to calculate the adapted wideband SINRs for all users  $n$ . Equation 4.12 defines the wSINRs for all MSs in the ALSF. Those are either users served by the MBS  $N_{MBS}$  or RNs  $N_{RN}$ .  $\bar{N}$  is

considered as the average white noise for each MS.

$$\overline{\text{wSINR}}_{\text{AL}}(n, i) = \dots \quad (4.12)$$

$$10\log_{10}\left(\frac{\overline{P}_{\text{rx}}(n, i, 1)}{\overline{I}_{\text{MBS}}(n, i, 1) + \overline{I}_{\text{RN}}(n, i) + \overline{N}(n, i)}\right),$$

$$\text{where } n \in \{N_{\text{MBS}}, N_{\text{RN}}\}$$

Equation 4.13 defines the wSINR in BHSFs with RNs ( $N_{\text{sRN}}$ ) in the reception mode and for MSs served by the MBS ( $N_{\text{MBS}}$ ). Here, no interference caused by the RNs is needed to be considered.

$$\overline{\text{wSINR}}_{\text{BH}}(n, i) = 10\log_{10}\left(\frac{\overline{P}_{\text{rx}}(n, i, 2)}{\overline{I}_{\text{MBS}}(n, i, 2) + \overline{N}(n, i)}\right), \quad (4.13)$$

$$\text{where } n \in \{N_{\text{MBS}}, N_{\text{sRN}}\}$$

#### 4.3.2.3 Calculation of the average supportable rates for direct and two hop connections

In the next step the average supportable data rates  $\overline{R}$  for all adapted wSINR values are calculated based on an adapted Shannon bound curve in Equation 4.14, where  $\alpha$  is a factor to consider the possible system overhead. Additionally, two boundaries are defined in 4.15 and 4.16. The minimum supported wSINR of the system as well as a maximum reachable supportable rate  $R_{\text{max}}$ . The  $w\text{SINR}_{\text{min}}$  is dependent on the design and robustness of the control channel of the system and the  $R_{\text{max}}$  depends on the supported types of MCS and spatial layers.

$$\overline{R} = \alpha * \log_2\left(1 + 10^{\frac{\overline{\text{wSINR}}}{10}}\right), \quad (4.14)$$

$$\text{subject to } \overline{R}(\text{wSINR} < \text{wSINR}_{\text{min}}) = 0, \quad (4.15)$$

$$\overline{R}(\overline{R} > \overline{R}_{\text{max}}) = \overline{R}_{\text{max}} \quad (4.16)$$

Equation 4.17 then, finally defines the delta  $\Delta$  compared to the supportable rate without applying the current PAVs pattern ( $\overline{R}_{\text{ref}}$ ) of the considered individual  $i$  for all users and

relays  $n$ .

$$\Delta\bar{R}_{BH,AL}(n,i) = \bar{R}(n,i) - \bar{R}_{ref}(n,i), \quad n \in \{M_{sRN}, N_{RN}, N_{MBS}\} \quad (4.17)$$

#### 4.3.2.4 Description of the fitness value calculation

In the previous Section 4.3.2.1 - 4.3.2.3 each calculation step is described to get the delta values of the supportable rates for all MSs or RNs in all subframe types for every individual  $i$  in a generation  $g$ . Now, the actual fitness value for each individual  $i$  can be derived out of the defined fitness function, which later represents each set of PAVs per individual for the selection process to create the offspring.

Two optimization functions  $FF_{o1,2}$  are defined and explained in the following. Equation 4.18 defines the first possible fitness function  $FF_{o1}$  to use.

$$\begin{aligned} FF_{o1}(g,i) = & \sum_{x=1}^{X_{MBS}} \left( \dots \right. & (4.18) \\ & \sum_{m=1}^{M_{sRN}} \bar{\omega}_{x,m} \cdot \Delta\bar{R}_{BH}(x,m) + \frac{N_{MBS}}{N_{RN}} \cdot \sum_{n=1}^{N_{MBS}} \Delta\bar{R}_{BH}(x,n) + \\ & \left. \frac{N_{RN}}{N_{MBS}} \cdot \left( \sum_{n=1}^{N_{MBS}} \Delta\bar{R}_{AL}(x,n) + \sum_{n=1}^{N_{RN}} \Delta\bar{R}_{AL}(x,n) \right) \right), \\ & \text{where } \frac{N_{MBS}}{N_{RN}} = 1, \text{ if } N_{RN} = 0 \text{ and } \frac{N_{RN}}{N_{MBS}} = 1, \text{ if } N_{MBS} = 0 \end{aligned}$$

The equation consists of a sum of sums over all MBSs. At first, the possible  $\Delta$ s of the supportable rates for the BHSFs are considered  $\Delta\bar{R}_{BH}$ . As explained previously, the algorithm aims to increase the supportable rates of the RNs, while protecting the supportable rates of the MBS MSs.

First, the delta of the RN backhaul  $m$  is weighted by a scalar  $\omega_m$ , which represents the number of two hop users to be served by an individual RN  $m$ . The higher  $\omega_m$  will be, the more important the  $\Delta$  rate becomes for the considered RN backhaul, because the RN needs to serve more two hop MSs.

Second, the sum of the  $\Delta$ s for all MBS users during the BHSF is taken into account. It is additionally weighted by the factor  $\frac{N_{MBS}}{N_{RN}}$  which represents the importance of the sum. The more MSs are attached to the MBS directly, the more important it will be to serve these MSs and thus, the rates of them are more important. On the other hand if the RNs ( $M_{sRN}$ ) attached to the MBSs, need to serve more MSs ( $N_{RN}$ ), the sum will be less prioritized.

Third, the next sum represents the value of the  $\Delta$  rates for the MSs attached directly to the MBS and possibly served during the ALSF. Here an additional weight takes into account the importance of the sum. If a high number of two hop MSs are needed to be served by the RN attached to the donor MBS the more important the sum of the  $\Delta$  rates in the ALSF becomes to counteract on losses for the directly attached users in the BHSF.

Forth, the sum of the RN ALSF is considered as well. This aims not to introduce additional interference caused by the RNs when the access link rate is low and therefore, more PRBs would be needed for transmissions. This becomes the more relevant, the more two hop users need to be served by RNs. Because of that, the additional weight  $\frac{N_{RN}}{N_{MBS}}$  gives the sum more importance when more two hop MSs have to be served. Furthermore, the term gets less important if a relatively higher number of MBS MSs are attached and need better conditions to compensate possible losses in the BHSF.

The second fitness function  $FF_{o2}$  which is defined by Equation 4.19, is more aggressive to find a good individual. It only focuses on the improvement of the RN backhaul link and the improvement of the direct MSs during the ALSF to protect them against losses in the BHSF. Basically the weighted sum for the  $\Delta$  rates of RN backhaul links is used, as already explained for Equation 4.18. The second sum consists of the deltas for the supportable rates of the users directly attached to MBSs for the ALSF, when the RNs are in sending mode.

$$FF_{o2}(g, i) = \sum_{x=1}^{X_{MBS}} \left( \sum_{m=1}^{M_{sRN}} \vec{\omega}_{x,m} \cdot \Delta \bar{R}_{BH}(x, n) + \sum_{n=1}^{N_{MBS}} \Delta \bar{R}_{AL}(x, n) \right) \quad (4.19)$$

In addition, the number of links which have a positive  $\Delta$  supportable rate are counted for ALSF and BHSF separately. Based on that, a percentage can be derived how many subbands the final individual should be applied in both subframe types to improve the system performance.

Besides that, prohibitive possible outages of users which might be introduced by the adapted power pattern is taken into account. Therefore, the algorithm controls whether MBS users might end up in outage in both possible transmission subframe types. If this is the case, the MS specific  $\Delta$  rate is set to -100, which represents the negative impact on the single user. To this end, the total fitness value of the considered individual is decreased and down prioritized in the parent selection process. The same procedure is applied for RNs in the BHSF. Here, RNs which might result in outage will influence even more the

fitness value of the individual, due to an additional weight, which represents the number of two hop MSs attached to the RN.

#### 4.3.2.5 Generation of the offspring

After the calculation of the total fitness values for the considered generation is done, the offspring needs to be created for the next optimization step. Therefore, half of the individuals with the highest fitness values are chosen as potential parents of an offspring. The other half with lower fitness values is discarded. For the selection process a fitness proportionate scheme based on Equation 4.20 is used, where a probability  $p_i$  based on each individuals fitness value is calculated to act as a parent. The exponential factor  $\alpha$  has influence on the probability distribution of the individuals. The higher  $\alpha$  is set, the higher the probability the best individuals are chosen as parents. Based on the outcome of a sensitivity test,  $\alpha$  was set to 4. The procedure increases the selection probability towards individuals with higher fitness values. As an example, Figure 4.8 presents the procedure as an illustration of a wheel of fortune.

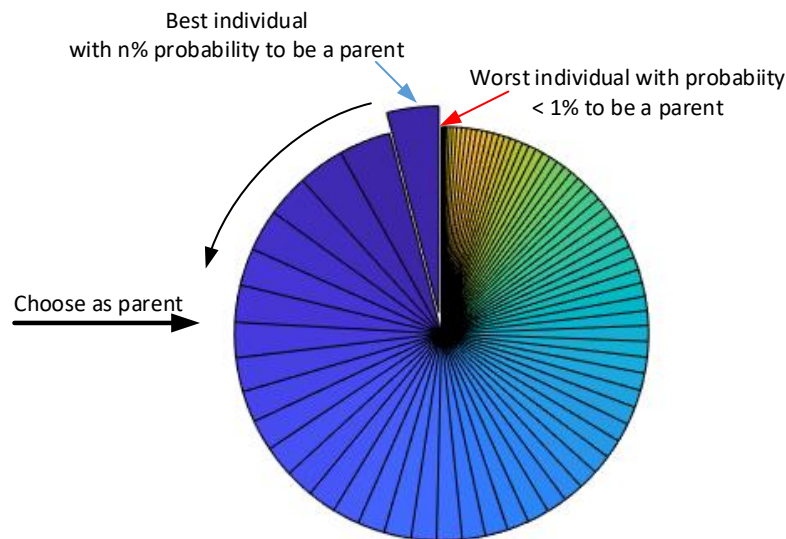


Figure 4.8: Fitness proportionate selection to create couples of parents

Each parent is chosen in a single process to finally create the target number of parents needed.

$$p_i = \frac{f_{V_i}^\alpha}{\sum_{n=1}^N f_{V_n}^\alpha} \quad (4.20)$$

Therefore, a random uniformly distributed number  $x$  between zero and one is determined and compared with the cumulated sum  $\vec{p}_{cs}$  of each individuals' probability, as defined in

Equation 4.21, for the total number of potentially survived individuals  $N$ .

$$\vec{p}_{cs}(i) = \sum_{n=1}^i p_i(n), \text{ for } i = 1, 2, \dots, N \quad (4.21)$$

Finally, a parent is chosen based on Equation 4.22, if:

$$\vec{p}_{cs}(i) \leq x < \vec{p}_{cs}(i+1), \text{ where } x \in \{\mathbb{R}^+ \mid x \leq 1\} \quad (4.22)$$

Once, the parents are determined an one point crossover mechanism is used to create the offspring, as depicted in Figure 4.9. This is used as the local intensification process as explained in the beginning of this Section. Here, two random integer values  $x, y$  are chosen, if the number of MBS does not equal the number of RNs in the system. Otherwise one integer would be sufficient. The first value  $x \in X_{MBS}$  is taken out of the total number of the MBS in the system, which equals the number of possible crossover points for the individual part of the MBSs. Second value  $y \in N_{sRN}$  is used to find crossover-points for the PAVs of the RNs. The couple of individuals reproduce themselves as depicted in Figure 4.9. For the next couples the process is repeated and different crossover points are determined until the total set of offspring PAVs is created.

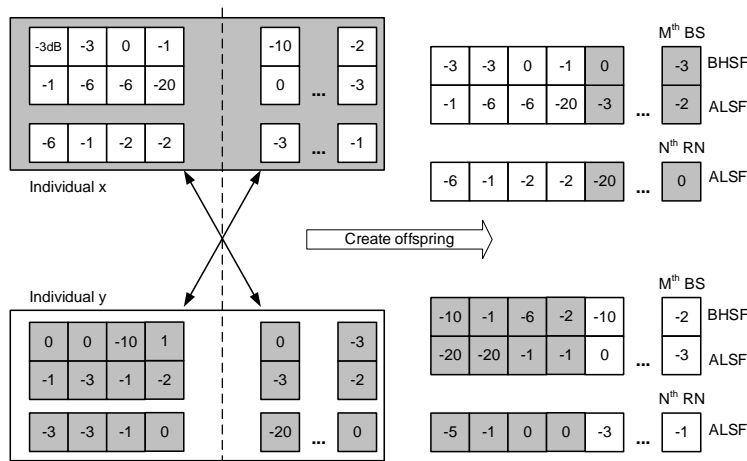


Figure 4.9: One point crossover mechanism to create offspring

Finally the offspring needs to be slightly changed to not stuck in a local optimum of the search space, when just reproducing the new set of PAVs based on the legacy. A small number of values have to be randomly changed, which is defined as the mutation process. This is used as the global diversification process, as explained before. The final outcome of the genetic algorithm is very sensitive to the mutation rate. Therefore, a sensitivity analysis has been carried out to adjust the mutation rate to result in the best possible

solution. Figure 4.10 gives the results of the performed sensitivity analysis.

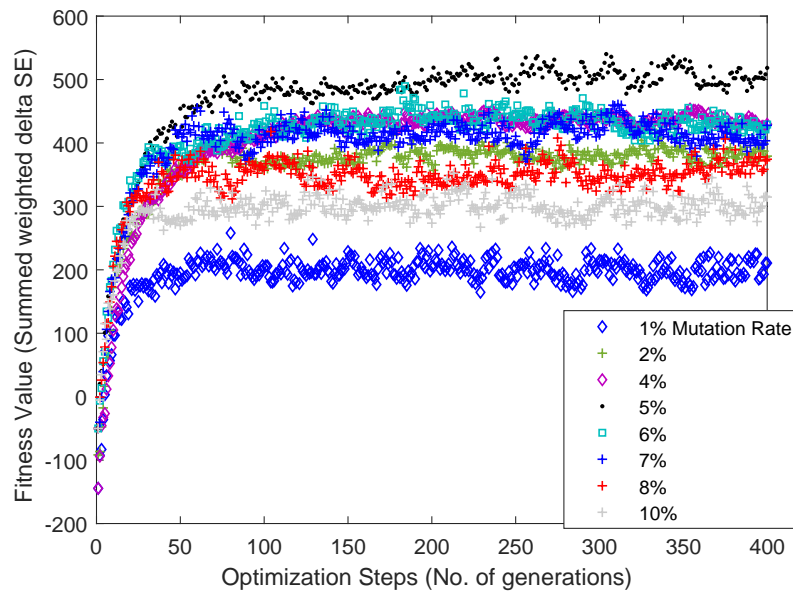


Figure 4.10: Sensitivity analysis with different mutation rates

The illustrated adjustment of the mutation rate was done based on Equation 4.19 with different percentage of mutation rates. For each generation only the maximum fitness value is depicted. It can be observed, that the best found mutation rate was 0.05 (dotted black curve), which means 5% of the total number of PAVs of the generation were mutated. All other tested mutation rates between 1 and 10 % didn't result in a higher maximum fitness value. In Figure 4.11 the maximum derived fitness values for different mutation rates are summarized.

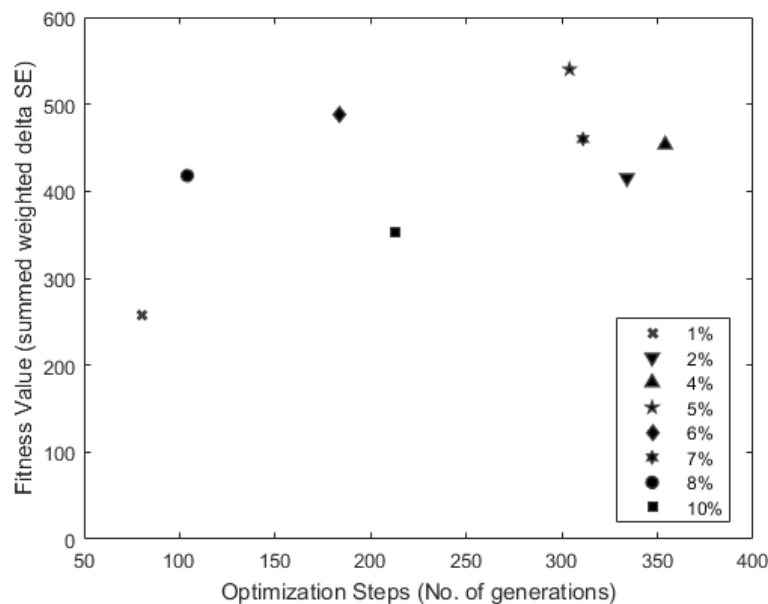


Figure 4.11: Maximum fitness values with different mutation rates

Finally, the best occurring individual with the highest fitness value is determined based on Equation 4.23 and saved. It will be only replaced if an offspring generation includes an individual with a higher fitness value.

$$p\vec{a}v_{\max} = \text{PAV}(\max [FF(g, i)]); \quad (4.23)$$

#### 4.3.2.6 Description of the final outcome of the optimization

Finally a promising optimized PAV pattern is found which improves for a certain percentage of MSs and RNs the total sum of the supportable rates of the MSs and RNs. Figure 4.12 gives an idea about the overall optimization process. As an example, the calculation process is shown based on Equation 4.19. As can be observed the individual with the maximum fitness value (marked in red) is found in generation 270 with a fitness value of 583.4.

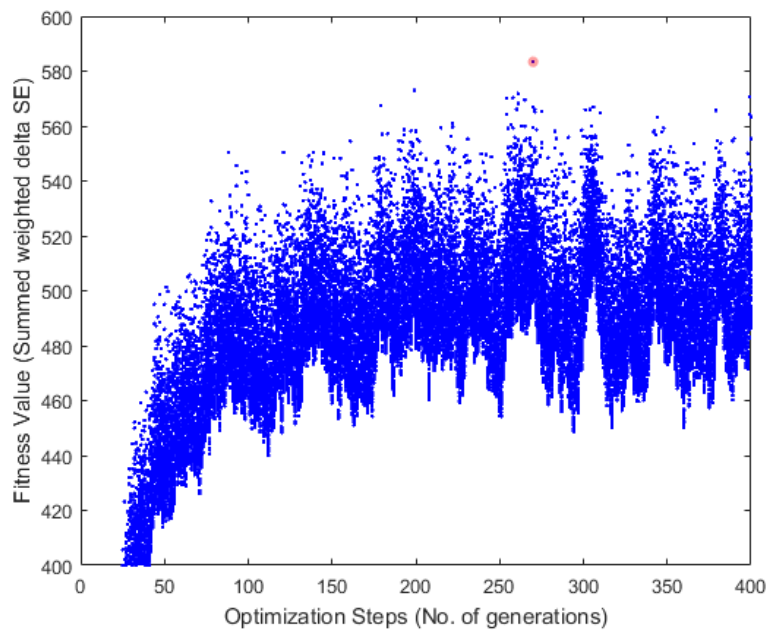


Figure 4.12: Example of GA optimization process with Equation 4.19

The final pattern which is found as the configuration with the highest fitness value can be seen as converged, if 100 optimization steps afterwards any pattern could not outperform the applied settings. This has been concluded based on the sensitivity analysis for different mutation rates, when the total length have been increased from 400 to 800 optimization steps in 4 steps with 100 additional calculations each. Figure 4.11 shows the different maximum fitness values for a number of mutation rates. None of the trial runs show an improved result after 100 additional optimization steps above 400 calculations.

In addition, Figure 4.12 shows a converged result after 270 calculation steps.

As an additional numerical example of the optimization result, Figure 4.13 shows a configuration found by the GA for two MBSs and two RNs, based on the final PAVs (individual) with the maximum fitness value. RN1 transmits with no adapted power, while RN2 has to decrease it by 3 dB in the ALSF. MBS1, MBS2 have an decreased transmission power by 6, 10db respectively, in the ALSF, while decreased power of 1dB, receptively 3dB, has to be applied during the BHSF.

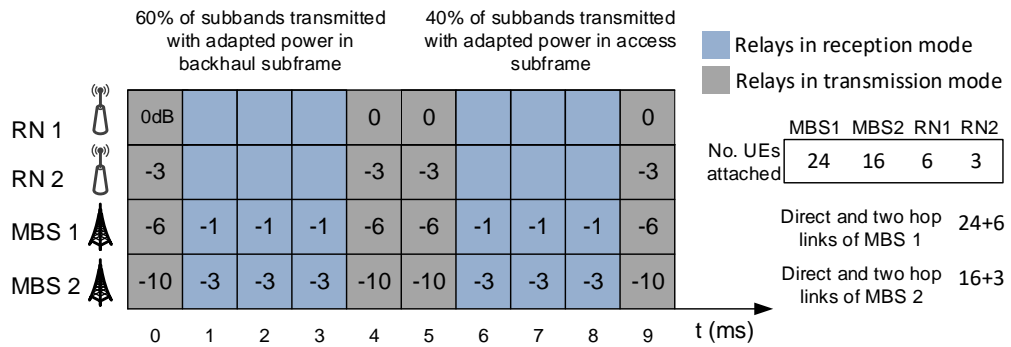


Figure 4.13: Numerical example of an optimized transmission power pattern

Furthermore, Figure 4.14 gives an impression how a configuration of the optimized subbands could look like in time domain, corresponding to the previously described example.

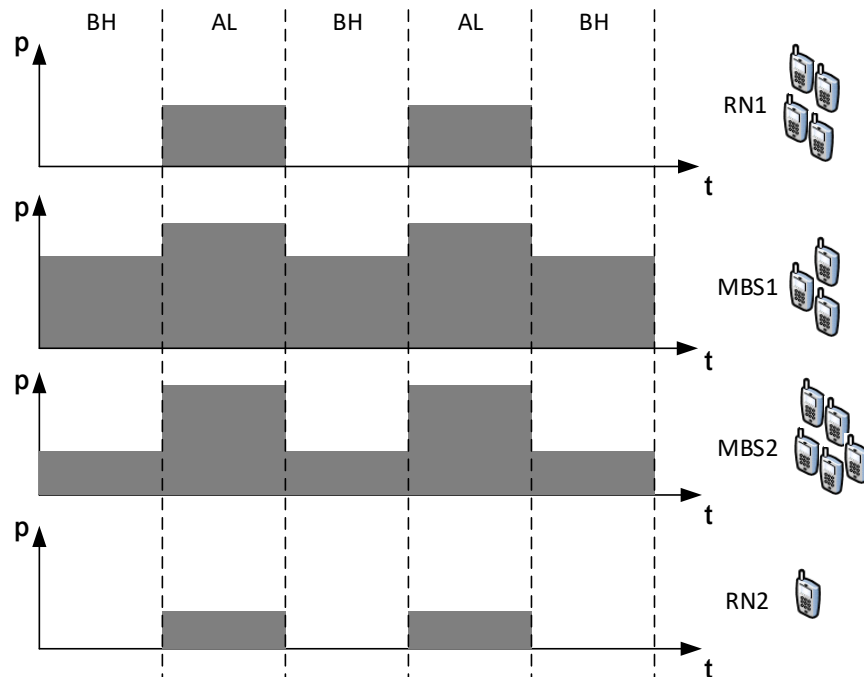


Figure 4.14: Example of possible optimized transmission power configuration over time

Figure 4.15 illustrates how a configuration could look like in the frequency domain.

As already explained in Sec. 4.3.2.4 the GA derives a percentage of subbands, based on the number of MSs and RNs which gain from the configuration. Here, as an example, half of the total system bandwidth is used with the derived optimized power pattern. The other half is transmitted with the default power settings of each serving node, to schedule MSs which have decreased supportable rates through the applied power pattern.

After the final configuration pattern is found, it is applied and the synchronous adapted two-hop proportional fair scheduler takes the newly set power patterns into account depending on the defined scheduling strategies as explained in the following section.

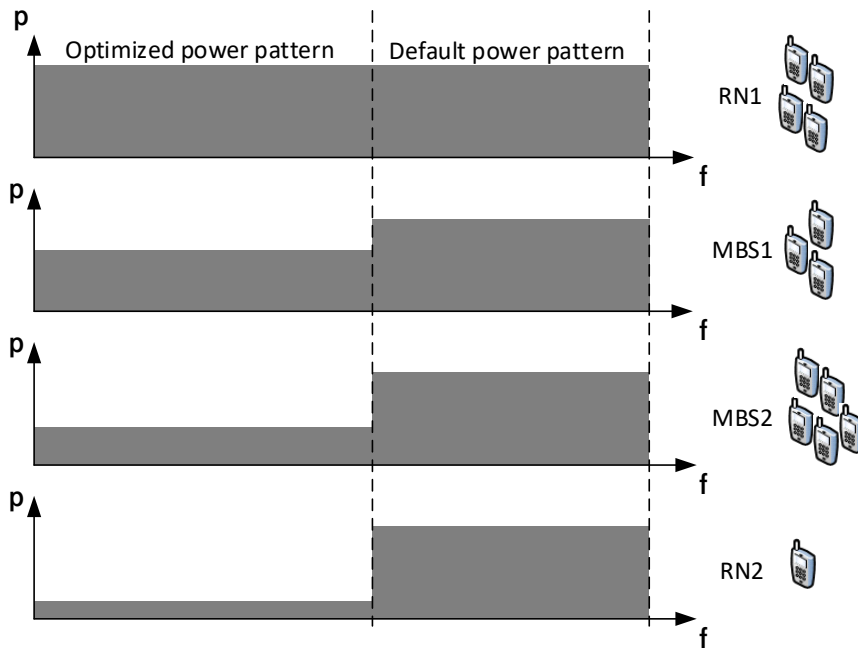


Figure 4.15: Example of possible optimized transmission power subband configuration over frequency in the ALSF

## 4.4 Cell-centralized synchronous adapted scheduling

While the optimization process in the previous section aims to improve the backhaul link of the RNs and thus, the overall network performance by adjusting the transmission power on a subset of subbands for each MBS and RN on a larger time scale, the TTI based scheduling strategy, which will be described in this section, aims to react on short term effects such as small scale fading as well as good performance of the link adaptation to meet the systems target block error rate (BLER). In addition, to this a proportionally fair distribution of the radio resources among users and RNs needs to be fulfilled. Due to the introduced asynchronous optimization, the short term scheduling strategy needs

to take into account the imbalanced power levels and thus, larger variations in terms of SINR on the resources. The asynchronous optimization keeps the newly adjusted relation of power levels stable over a period of time, so that the CQI reports from the MSs are not outdated and the appropriate link adaptation can be performed. However, there are different strategies possible, how to make use of the optimized subbands.

In the following the adapted short term scheduler is described and different strategies are defined to allocate resources of the optimized subbands. Further, different types of two-hop CQI feedback reports are compared which mainly increases the signalling overhead, since the information needs to be collected and fed back from RN to MBS to distribute the radio resources in a proportional fair manner, as discussed before. Finally those are compared by means of SLS presented in Section 5.3. Figure 4.16 shows the flow chart of the TTI based adapted two hop proportional fair scheduling process. In the

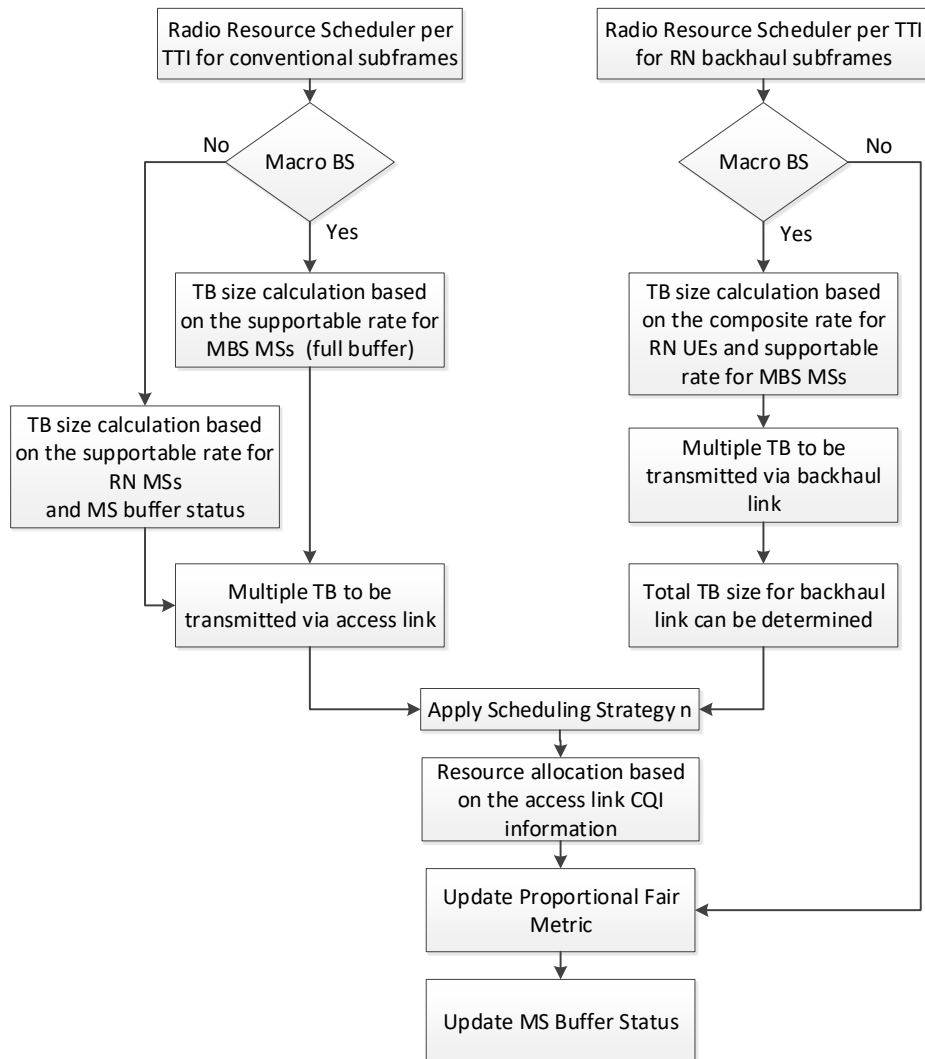


Figure 4.16: Flow chart of the adapted two hop proportional fair scheduler

first step it is determined if either a BHSF or an ALSF is present. In the second step,

either an RN or an MBS is considered in the following scheduling procedure. For simplicity of the figure, the procedure to allocate resources for possible retransmissions is not shown here. In the case of an ALSF and an MBS the Transport Block Size (TBS) of each schedulable MS is determined based on a conventional PF metric, as defined in Equation 2.14 and 2.15 in Section 2.3.7.4. Moreover, the MBS to MS/RN transmission is done with infinite full buffer size, while in the case of an RN to MS transmission in an ALSF only the data is transmitted which was delivered via the MBS-RN backhaul transmission (most left case in Figure 4.16). Therefore, the resource allocation is done under each MSs buffer limitation. The calculation of Equation 2.16 is only done if the buffer size of the MS is larger than or equals the total TBS of the MS. Otherwise the considered MS is excluded by setting the MS specific priorities on the remaining free PRBs to  $-\infty$  in the considered TTI. If the buffers of the remaining schedulable MSs are smaller as well, not all PRBs are used for transmission. This situation relaxes the interference situation on several PRBs but introduces a higher probability of outdated feedback in neighbouring cells which might influence the effectiveness of the link adaptation, when the RN appears as a strong interferer. In case of a BHSF transmission the available PRBs at the MBS need to be shared among one hop MSs and RNs at the MBSs. That is why the adapted two-hop metric with the co-scheduling feature needs to be used as a promising solution. Therefore, the following process which is depicted in Figure 4.17 is performed at the MBS scheduler until the final scheduling decision is taken as granted.

1. Get the schedulable PRBs (after the resources for retransmissions are taken into account).
2. Iterative consideration of each PRB.
3. Resource pre-allocation based all possible one hop and two hop rates.
4. Check if all PRBs are pre-allocated.
5. Calculate the MS specific transport block sizes (TBS)s.
6. Start again an iterative consideration of each PRB.
7. Final resource allocation based on all possible one hop rates.
8. Exclude MS/RN from process if TBS is fulfilled

9. If all TBSs are reached check if any resources are left and allocate them by repeating the process
10. If any TBS is not fulfilled by the process cut to the reached TBS and leave remaining bits for the next TTI

The TBSs during the resource allocation are determined with the MIESM interface which is the used link adaptation algorithm in the DT SLS. For further information the reader is referred to Section 3.3.4.1 and [99, 116, 117].

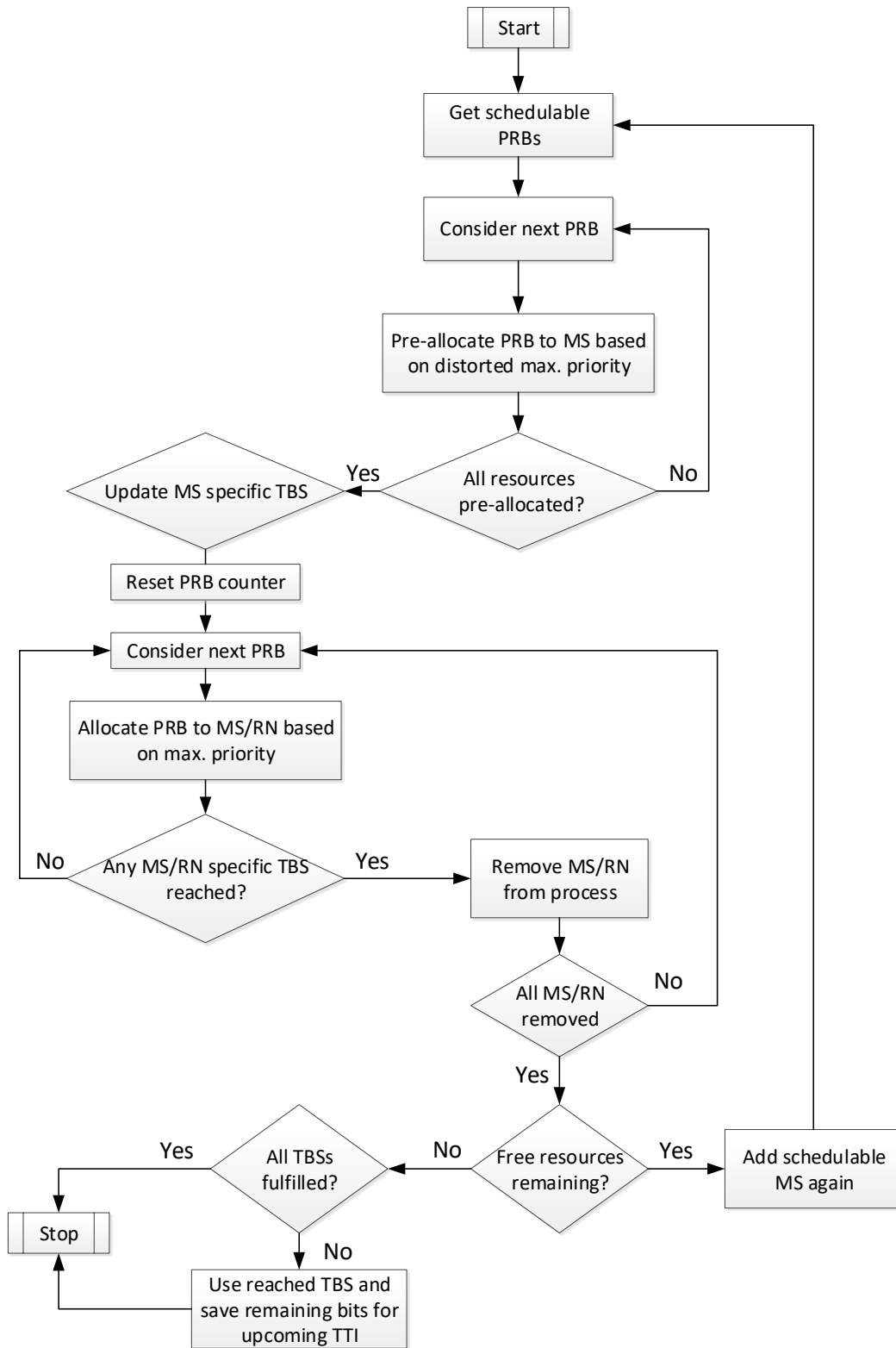


Figure 4.17: Flow chart for the resource allocation considering co-scheduling, two-hop proportional fairness and frequency selectivity

To remind the reader of how the priorities for MBS MSs are calculated the Equation 2.14 of Section 2.3.7.4 is shown again, where  $k$  is the considered user on the  $n^{th}$  PRB in

TTI  $i$ .

$$P_{k,n}(i) = \frac{R_{k,n}(i)}{T_k^\alpha}$$

The composite rate (CR) of the two-hop connections based on Equation 2.17 in Section 2.3.7.5 is extended in Equation 4.24. Due to the introduced buffers and the decode and forward functionality of the RNs all possible combinations between backhaul link and RN access link rates need to be taken into account to derive the most precise scheduling decision. Based on that each RN access link rate of PRB  $m$  is considered in addition, which results in a larger priority matrix  $P_{j,n}$  for the two hop users  $j$ .

$$CR_{j,n}(i) = \left( \frac{1}{R_{n,BH}(i)} + \frac{1}{R_{m,AL}(i)} \right)^{-1} \quad (4.24)$$

Finally, two priorities are calculated with the summed throughput history  $T$  of the access link  $T_{AL}$  and the BH link  $T_{BH}$ . The maximum is used as a priority of the two hop MSs. In most of the cases the priority of the AL might be used, because the MS individual past throughput might be equal or less then the total past throughput of the BH link.

$$P_{j,n}(i) = \max \left( \frac{CR_{j,n}(i)}{T_{j,AL}^\alpha}, \frac{CR_{j,n}(i)}{T_{k,BH}^\alpha} \right) \quad (4.25)$$

Finally, the calculated priorities for one and two-hop MSs are compared and the resources are allocated to the MSs with the maximum priority on each PRB, as in Equation 4.26.

$$P_{k,n}(i) = \max \left( P_{k,n}(i), P_{j,n,m}(i) \right) \quad (4.26)$$

The principle of the adapted frequency selective, proportional fair co-scheduling process is summarized in Figure 4.18. The coloured MS one to three represent two hop MSs while the white coloured MSs are one hop MSs. The blue marked MS1 and the green marked MS2 are attached to the light orange marked RN1. The red coloured MS3 is served by the RN2. On the left side of the figure the pre-allocation decisions are depicted. Then the re-allocation process is done as explained above. Finally the RNs share the resources in one TTIs with the attached one hop MSs. As shown in the figure the final number of the PRBs has not necessarily to be the same as in the pre-allocation process. For instance in the third TTI RN2 has allocated one more PRB than during the pre-allocation process to fulfil the calculated TBS for MS3.

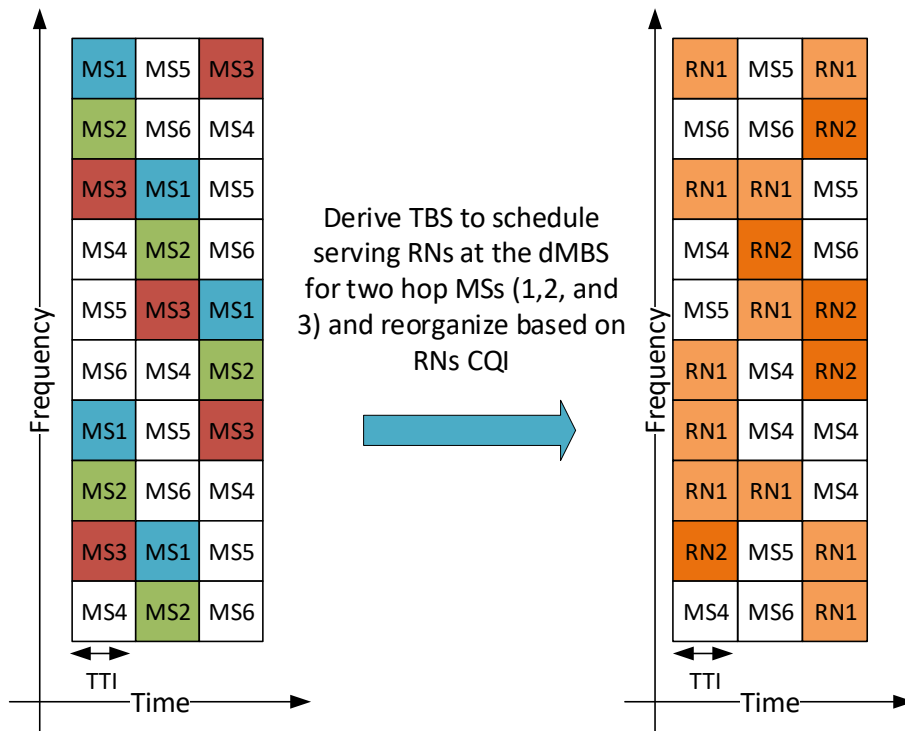


Figure 4.18: Two hop co-scheduling among directly attached UEs and RNs with correct frequency selective decisions

#### 4.4.1 Scheduling strategies for optimized subbands

As already mentioned different scheduling strategies are applied to handle the radio resource allocation to the users for the power adapted subband. Advantages and drawbacks of the proposed strategies are discussed in the following.

Figure 4.19 illustrates the different scheduling strategies compared in this work. For clarification the red and pink coloured MSs did not gain from the centralized power adaptation, while the light and dark green coloured MSs profit from it in this example.

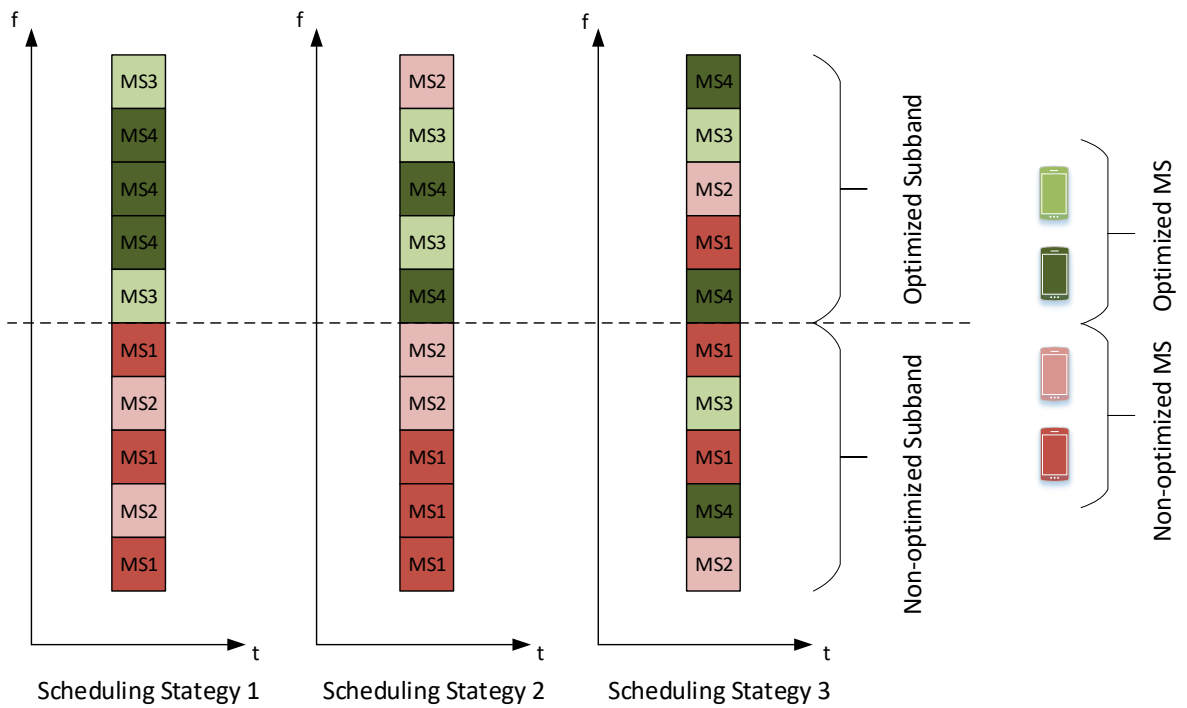


Figure 4.19: Illustration of the compared synchronous scheduling strategies after subband power optimization

The scheduling strategies are defined as follows:

- Scheduling strategy 1:

Only users with previously calculated chance to gain from optimized subband are allowed to use such resources, based on the MS specific individual positive  $\Delta$  supportable rates. If no user with potential benefit is attached to MBS or RNs the resources will be left unallocated. This results in a better SINR in neighbouring cells on the one hand, but higher loss in terms of unallocated radio resources on the other.

As an example, based on this strategy the constellation in Figure 4.19 can appear as follows: MS1 and 2 are exclusively scheduled in the non-optimized subband and MS3 and 4 are exclusively scheduled in the optimized part.

- Scheduling strategy 2:

Users which potentially loose from the optimization process can also make use of the optimized subband if the channel conditions are still favourable for them. It is possible to allocate the total amount of resources independent if transmitted with optimized or default power. This results in a higher variation of SINR values for a single user transmission and thus in potentially less efficient link adaptation. In

contradiction to that the short-term scheduler can achieve higher channel diversity gains.

As an example, based on this strategy the constellation in Figure 4.19 can appear as follows: MS1 and 2 are exclusively scheduled in the non-optimized subband and MS3 and 4 are not exclusively scheduled in the optimized part any more.

- Scheduling strategy 3:

No restriction regarding the radio resource allocation of both parts of the system bandwidth. Users with less rates can also make use of the optimized subband and users with better rates in the improved subbands can also use resources from the non optimized area. On the one hand, possible high SINR variations are not prevented within the user specific transmission. On the other hand, the users might experience higher frequency selective diversity gains if the error rates are not increased due to a worse performance of the link adaptation.

As an example, based on this strategy the constellation in Figure 4.19 can appear as follows: MS1 to 4 are scheduled in the optimized and non-optimized subband.

The performance of the defined scheduling strategies are compared by means of SLS results in Chapter 5.

#### **4.4.2 Numerical examples for the two-Hop proportional fair metric**

Before the two-hop proportional fair metric was adapted during the work of this Thesis is was at first necessary to understand the behaviour of the conventional two-hop proportional fair scheduling metric described in Section 2.3.7.5. Therefore some numerical examples for a simplified network are described as follows.

A network consisting of a single donor MBS with 1 RN and 3 attached MSs is considered in Figure 4.20. MS1 and 2 (marked as blue and black in the following Figures) are attached to the dMBS while MS3 is served by the RN (marked as green). For further simplification only one PRB can be allocated per TTI and the supportable rate per MS is set as a fixed value over time.

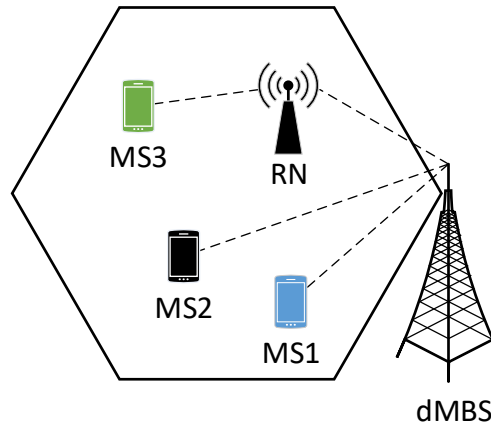


Figure 4.20: Simple network scenario for numerical examples of the two-hop proportional fair metric

In the first example, presented in Figure 4.21 it is assumed, that all MSs have the same supportable rate on the considered PRB. While MS1 and 2 have a direct link supportable rate of 2bps/Hz, two hop MS3 has a supportable rate of 4bps/Hz on both backhaul and access link, to compensate the loss in time based on Equation 2.17, resulting in an end-to-end two-hop supportable rate of 2 bps/Hz, as well. The upper subplot depicted in Figure 4.21 shows the variations of the PF metric over time based on Equation 2.14, 2.15 and 2.16 in combination with 2.17. As it can be observed, the metric compensates the loss over time, under the assumption that the RN can receive only in 60% of the time, represented as the gaps of the green curve for the scheduling metric. Within the sending TTIs only the history information in Equation 2.15 is updated. In the lower subplot of Figure 4.21 it can be observed, that the scheduler allocates equal amount of resources, which is proportional fair in the case when the supportable rate equal to each other. Finally, each MS gets one third of the available resources.

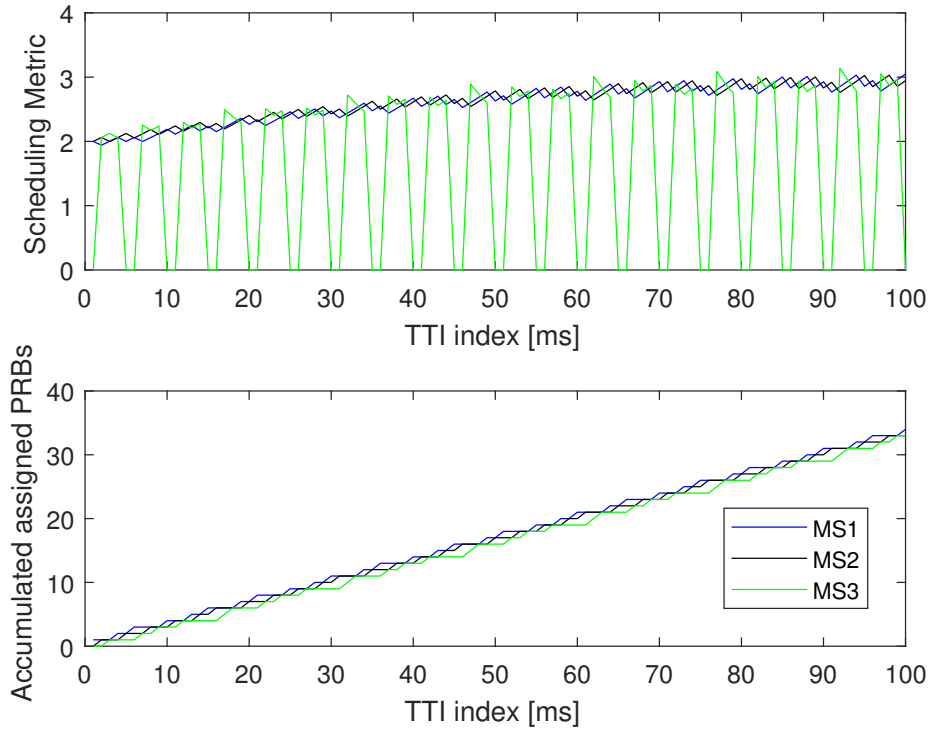


Figure 4.21: Example with equal supportable rates among MSs

Within the next example illustrated in Figure 4.22 it is assumed, that the one hop MS1 has an increased supportable rate of 5bps/Hz. This results in a proportional higher amount of allocated PRBs for MS1. MS1 gets 40 PRBs in total within the considered 100 TTIs, while MS2 and 3 get 30 PRBs each. The metric compensates the loss in time for the two hop MS, as well. Moreover, it could be observed that the proportion of the allocated resources among MSs depends on the forgetting factor  $\beta$ , which is here set to 0.97. The higher  $\beta$  the higher the amount of resources MSs with higher supportable rates get allocated. If  $\beta$  is equal to one no past decisions are taken into account and the metric equals a Max-Min SINR scheduler without considering fairness any more, as described in Section 2.3.7.3. If  $\beta$  would be set to 0 the metric would end in a round robin scheduler, as described in Section 2.3.7.1. Further results for clarification can be found in the Appendix A.

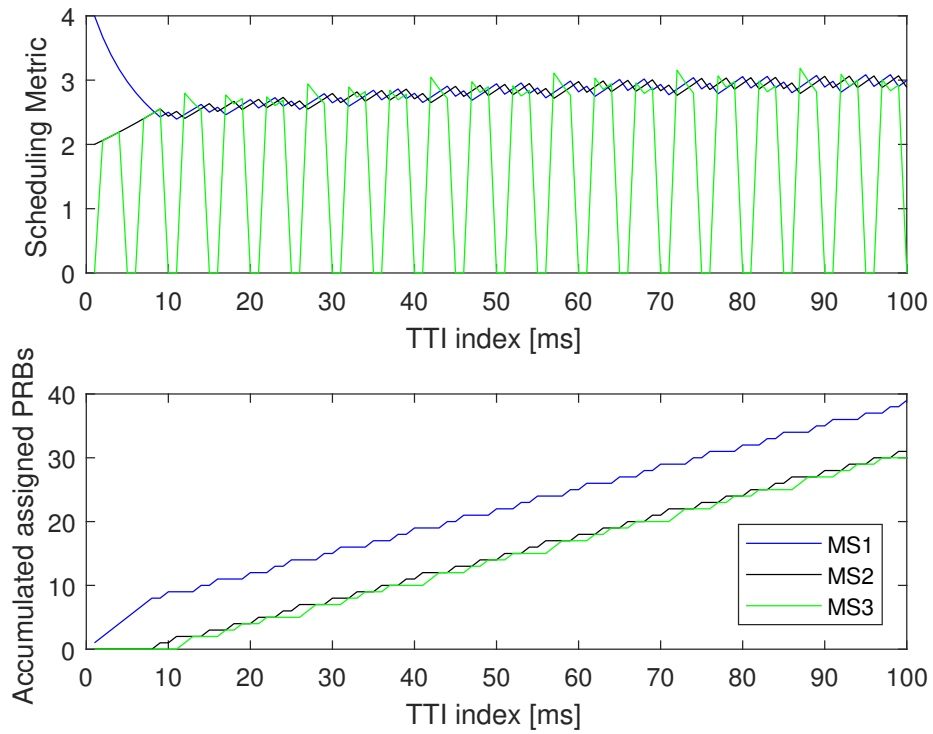


Figure 4.22: Example with higher supportable rate for MS1 and equal supportable rates of MS2 and two-hop MS3

The third numerical example presented in Figure 4.23 shows the outcome of the assumption if the two hop link has the highest supportable rate set to 2.5 bps/Hz, while MS1 and MS2 have only a rate of 2 and 1 bps/Hz, respectively. As it can be observed independent of the loss in time the two hop MS3 gets the highest amount of resources, while MS1 gets more than MS2 due to the higher rate.

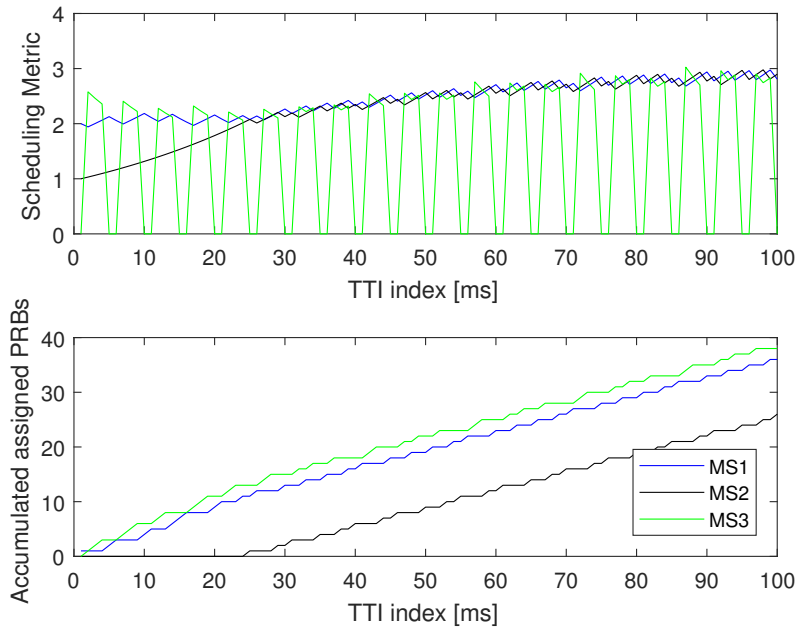


Figure 4.23: Example with higher supportable rate for two-hop MS3 and equal supportable rates of MS1 and 2

In the last example shown in Figure 4.24, an extreme case is considered to show possible limitations for two hop MSs. For instance, the two hop MS has an end-to-end supportable rate of 3bps/Hz which means high supportable rate values on both links. A further assumption is, that both MSs directly attached to the dMBS are cell edge users and only support a supportable rate of 0.11bps/Hz which equals Quadrature Phase Shift Keying (QPSK) with code rate 1/9, which is the lowest possible MCS of the system. It can be seen the limitation of the two hop transmission, due to the maximum number of TTIs for the backhaul transmission. While the two hop MS gets the maximum 60 available PRBs over time during the RN receive TTIs, MS1 and 2 get the left resources in the sending TTIs. In a conventional system typically MS3 as a single hop MS would get all resources until the scheduling metric of one of the cell edge MSs 1 and 2 outperforms the priority. This shows the general limitation for the two hop MSs in the overall maximum achievable data rate in HD extended systems.

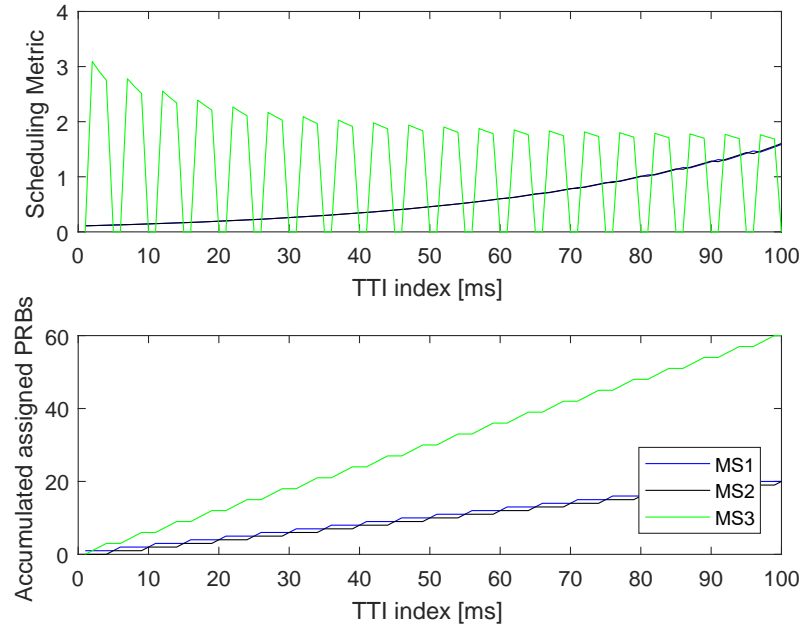


Figure 4.24: Example with highest supportable rate for two-hop MS3 and equal lowest supportable rates of MS1 and 2

## 4.5 Additional signalling and overhead consideration

When frequency selective scheduling is applied, typically subband CQI reports are used to gain knowledge of the channel states and derive a resource allocation decision with better resource utilization. Typically, in conventional networks the MSs take measurements and send back the reports to the MBSs where the radio scheduler uses the reports to derive a decision. In RN extended networks, it is additionally necessary to feedback the reports from RNs to the dMBS for all MSs attached to the RN. This can heavily increase the additional signalling overhead in the uplink (UL) and influence the performance. Besides that, the control signalling overhead is already increased, as different subframe types occur and the MBS needs accurate information of the subframe (SF) types. For instance, if periodic CQI reporting is assumed, the MS needs to generate at least two CQI reports per frame, one for each occurring SF type, where different interference situations appear and additionally different optimized power patterns are applied as described in the previous Section 4.1. The MS/RN specific reports consist of a defined number of subband reports including MCSs recommendations among other information as described in Section 2.2.3. The reports of all two-hop MSs need to be collected and sent back to the MBS. To reduce this potential large amount of overhead, different types of reports with reduced amount of overhead are compared in this Thesis. The reference case assumes a full multiple

subband report for frequency selective decisions as input for Equation 2.17. Alternative RN to MBS feedbacks with a potential overhead reduction are used and compared in terms of throughput, SINR and fairness in Section 5.3.1. Instead of frequency selective subband CQI reports either the recommended maximum or average supportable rate for the RN access links is forwarded to the corresponding dMBS. This reduces the amount of signalling by  $\frac{1}{N}$ , where N is the defined number of subband reports per MS. For further clarification it should be kept in mind, that the actual scheduling decision at the RN is still done in a frequency selective manner based on RN MSs' CQI feedback to the RNs as explained in Section 4.4.

In the following Table 4.1 a summary of the necessary additional feedback for the proposed hybrid RRM scheme is listed. It is distinguished between the defined three sub-problems. Figure 4.25 illustrates the required feedback for the hybrid RRM scheme of this Thesis.

Table 4.1: Summary of the required additional feedback information for the hybrid RRM scheme

<b>Sub-problem</b>	<b>Parameter description</b>	<b>Value</b>
1. Decentralized cell-selection	RSRP of the backhaul link needs to be broadcasted by the attached RNs to the MSs	7 bits for one dBm step wise resolution. In total 128 values possible (e.g. in LTE-A typically broadcasted every 40ms)
1. Decentralized cell-selection	Time ratio between backhaul and access link needs to be broadcasted by the attached RNs to the MSs	3 bits to define the ratio (e.g. in LTE-A the maximum BH transmission time per frame is 60%. See Section 3.5.3)
2. Cell-centralized synchronous RRM	Recommended second hop maximum MCS indices need to be forwarded from RN to dMBS	5 bits per two-hop MS with a periodicity like the CQI feedback (e.g MCS index 0 - 32 every 5ms)
3. Network cell-centralized asynchronous RRM	RSRP of the backhaul and access links to be fed back to the central unit (CU)	7 bits per link with a one dBm step wise resolution (e.g 128 values possible (e.g -30 to -158dBm) with a periodicity of 300ms)

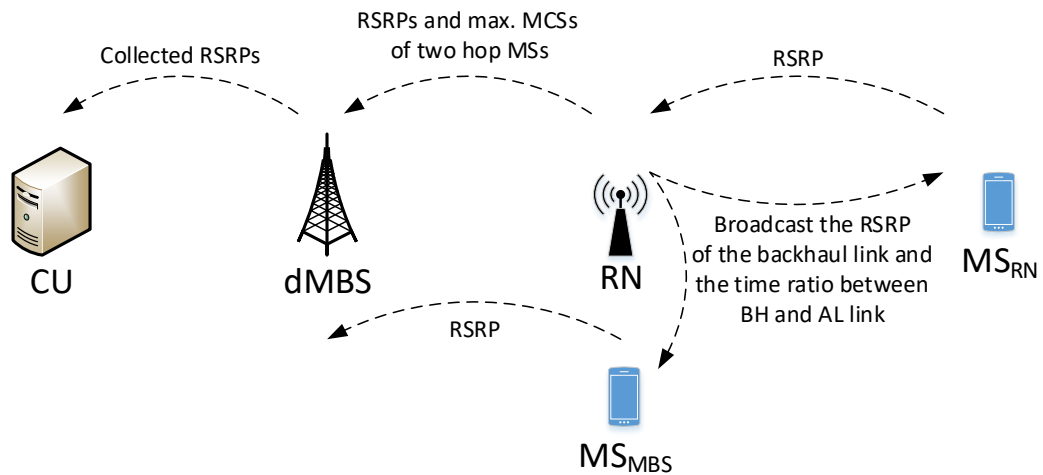


Figure 4.25: Required signalling for the proposed hybrid RRM scheme

## 4.6 Summary

In this Chapter the major contributions of this Thesis have been described. The general problem formulation defined in Section 2.3.2 is decomposed in three sub-problems to be able to improve the system capacity in a realistic large scale RN-extended OFDMA network.

- The first sub-problem is defined as a adapted cell selection procedure discussed in Section 4.2. The cell selection is done under the consideration of the available backhaul and access link TTIs. In addition to that the cell selection scheme considers the link qualities of all links and takes into account the higher importance of the non-ideal backhaul link quality for the two hop transmissions by the introduction of an additional weighting factor. This is the decentralized functionality of the hybrid RRM scheme.
- The second sub-problem is defined in Section 4.3 as a heuristic which adapts the transmission power of MBS and RNs based on RSRP values, to improve the backhaul link quality for RNs while keeping link qualities for the users attached to the MBSs stable. This is the network centralized part of the proposed hybrid RRM scheme.
- Finally the third sub-problem is defined as the adapted two-hop proportional fair scheduling metric and the cell-centralized part of the hybrid RRM scheme. The scheduler allocates resources in a proportional fair manner under consideration of

frequency selective correct decisions and buffer limitations with a very high degree of freedom using the co-scheduling functionality, as defined in Section 4.4.

# Chapter 5

## Performance analysis

In this section, the assumptions and results of the carried out SLS analysis for the proposed hybrid radio resource management (RRM) scheme are presented. A flow chart of the applied system level simulations is illustrated in Figure 5.1 with respect to the decomposed sub-problems of the hybrid RRM scheme defined in Chapter 4 in this Thesis. It has to be mentioned that the schemes for the sub-problem one and three is recalculated only once per MS drop, as the adapted cell selection scheme and the adapted transmission power pattern is set for the whole snapshot loop. In contradiction to that, the sub-problem two is re-calculated in each snapshot, TTI, respectively.

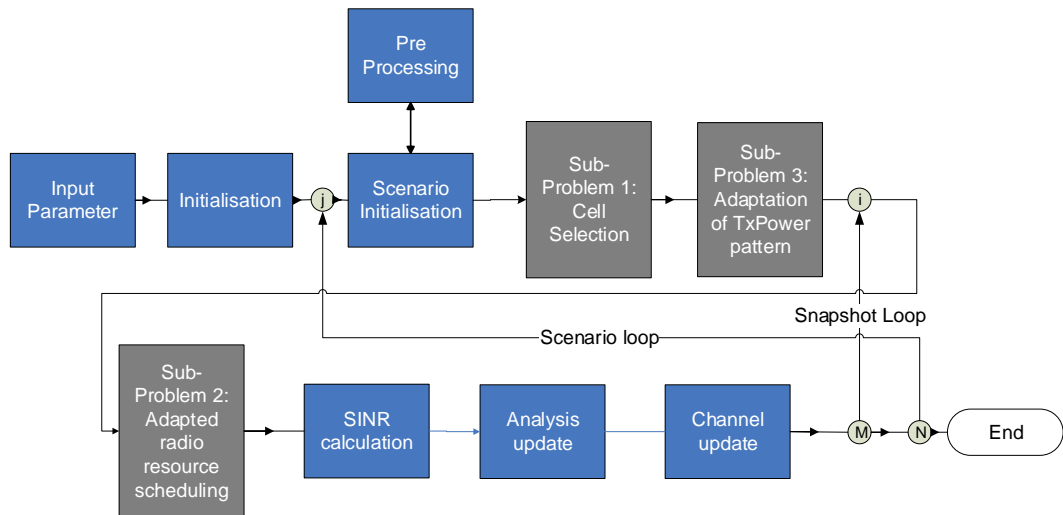


Figure 5.1: Principle flow chart of the DT SLS with respect to the hybrid RRM scheme

For the analysis the used example network scenario consists of the following.

## 5.1 Assumptions of the network scenario

In each sector 4 RNs are placed randomly with a minimum distance of 40m to each other. Each cell sector is equipped with a 3D directional antenna with a 3dB horizontal beamwidth of  $70^\circ$  and a vertical 3dB HPBW of  $10^\circ$ . The transmitting antennas of the RNs and the receiving antennas of the RNs/MSs are omni directional. A hotspot MS distribution with 30 MSs in average per cell is considered.  $2/3$  of the users within a macro cell sector are dropped into the defined hotspots. The remaining MSs are dropped randomly across the cell area. A hotspot occurs in the vicinity of the RNs. As an example, Figure 5.2 shows one MSs/RNs drop of the simulated RN extended LTE-A network with 19 hexagonal cell sites and 3 sectors per site. The RNs are marked as blue in the macro sector areas while the MSs are marked as red.

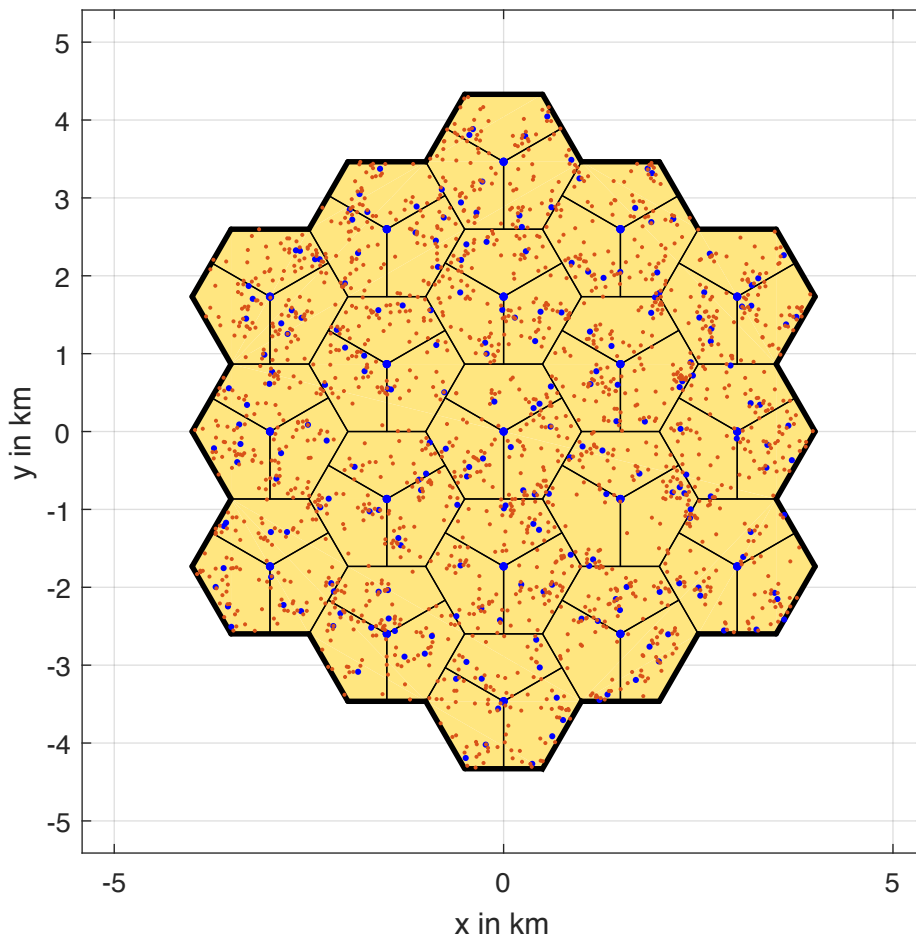


Figure 5.2: Network Layout, 19 MBSs, 3 Sectors/Site, e.g. 4 RNs per Sector

The cell selection scheme of the MSs is based on the comparison of one and two-hop adapted supportable rates based on Equation 4.4, 4.7 and 4.8, which enhances the end-to-end optimal routing strategy proposed in [73] as explained in Section 4.2. To prevent

border effects, the wrap around technique is applied. The WINNER+ sub urban macro (SUMa) channel model is used for the MBS-MS direct links (DL) and the MBS-RN backhaul links (BH). For the RN-MS access link (AL) the urban micro (UMi) channel model is used. The LoS probability of the MBS-RN BH link is slightly increased as a higher antenna height is assumed for the deployed relays compared to the MSs, according to [29,98].

It has to be kept in mind, that the chosen scenario is a very challenging, but one of the most realistic scenario for RN deployments. On the one hand RNs deployed at user hotspots give a very high probability to provide excellent AL channel quality. On the other hand, due to the random placement of the user hotspots and the RNs in its vicinity it can happen that the hotspot occurs in the main beam direction of the MBS antenna. In such scenarios it is quite unlikely that RNs might outperform the direct link performance, even if in such scenarios the backhaul link quality will be excellent as well. In a nutshell the chosen scenario is one of the most realistic but also one of the most challenging ones to outperform the conventional MBS network. Within the applied 2x2 MIMO system a brute force algorithm is used to create the CQI report of each MS. Based on the best derived SINRs of all possible transmission modes and codebook based precoding matrices the MCS, RI and PMI indices are chosen and the subband CQI report is created. A CQI feedback delay of 5ms is assumed until the report can be taken into account at the serving node (MBS or RN). In addition the derived feedback delay model for the two-hop information throughout this Thesis is applied, which is defined in Section 3.5.4. The MSs attached to MBSs are instructed to generate two CQI feedback reports, during the RN reception and transmission times.

For the link adaptation (LA) the mutual information effective SINR mapping (MIESM) interface is used according to [99]. Based on the subband CQI indices which are fed back by the MSs the scheduler of each serving node estimates the corresponding SINR values and calculates an effective SINR for the allocated PRBs of each specific MS. Based on that a preferred MCS is chosen for the transmission. A full buffer at the MBS and a resulting limited buffer traffic model at the RNs is used. MS individual buffers are used at each RN. For all link types the LTE-A corresponding HARQ retransmission procedure is applied based on the chase combining model. In Tab. 5.1 the most important simulation assumptions are summarized which follow [98].

Table 5.1: System Level Simulation Parameters

<b>Parameter</b>	<b>Value</b>
Cellular Layout	Hexagonal grid, 19 sites, 3 sectors per site
Inter Site Distance	1732m (3GPP sub urban case)
Carrier Frequency	2 GHz
System Bandwidth	10MHz, Downlink FDD
MBS TxPower	46dBm
MBS antenna pattern	3GPP 3D Ant. Model with 16dBi max. gain
RN, MS height	5, 1.5m
RN Tx Power	30dBm
RN Tx antenna pattern	Omni directional with 0dBi gain
RN Rx antenna pattern	Omni directional with 0dBi gain
No. of RN backhaul sf	6 out of 10 (Non-exclusive BS-RN transmission)
Propagation Model	Distance dependent model according to [98]
Channel Model	WINNER+
No. of RN per cell	4
RN location	Random without planning gain
MS distribution	2/3 hotspot at RN, 1/3 randomly distributed
MS velocity	3km/h
Avg. number of MSs per cell	30
Scheduler	Adapted 2 Hop Proportional Fair
Transmission schemes	2x2 MIMO (Closed Loop SU-Beamforming, Spatial Multiplexing)
Supported MCS	LTE Rel.12 (QPSK - 256 QAM) [95]
Traffic Model	Full buffer @ MBS, limited buffer @ RN
CQI feedback	periodic subband CQI (5PRBs per group) (MCS, RI, PMI index) for ALSF and BHSF
Link Adaptation	MIESM based on [99]
Control Channel Overhead	MBS: 3 symbols (DL PDCCHs per SF) RN: 3 symbols (1 DL R-PDCCH, 1Tx-Rx, 1Rx-Tx switching per SF) plus demodulation of reference symbols

Regarding the proposed network-centralized GA defined in Section 4.3, the number of generations and individuals, the applied crossover type, the derived mutation rate and the defined fitness functions are used, as listed in Table 5.2.

Table 5.2: Summary of the parameters applied for the network-centralized scheme

Parameter	Value
Fitness Function type	Eq. 4.18 and 4.19
Number of generations	400
Number of individuals	160
Parental selection	Fitness proportionate, exp. factor equals 4
Crossover inheritance type	Random one point
Mutation rate	0.05
TX power adaptation values (PAV)	-46, -40, -30, -20, -10, -6, -3, -2, -1, 0dB

## 5.2 Studies of important aspects in RN extended networks

In this Section two studies are presented considering the comparison of different cell selection schemes and the co-scheduling functionality to show the potential benefit of both as discussed in Section 4.2 and 4.4. For the final results the best cell selection scheme and the co-scheduling functionality has been applied to result in the highest possible improvement of the MS throughput under fairness constraints.

### 5.2.1 Comparison of different cell selection metrics

As discussed in Section 4.2 a novel cell selection scheme is proposed in this Thesis. In addition to the varying interference situations of the possible one-hop connections to the MBSs it takes into account possible link quality imbalances between the backhaul links and the access links of the possible two-hop connections to the RNs.

Figure 5.3 shows the assignment rates for the three considered cell selection schemes. The RSRP based selection is done as in a conventional MBS network, illustrated as the black coloured bar. The cell with the highest received serving link power is used to attach the MSs without considering the backhaul link quality of the RNs. Based on that, 50.91% are attached to one of the deployed RNs in the applied scenario.

The blue bar represents the MS assignment rate in the case of the end-to-end optimal routing scheme based on the composite rate (CR) which has been described in Section 2.3.6. The scheme takes into account the quality of the backhaul links but not the possible imbalance of transmission intervals for each possible two-hop link. Further it does not take into account the different interference situations of the possible one-hop connections and the higher importance of the backhaul link quality, which is considered as the bottleneck of the possible two-hop connections. 41.02% of the users in the network have been

attached to the relay nodes with this cell selection procedure.

Finally, the light blue bar shows the MS assignment rate when the proposed scheme of this Thesis is applied. The MSs which have selected an RN as the serving cell have been reduced to 31.73%. As already explained in the considered scenario an unplanned RN deployment is assumed with no planning gains and no backhaul improvements without applying the proposed network-centralized scheme. Therefore, the possible two-hop connections provide a lower probability to outperform the possible direct links. In addition to that it is quite likely that the possible two-hop connections provide an excellent channel quality on the access link but lower quality on the backhaul connection. This is now taken into account in the proposed cell selection scheme which has been described in Section 4.2.

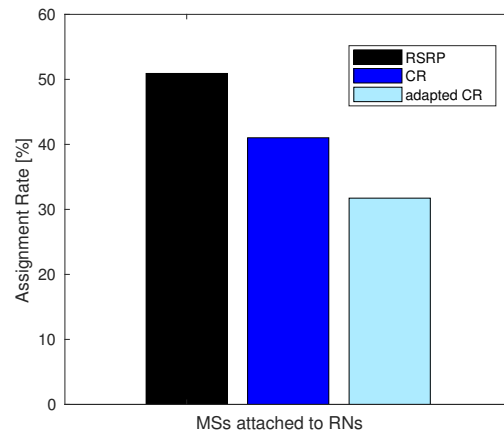


Figure 5.3: MS Cell Selection Rates for the RSRP, the CR and the adapted CR metric

The Figure 5.4 shows the comparison of the MSs throughput and the fairness for the three considered cell selection schemes. It turns out that in the considered RN deployment scenario the proposed cell selection scheme outperforms the RSRP and the CR based schemes. Especially below the 65 percentile in the CDF of the overall MS throughput the proposed scheme provides a better performance. The lower amount of MSs which are served by the RNs profit from the proposed scheme below the 55 percentile due to the aforementioned reasons. Furthermore, the RN backhaul connection needs to transport more data to the higher number of attached MSs in the case when the RSRP based selection is applied. Due to that a higher number of resources is used to serve the relays. On the one hand the users attached directly to the MBS suffer from less available resources but on the other hand a lower amount of users need to be served directly by the MBSs. This compensates the potential loss specially in the TTIs when relays are in the sending

mode and the MSs at the MBSs can be served exclusively. In the right figure it can be observed that the proposed cell selection scheme provides a better fairness, as the CDF is shifted to the right below the 65 percentile and shifted to the left above the 90 percentile.

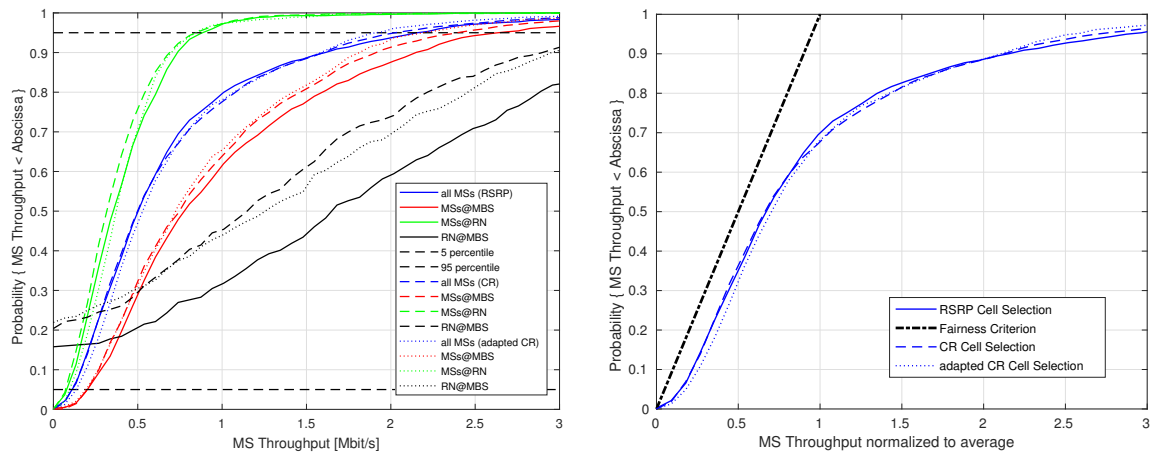


Figure 5.4: Throughput and fairness of all MSs and RN BH for the different cell selection metrics

It is also interesting to see, that the CR based scheme does not outperform the conventional RSRP based cell selection. This can be explained by the imbalanced link qualities of the backhaul and access links. There are still too many MSs attached to RNs due to the high access link qualities while the backhaul link cannot transport enough data to the RNs to gain from it.

Based on the improved fairness and throughput below the 65 percentile the proposed adapted cell selection scheme is used for the following analyses.

## 5.2.2 Comparison of exclusive backhaul scheduling and co-scheduling

In Section 2.3.7.6 the co-scheduling functionality has been identified as an important feature to increase the flexibility of the possible radio resource scheduling decisions at the MBS. The scheduler is able to schedule the attached RNs and MS in a frequency selective manner in the same TTIs. A comparison of the simulation results when the co-scheduling functionality is either disabled or enabled is presented in Figure 5.5. It is assumed, that 60% of the TTIs are used for the backhaul subframes, which is the maximum possible value in LTE-A, as explained in the Section 3.5.3. In the left figure the MS throughput is shown. It can be observed that in the case of exclusively scheduling the RNs at the MBSs (dashed lines) the transmitted data over the backhaul link is much higher than for the co-scheduling case (solid lines). The two-hop MSs profit from that very much (green dashed

line). The users served by the MBSs (red lines) suffer from it as not enough resources are available to serve them in a fair manner. The overall MS throughput performance (blue lines) shows that approximately below the 60 percentile the users suffer from the exclusive backhaul scheduling, while above the 60 percentile the users gain from it. The users below the 60 percentile are mainly the macro cell users. An increased outage probability can be observed for the macro users considering the intersection with the y-axis of the dashed red curve. Overall, this results in a worse fairness situation of the network, which can be seen in the right Figure. The co-scheduling feature provides a much better fairness (solid blue line).

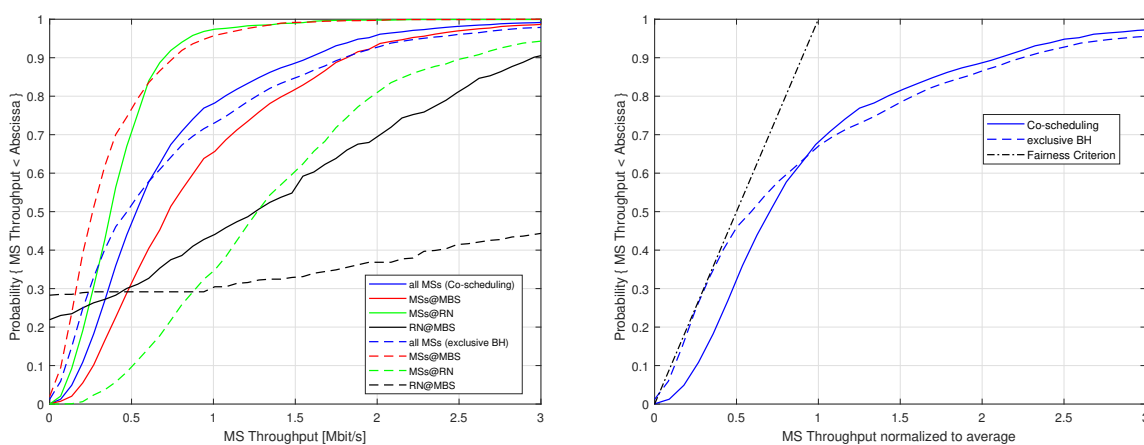


Figure 5.5: Throughput and fairness of all MSs and RN BH for with and without co-scheduling functionality

For the final results the co-scheduling functionality is enabled to improve the fairness of the network.

### 5.3 Final results of the hybrid radio resource management scheme

In the following the final results of the Thesis are presented. A comparison of the resulting MS throughput, SINR, fairness and potential energy savings on the DL physical shared channel is described in the following. In the reference simulation a conventional MBS network is considered and compared to the results of the proposed hybrid RRM scheme in this Thesis.

In the first step, the scheduling strategy based on the decentralized adapted two-hop proportional fair metric, defined in Section 4.4 is enabled, while the centralized heuristic

algorithm is disabled. To reduce RN signalling to the MBS a comparison is carried out for the different aforementioned signalling information. Finally the network-centralized algorithm is additionally enabled based on the defined fitness functions in Equation 4.18 and 4.19, as described in Section 4.3 and further defined as o1 and o2.

### **5.3.1 Throughput comparison of different two-hop MS feedbacks forwarded from RN to MBS**

The Figures 5.6 and 5.7 show the comparison of the CDFs for the MS specific throughput. For further clarification it is distinguished between three user groups and the RN backhaul performance within each simulation run. The light grey coloured curve is set as the reference MBS network performance results. The blue coloured CDFs are dedicated to the total amount of MSs served during the simulation run in the heterogeneous deployment. Obviously the wireless RN backhaul throughput is excluded here. Therefore, the black coloured CDFs show the RN wireless backhaul link performance. The red coloured curves refer to the users attached to the MBSs, while the green CDFs represent the user performance served by the RNs. Further it is distinguished between different RN to MBS forwarded feedback information. As described in Section 4.4 the additional signalling traffic is defined as the full CQI report which includes frequency selective subband information (FSS), while the reduced signalling is either the maximum (MAX) or average (AVG) recommended MCS of the individual two hop user. A further explanation can be found in the legend of the corresponding results.

The Figure 5.6 shows clearly the higher performance for the heterogeneous network compared to the reference. An average gain of approximately 18% can be observed at the 60 percentile of the CDF. The performance is kept stable, when the lower signalling overhead is used. Additionally it can be observed, that in the case of the results with AVG feedback slightly improves the performance below 60 percentile, while decreasing a bit above it. This may come from the fact that RN MSs are slightly higher prioritized, when the MBS allocates the resources to either direct users or RNs. This is also confirmed due to the higher RN backhaul throughput in the case of the reduced overhead illustrated as the black curves. In addition it can be observed in Figure 5.7 that the RN MSs experience a higher throughput in case of AVG or MAX feedback while the MBS MSs' throughput is slightly decreased. Furthermore, the RN MSs throughput is well below then for the MBS MSs since only the worst MSs are served by the RNs, keeping the applied adapted cell

selection scheme in mind.

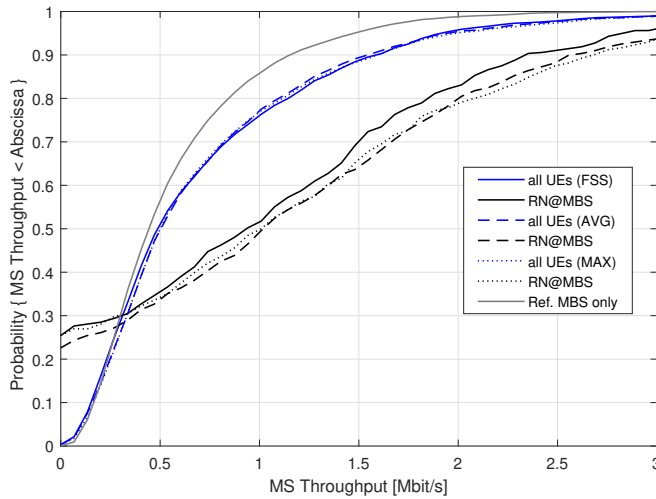


Figure 5.6: Throughput of all MSs and RN BH with different RN AL CQI feedbacks

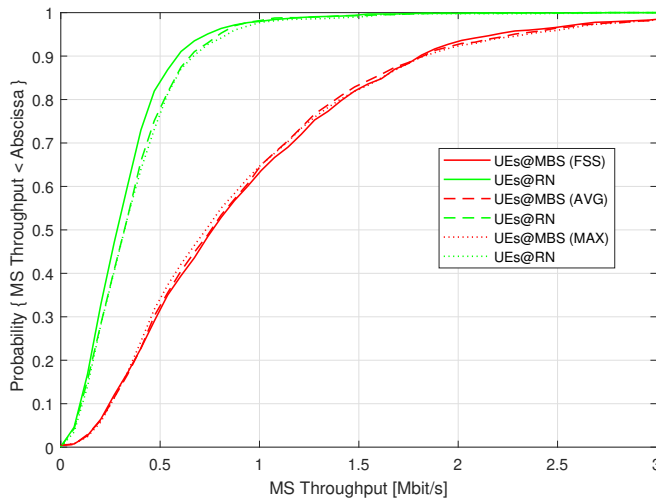


Figure 5.7: Throughput of MBS and RN MSs with different RN AL CQI feedbacks

### 5.3.2 Throughput comparison with different fitness functions and scheduling policies

In the next step the network-centralized heuristic is enabled. In the first part fitness function  $\phi_1$  is used and the results are shown in the Figures 5.8 and 5.9. Unfortunately, the optimization approach doesn't clearly outperform the previous explained results. Due to the design of fitness function  $\phi_1$ , there are too many counteraction terms in the equation, which wipe out possible gains. In this case, the different scheduling strategies based on Section 4.4.1 does not show significant influence in the performance with the defined fitness function  $\phi_1$ . It can be concluded that, the network-centralized heuristic did not derive

a proper power reduction pattern. However, the performance is kept stable and at least no decreased throughput is observed.

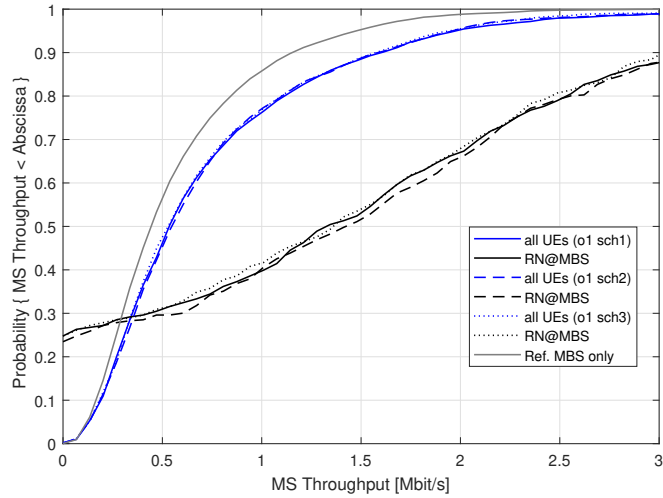


Figure 5.8: Throughput of all MSs and RN BH with fitness function o1 and scheduling policy 1,2 and 3

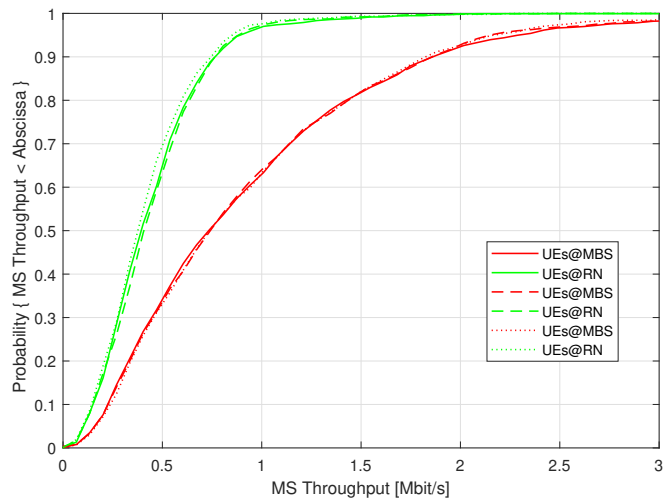


Figure 5.9: Throughput of all MBS and RN MSs with fitness function o2 and scheduling policy 1,2 and 3

As an alternative, fitness function o2 is now enabled and presented. As already described in Section 4.3 the design of the fitness function is much more aggressive to find a promising subband power reduction pattern. Only the possible improvement of the RNs in the backhaul subframes and the MBS MS improvements in the access link subframes are in focus without the consideration of possible losses of MBS MSs during backhaul subframes and RN MSs in the AL subframes. Figure 5.10 shows the performance comparison when fitness function o2 is applied in combination with the proposed scheduling

strategies. It can be observed the best performance when scheduling strategy 2 is used. To remind the reader strategy one leaves the radio resources free, when no MS individual  $\Delta$  supportable rate promises possible gains in the considered cell. On the one hand, this might improve the SINR in the surrounding cells but decreases the number of available resources to be scheduled to MS/RNs. Scheduling strategy 2 provides access to all available resources for the non-optimized users. In contrast to this scheduling strategy 3 gives the opportunity to allocate resource to every single MS from both resource regions. As can be observed scheduling strategy 2 outperforms 1 and 3. A closer look discloses, that scheduling strategy 3 slightly outperforms one. The difference between 2 and 3 is explained by the higher SINR variance in case of strategy 3 for a single MS. The link adaptation targets a BLER of 10 percent to provide best performance of the network. In case of strategy 3 the target BLER was narrowly missed due to higher SINR variations on the transport blocks. In Figure 5.11 it can be observed, that especially in case of the MBS MS throughput the performance strategy 2 outperforms 1 and 3. For the RN MSs the difference between strategy 2 and 3 can be neglected, as the RN MSs are buffer limited and rarely use both bandwidth parts simultaneously due to the smaller Transport Block Sizes (TBS)s.

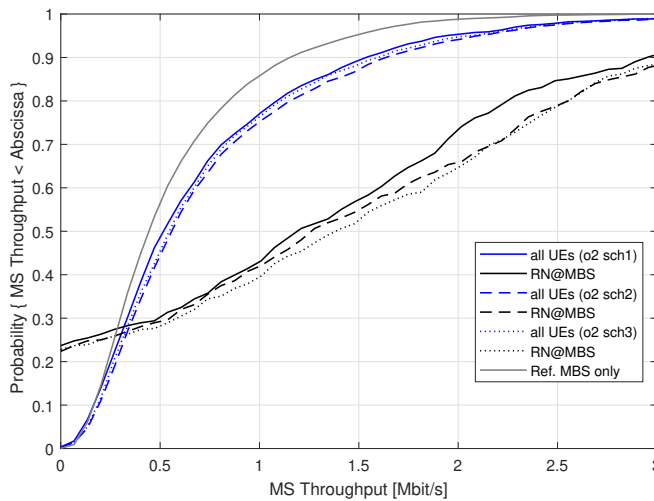


Figure 5.10: Throughput of all MSs and RN BH with fitness function o2 and scheduling policy 1,2 and 3

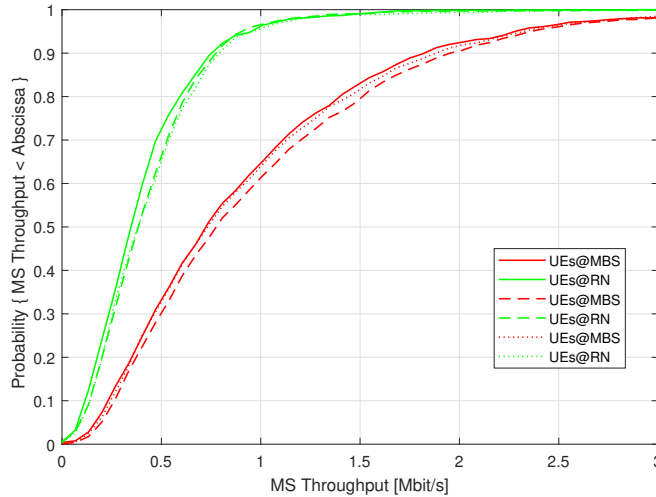


Figure 5.11: Throughput of all MBS and RN MSs with fitness function o2 and scheduling policy 1,2 and 3

### 5.3.3 Final comparison for best feedback, power reduction pattern and scheduling settings

Figure 5.12 shows the final result of the comparison in this Thesis. The user throughput for all distinguished user groups is shown. It can be observed, that much more data is transmitted to the RNs when the GA was applied (black solid vs. dashed curves). This comes from a higher prioritization of the RN backhaul transmission after the optimized power adaptation. A clear throughput gain can be observed for all users when the hybrid RRM approach with fitness function o2 and scheduling strategy 2 is applied. At 60 percentile which represents the average throughput, approximately 10 percent gain is reached, without any loss in other regions. From 0 to 100 percentile the CDF runs on the right side compared to the cell-centralized approach. This result gives a clear impression that the genetic algorithm optimized the backhaul link quality (improved throughput of RN MSs) and additionally compensated possible losses for the macro users in the second subframe type when RNs are receiving. Even for the MBS MSs the performance is increased, when the interference situation is adapted by the network-centralized scheme.

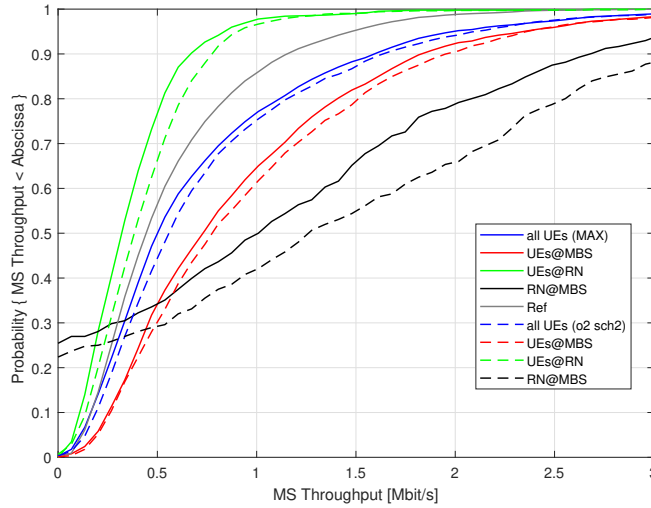


Figure 5.12: Final Comparison of the UE and RN throughput for reduced feedback based on max value and fitness function o2 with scheduling policy 2

### 5.3.4 SINR comparison for best settings

To give some more insights how the system behaves the SINR values for the best derived hybrid settings (MAX feedback, fitness function o2 with scheduling strategy 2) are analysed. The SINR values are calculated on 3 subcarriers per PRB depending on the applied power per PRB, used transmission mode (spatial multiplexing or single user beamforming), channel variations in time and frequency, and codebook based precoding vectors (PMI) used for each individual transmission. Here, the CDF shows the individual sub-carrier related SINR per link type. In Figure 5.13 the comparison of the SINR values for the RN backhaul (BH) links (black curves) are presented when the centralized scheme is enabled compared to the best found cell-centralized result. A clear gain of approximately 2.2dB in average (60 percentile) can be observed for the BH due to the applied optimized transmission power pattern. Furthermore in Figure 5.14 the CDFs of SINR for the total amount of MSs (blue curves) is illustrated. The dashed dark blue CDF (fitness function o2, scheduling strategy 2) clearly shows a higher improvement than the solid blue curve representing the cell-centralized approach compared to the reference simulation result.

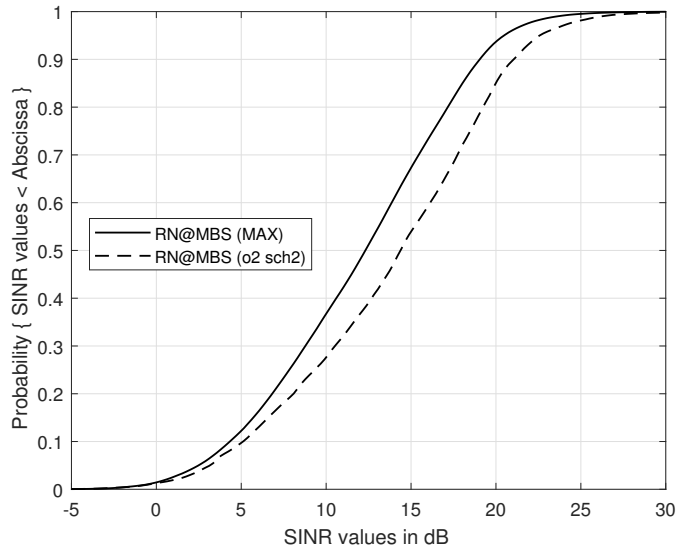


Figure 5.13: Comparison of the RN BH SINR values for reduced feedback based on max value and fitness function o2 with scheduling policy 2

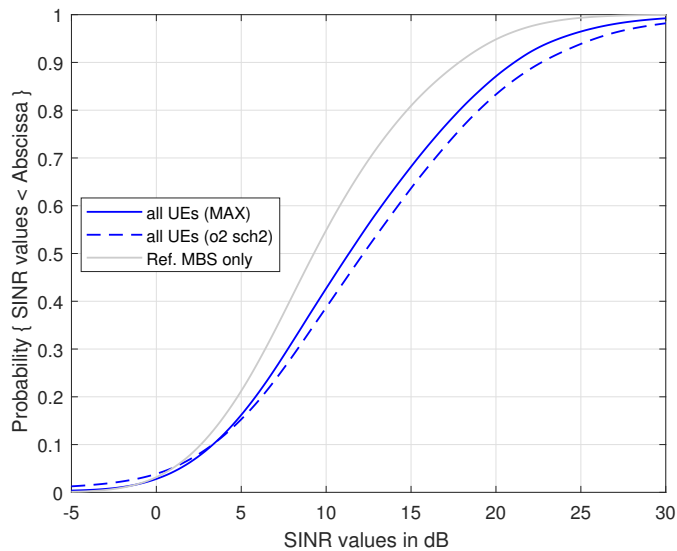


Figure 5.14: Comparison of the MBS and RN UE SINR values for reduced feedback based on max value and fitness function o2 with scheduling policy 2

In Figure 5.15 the SINR values for the two user groups are depicted. The red curves represent the MSs attached to the MBSs, while the green curves show the behaviour for the MSs at the RNs. As required no degradation for the MBS MSs can be seen. Even a slight SINR improvement of roughly 0.5dB is observed as mean value (approximately 60 percentile) for the GA with scheduling strategy 2. For the RN MSs decreased SINR values are observed below 80 percentile. This comes from the defined fitness function, which tries to compensate the potential loss in the backhaul subframe for MBS MSs by reducing the interference. Above 80 percentile, the SINR it is slightly improved. However, the loss

in the RN access link did not result in a performance degradation, due to the applied reuse one scheme, which means that all RNs have access to the total system bandwidth to serve their MSs. Thus, the lower SINR will be compensated with higher amount of resources in use at the RNs. This is also confirmed considering the results in Figure 5.12. Due to the improved SINR on the backhaul link, the RNs are higher prioritized to be scheduled and thus, the RN MSs profit from that in terms of increased throughput. In the overall SINR consideration depicted in Figure 5.14 only below 5 percentile the SINR is decreased due to the aforementioned effect on the RN-MS links, without any loss in the throughput performance.

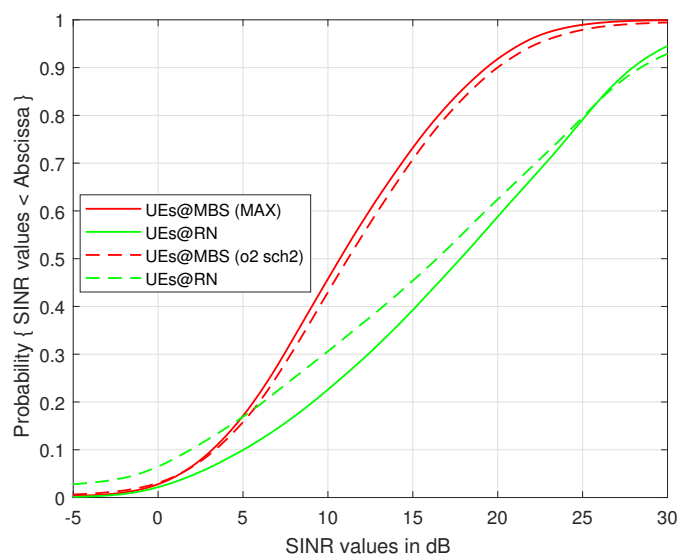


Figure 5.15: Comparison of the MBS and RN UE SINR values for reduced feedback based on max value and fitness function o2 with scheduling policy 2

### 5.3.5 Fairness comparison for best settings

The fairness index is defined according to the 3GPP criteria in [102]. As previously explained in Section 3.4.3 it is defined as the normalized user throughput CDF with respect to the average. If it proceeds on the right side of the identity function the system performance fulfils a fair throughput distribution among users. The limit defines a linear relation between the user throughput and the probability to experience a certain throughput. In Figure 5.16 the fairness evaluation of the investigated system is presented. Compared to the reference network (light grey) the RN extended network has a slightly higher variance of throughput values, since it is a bit flatter. However, all example RN network settings shown here fulfil the fairness requirement of the 3GPP. The fairness of the network is kept stable by the applied hybrid RRM scheme.

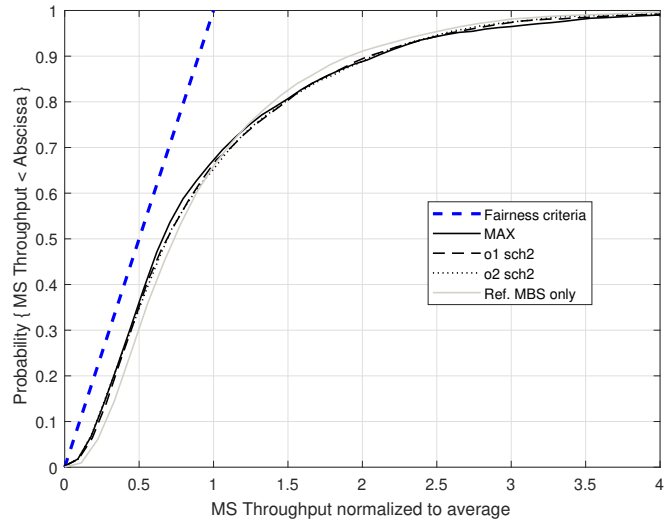


Figure 5.16: Final Comparison of the Fairness Criterion

### 5.3.6 Energy consumption

Due to the network-centralized asynchronous optimization as defined in Section 4.3 a smaller amount of energy is used for transmission on a number of PRBs in the downlink data channel. Dependent on the MBS or RN specific power adaptation possible energy savings can be reached. Figure 5.17 shows the CDF with the probability of potential power savings for MBS, RNs respectively. Here, the best found setting (fitness function o2 with scheduling policy 2) provides also the highest power savings. Approximately up to 2.7 dB for MBS as well as 3.2 dB for RN transmissions could be saved.

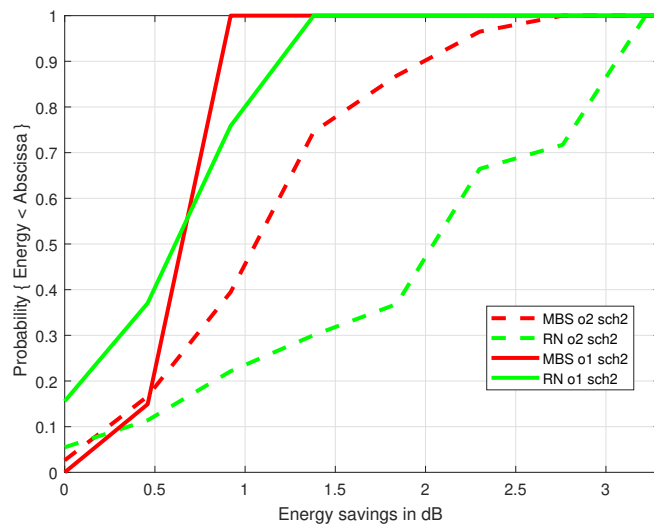


Figure 5.17: Final Comparison of potential MBS and RN transmission power savings on the DL data channel

# Chapter 6

## Conclusions and outlook

### 6.1 Conclusions

In order to fulfil the growing data demand in mobile networks the work in this Thesis shows that the proposed hybrid radio resource management scheme is able to increase the system capacity in relay-extended networks.

It contributed an answer to the question, if it is possible to improve the overall user throughput of the system by designing an hybrid radio resource management approach under full practical limitations. That is why, the wireless backhaul link is considered as the bottleneck of the possible two-hop connections. Moreover, an realistic additional feedback delay model is defined and applied during the system level simulations to evaluate the hybrid RRM scheme. The analysis of this work shows performance improvements in terms of the overall user throughput by adapting:

1. The decentralized cell selection scheme, by taking into account the imbalances of the sending and receiving time and the link type qualities for the MS attachment.
2. The synchronous cell-centralized radio resource scheduler to derive a two-hop proportional fair and frequency selective accurate resource allocation decision in each transmission time interval.
3. The asynchronous network-centralized transmission power, which finds an improved transmission power setting for each serving node on a part of the system bandwidth in time intervals when the RNs are in the sending or the receiving mode.

The possible improvements based on the proposed hybrid radio resource management have been verified by detailed system level simulations.

In addition to this the Thesis shows the possibility to introduce relays to a mobile network without additional costs related to planning effort or additional hardware, such as an receiving antenna for the relay wireless backhaul link. It also takes into account the limited possible sites to deploy relays in realistic networks. Moreover, possible energy savings are shown by reducing the applied transmission power in the network. The Thesis also discusses the necessary additional signalling effort which is needed to apply the proposed hybrid RRM scheme.

For further standardization it is recommended to take the necessary signalling into account in the 3GPP study item on RNs for 5G NR [5]. Furthermore, the Thesis gives valuable information about the co-scheduling functionality among RN and MSs, which is not solved yet.

## 6.2 Future work

In the future, the work of this Thesis can be extended in different directions:

- Further increase the flexibility of the radio resource scheduler by introducing a higher amount of antennas and thus a higher amount of spatial layers. In combination with a multi user MIMO scheduler it might be further improve the qualities of the wireless backhaul links. However, the additional necessary signalling traffic would be increased.
- The time ratio between the backhaul and the access transmission can be adapted in addition. Here, still an asynchronous scheme might make sense due to the increased probability of outdated feedback when switching the time ratio dynamically. Furthermore, the time ratio needs to be network centralized to prevent unwanted relay to relay interference. The applied heuristic could be extended by considering the target time ratio in the defined fitness functions.

The gained knowledge of this Thesis can also be used to develop a sophisticated RRM scheme for full duplex relay nodes in the future. It will be necessary to adapt the proposed scheme in such a way, that the large imbalances of the received and sent power at the relays are taken into account and compensated to prevent prohibitive self-interference as one of the most problematic research challenges for full duplex relays. Furthermore, the

proposed hybrid scheme could be adapted for a network infrastructure supported device-to-device network to improve the coverage of the system. Especially, as the worst case assumptions for the wireless backhaul links are taken into account, the proposed scheme could be used for a device-to-device extended network.

# Appendices

# Appendix A

## Numerical Examples for different scheduling metrics

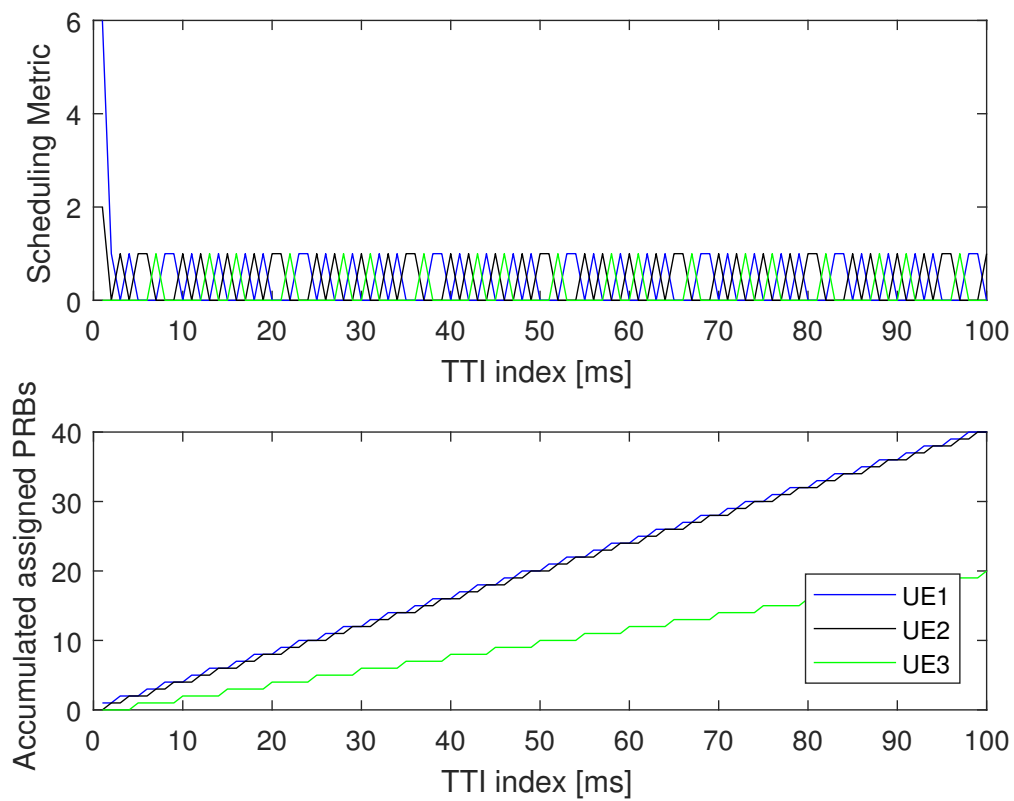


Figure A.1: Numerical example for a round robin scheduler

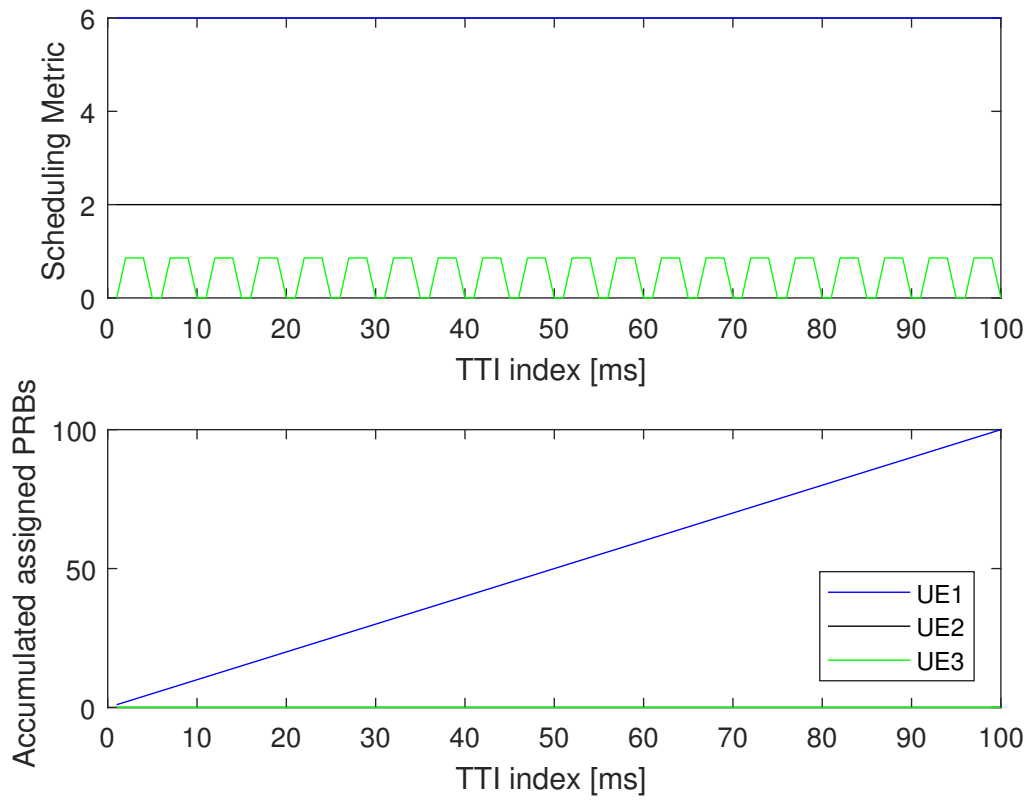


Figure A.2: Numerical example for a Max-Min scheduler

# Bibliography

- [1] Afif Osseiran, Federico Boccardi, Volker Braun, Katsutoshi Kusume, Patrick Marsch, Michal Maternia, Olav Queseth, Malte Schellmann, Hans Schotten, Hidekazu Taoka, Hugo Tullberg, Mikko A. Uusitalo, Bogdan Timus, and Mikael Fallgren. Scenarios for 5G mobile and wireless communications: the vision of the METIS project. *IEEE Communications Magazine*, 52(5):26–35, may 2014.
- [2] Monica (Senza Fili Consulting) Paolini. White paper Crucial economics for mobile data backhaul. 2011.
- [3] Christian Hoymann, Wanshi Chen, Juan Montojo, Alexander Golitschek, Chrysostomos Koutsimanis, and Xiaodong Shen. Relaying operation in 3GPP LTE: challenges and solutions. *IEEE Communications Magazine*, 50(2):156–162, feb 2012.
- [4] 3GPP. TR 36.806 v9.0.0, Relay architectures for E-UTRA (LTE-Advanced). Technical Report Release 9, 2010.
- [5] 3GPP. 3GPP TR 38.874 V0.2.1 (2018-05) Study on Integrated Access and Backhaul; (Release 15), 2018.
- [6] 3GPP. 3GPP TS 23.002 V15.0.0 (2018-03) Technical Specification Group Services and System Aspects; Network architecture (Release 15), 2018.
- [7] 3GPP. 3GPP TS 23.401 V15.3.0 (2018-03) Evolved Universal Terrestrial Radio Access Network (E-UTRAN) access (Release 15), 2018.
- [8] 3GPP. 3GPP TS 23.101 V14.0.0 (2017-03) General Universal Mobile Telecommunications System (UMTS) architecture (Release 14), 2017.
- [9] 3GPP. 3GPP TS 36.300 V15.1.0 (2018-03) Evolved Universal Terrestrial Radio Access (E-UTRA) and Evolved Universal Terrestrial Radio Access Network (E-UTRAN); Overall description; Stage 2 (Release 15), 2018.

- [10] 3GPP. 3GPP TS 36.423 V15.1.0 (2018-03) X2 application protocol (X2AP) (Release 15), 2018.
- [11] 3GPP. 3GPP TR 36.806 V0.2.0 (2009-11) Relay architectures for E-UTRA (LTE-Advanced (Release 9), 2011.
- [12] 3GPP. 3GPP TS 38.300 V15.1.0 (2018-03) NR; NR and NG-RAN Overall Description; Stage 2 (Release 15), 2018.
- [13] 3GPP. 3GPP TS 38.401 V15.1.0 (2018-03) NG-RAN; Architecture description (Release 15), 2018.
- [14] Stefan Brueck. Heterogeneous Networks in LTE-Advanced. *Management*, pages 171–175, 2011.
- [15] Naga Bhushan, Junyi Li, Durga Malladi, Rob Gilmore, Dean Brenner, Aleksandar Damnjanovic, Ravi Sukhavasi, Chirag Patel, and Stefan Geirhofer. Network densification: the dominant theme for wireless evolution into 5G. *IEEE Communications Magazine*, 52(2):82–89, feb 2014.
- [16] Mona Jaber, Muhammad Ali Imran, Rahim Tafazolli, and Anvar Tukmanov. 5G Backhaul Challenges and Emerging Research Directions: A Survey. *IEEE Access*, 4:1743–1766, 2016.
- [17] Paul Arnold, Nico Bayer, Jakob Belschner, and Gerd Zimmermann. 5G radio access network architecture based on flexible functional control / user plane splits. *2017 European Conference on Networks and Communications (EuCNC)*, pages 1–5, 2017.
- [18] Ying Loong Lee, Teong Chee Chuah, Jonathan Loo, and Alexey Vinel. Recent Advances in Radio Resource Management for Heterogeneous LTE/LTE-A Networks. *IEEE Communications Surveys & Tutorials*, 16(4):2142–2180, 2014.
- [19] Volker Jungnickel, Konstantinos Manolakis, Stephan Jaeckel, Moritz Lossow, Peter Farkas, Michael Schlosser, and Volker Braun. Backhaul requirements for inter-site cooperation in heterogeneous LTE-Advanced networks. In *2013 IEEE International Conference on Communications Workshops (ICC)*, pages 905–910. IEEE, jun 2013.

- [20] Volker Jungnickel, Konstantinos Manolakis, Wolfgang Zirwas, Berthold Panzner, Volker Braun, Moritz Lossow, Mikael Sternad, Rikke Apelfröjd, and Tommy Svensson. The role of small cells, coordinated multipoint, and massive MIMO in 5G. *IEEE Communications Magazine*, 52(5):44–51, 2014.
- [21] 3GPP. TR 36.913, Requirements for further advancements for Evolved Universal Terrestrial Radio Access (E-UTRA). Technical report, 2011.
- [22] M Salem, A Adinoyi, H Yanikomeroglu, and D Falconer. Opportunities and Challenges in OFDMA-Based Cellular Relay Networks: A Radio Resource Management Perspective. *IEEE Transactions on Vehicular Technology*, 59(5):2496–2510, 2010.
- [23] Ashutosh Sabharwal, Philip Schniter, Dongning Guo, Daniel W. Bliss, Sampath Rangarajan, and Risto Wichman. In-Band Full-Duplex Wireless: Challenges and Opportunities. *IEEE Journal on Selected Areas in Communications*, 32(9):1637–1652, sep 2014.
- [24] Zhongshan Zhang, Xiaomeng Chai, Keping Long, Athanasios V. Vasilakos, and Lajos Hanzo. Full duplex techniques for 5G networks: self-interference cancellation, protocol design, and relay selection. *IEEE Communications Magazine*, 53(5):128–137, may 2015.
- [25] Vaneet Aggarwal, Melissa Duarte, Ashutosh Sabharwal, and N. K. Shankaranarayanan. Full- or half-duplex? A capacity analysis with bounded radio resources. In *2012 IEEE Information Theory Workshop*, pages 207–211. IEEE, sep 2012.
- [26] Zhongshan Zhang, Keping Long, Athanasios V. Vasilakos, and Lajos Hanzo. Full-Duplex Wireless Communications: Challenges, Solutions, and Future Research Directions. *Proceedings of the IEEE*, 104(7):1369–1409, jul 2016.
- [27] 3GPP. 3GPP TS 36.213 V15.1.0 (2018-03) Physical layer procedures (Release 15), 2018.
- [28] 3GPP. 3GPP TR 36.819 - Coordinated multi-point operation for LTE physical layer aspects. Technical report, 2013.

- [29] Yifei Yuan. *LTE-Advanced Relay Technology and Standardization*. Signals and Communication Technology. Springer Berlin Heidelberg, Berlin, Heidelberg, 2013.
- [30] Xiaohu Ge, Hui Cheng, Mohsen Guizani, and Tao Han. 5G wireless backhaul networks: challenges and research advances. *IEEE Network*, 28(6):6–11, nov 2014.
- [31] Ning Wang, Ekram Hossain, and Vijay K Bhargava. Backhauling 5G small cells: A radio resource management perspective. *IEEE Wireless Communications*, 22(5):41–49, oct 2015.
- [32] Claudio Coletti, Preben Mogensen, and Ralf Irmer. Deployment of LTE in-band relay and micro base stations in a realistic metropolitan scenario. *IEEE Vehicular Technology Conference*, pages 0–4, 2011.
- [33] Claudio Coletti, Preben Mogensen, and Ralf Irmer. Performance analysis of relays in LTE for a realistic suburban deployment scenario. In *IEEE Vehicular Technology Conference*, 2011.
- [34] Li Chen, Wenwen Chen, Bin Wang, Xin Zhang, Hongyang Chen, and Dacheng Yang. System-level simulation methodology and platform for mobile cellular systems. *IEEE Communications Magazine*, 49(7):148–155, jul 2011.
- [35] Josep Colom Ikuno. *System Level Modeling and Optimization of the LTE Downlink*. PhD thesis, 2012.
- [36] T.F. Maciel and Anja Klein. On the Performance, Complexity, and Fairness of Suboptimal Resource Allocation for Multiuser MIMOOFDMA Systems. *IEEE Transactions on Vehicular Technology*, 59(1):406–419, jan 2010.
- [37] International Telecommunication Union Radiocommunication Sector. IMT traffic estimates for the years 2020 to 2030. Technical report, 2015.
- [38] Hossein Falaki, Dimitrios Lymberopoulos, Ratul Mahajan, Srikanth Kandula, and Deborah Estrin. A first look at traffic on smartphones. *Proceedings of the 10th annual conference on Internet measurement - IMC '10*, page 281, 2010.
- [39] Mi Kyoung Kim and Hwang Soo Lee. Radio Resource Management for a Two-hop OFDMA Relay System in Downlink. *2007 IEEE Symposium on Computers and Communications*, pages 25–31, jul 2007.

- [40] Mehrdad Shariat, Emmanouil Pateromichelakis, Atta Ul Quddus, and Rahim Tafazolli. Joint TDD Backhaul and Access Optimization in Dense Small-Cell Networks. *IEEE Transactions on Vehicular Technology*, 64(11):5288–5299, nov 2015.
- [41] Guocong Song and Ye Li. Cross-layer optimization for OFDM wireless networks-part I: theoretical framework. *IEEE Transactions on Wireless Communications*, 4(2):614–624, mar 2005.
- [42] Guocong Song and Ye Li. Cross-layer optimization for OFDM wireless networks-part II: algorithm development. *IEEE Transactions on Wireless Communications*, 4(2):625–634, mar 2005.
- [43] Jieying Chen, Randall Berry, and Michael Honig. Limited feedback schemes for downlink OFDMA based on sub-channel groups. *IEEE Journal on Selected Areas in Communications*, 26(8):1451–1461, oct 2008.
- [44] Niko Kolehmainen, Jani Puttonen, Petteri Kela, Tapani Ristaniemi, Tero Henttonen, and Martti Moision. Channel quality indication reporting schemes for UTRAN long term evolution downlink. In *IEEE Vehicular Technology Conference*, pages 2522–2526. IEEE, may 2008.
- [45] Sanam Sadr, Alagan Anpalagan, and Kaamran Raahemifar. Radio Resource Allocation Algorithms for the Downlink of Multiuser OFDM Communication Systems. *IEEE Communications Surveys & Tutorials*, 11(3):92–106, 2009.
- [46] Jieying Chen, Randall A Berry, and Michael L Honig. Performance of Limited Feedback Schemes for Downlink OFDMA with Finite Coherence Time. In *2007 IEEE International Symposium on Information Theory*, pages 2751–2755. IEEE, jun 2007.
- [47] 3GPP. 3GPP TS 36.211 V15.1.0 (2018-03) Physical channels and modulation (Release 15), 2018.
- [48] A.J. Goldsmith and S.-G. Chua. Adaptive coded modulation for fading channels. *IEEE Transactions on Communications*, 46(5):595–602, may 1998.
- [49] Peng Tan, Yan Wu, and Sumei Sun. Link adaptation based on adaptive modulation and coding for multiple-antenna OFDM system. *IEEE Journal on Selected Areas in Communications*, 26(8):1599–1606, oct 2008.

- [50] Sungho Yun and Constantine Caramanis. Reinforcement Learning for Link Adaptation in MIMO-OFDM Wireless Systems. In *2010 IEEE Global Telecommunications Conference GLOBECOM 2010*, pages 1–5. IEEE, dec 2010.
- [51] Huiling Dai, Ying Wang, Ke Zhang, and Cong Shi. Link adaptation algorithms for channel estimation error mitigation in LTE systems. In *2012 IEEE Global Communications Conference (GLOBECOM)*, pages 1835–1840. IEEE, dec 2012.
- [52] Jung Hyun Bae, Jungwon Lee, and Inyup Kang. Outage-based ergodic link adaptation for fading channels with delayed CSIT. In *2013 IEEE Global Communications Conference (GLOBECOM)*, pages 4098–4103. IEEE, dec 2013.
- [53] David Gesbert, Saad Ghazanfar Kiani, Anders Gjøendemsjø, and Geir Egil Oien. Adaptation, Coordination, and Distributed Resource Allocation in Interference-Limited Wireless Networks. *Proceedings of the IEEE*, 95(12):2393–2409, dec 2007.
- [54] Andras Racz, Norbert Reider, and Gabor Fodor. On the Impact of Inter-Cell Interference in LTE. In *IEEE GLOBECOM 2008 - 2008 IEEE Global Telecommunications Conference*, pages 1–6. IEEE, 2008.
- [55] Guoqing Li and Hui Liu. Resource Allocation for OFDMA Relay Networks With Fairness Constraints. *IEEE Journal on Selected Areas in Communications*, 24(11):2061–2069, nov 2006.
- [56] Xiaojun Tang and Yingbo Hua. Optimal design of non-regenerative MIMO wireless relays. *IEEE Transactions on Wireless Communications*, 6(4):1398–1406, 2007.
- [57] Lei Huang, Mengtian Rong, Lan Wang, Yisheng Xue, and Egon Schulz. Resource Allocation for OFDMA Based Relay Enhanced Cellular Networks. *2007 IEEE 65th Vehicular Technology Conference - VTC2007-Spring*, pages 3160–3164, 2007.
- [58] Jintao Du and Jihong Zhao. RRM strategy based on throughput and fairness in LTE-A relay system. In *16th International Conference on Advanced Communication Technology*, pages 1059–1064. Global IT Research Institute (GIRI), feb 2014.

- [59] Ying Cui, V.K.N. Lau, and Rui Wang. Distributive subband allocation, power and rate control for relay-assisted OFDMA cellular system with imperfect system state knowledge. *IEEE Transactions on Wireless Communications*, 8(10):5096–5102, oct 2009.
- [60] Jeong Ae Han and Wha Sook Jeon. Proportional fair scheduling combined with adjustment of two hop transmission time for relay-aided OFDMA systems. In *2009 International Conference on Wireless Communications & Signal Processing*, pages 1–5. IEEE, nov 2009.
- [61] Wha Sook Jeon, Jeong Ae Han, and Dong Geun Jeong. Distributed Resource Allocation for Multi-Cell Relay-Aided OFDMA Systems. *IEEE Transactions on Mobile Computing*, 13(9):2003–2015, sep 2014.
- [62] G Boudreau, J Panicker, Ning Guo, Rui Chang, Neng Wang, and S Vrzic. Interference coordination and cancellation for 4G networks. *IEEE Communications Magazine*, 47(4):74–81, apr 2009.
- [63] Husam Eldin Elmutasim Osman Mohamed Elfadil, Mohammed Adil Ibrahim Ali, and Mohammed Abas. Fractional frequency reuse in LTE networks. *2015 2nd World Symposium on Web Applications and Networking (WSWAN)*, pages 1–6, 2015.
- [64] Lei Zhang, Hong Chuan Yang, and Mazen O. Hasna. Analysis of cell spectral efficiency of infrastructure relay-enhanced cellular system. *2011 International Conference on Wireless Communications and Signal Processing, WCSP 2011*, 2011.
- [65] Miguel Eguizabal and Angela Hernandez. Dynamic, fair and coordinated resource allocation for backhaul links for heterogeneous load conditions in LTE-advanced relay systems. In *2014 6th International Congress on Ultra Modern Telecommunications and Control Systems and Workshops (ICUMT)*, volume 2015-Janua, pages 33–40. IEEE, oct 2014.
- [66] Abdelbaset S. Hamza, Shady S. Khalifa, Haitham S. Hamza, and Khaled Elsayed. A Survey on Inter-Cell Interference Coordination Techniques in OFDMA-Based Cellular Networks. *IEEE Communications Surveys & Tutorials*, 15(4):1642–1670, 2013.

- [67] Shuqin Zheng, Hui Tian, Zheng Hu, Lan Chen, and Jianchi Zhu. QoS-Guaranteed Radio Resource Allocation with Distributed Inter-Cell Interference Coordination for Multi-Cell OFDMA Systems. *2010 IEEE 71st Vehicular Technology Conference*, pages 1–5, 2010.
- [68] Yicheng Lin, Student Member, Wei Yu, and Senior Member. Fair Scheduling and Resource Allocation for Wireless Cellular Network with Shared Relays. *30(8):1530–1540*, 2012.
- [69] Chen Sun, Weidong Wang, Yinghai Zhang, and Xiaojun Wang. Distributed two-hop proportional fair resource allocation in Long Term Evolution Advanced networks. *Wireless Communications and Mobile Computing*, 16(3):264–278, feb 2016.
- [70] Long Wang, Qinghe Du, Pinyi Ren, Li Sun, and Yichen Wang. Buffering-aided resource allocation for Type I relay in LTE-Advanced cellular networks. In *2014 IEEE Global Communications Conference*, number 20110201120014, pages 4484–4489. IEEE, dec 2014.
- [71] Su Yi and Ming Lei. Backhaul resource allocation in LTE-Advanced relaying systems. In *2012 IEEE Wireless Communications and Networking Conference (WCNC)*, pages 1207–1211. IEEE, apr 2012.
- [72] 3GPP. 3GPP TS 36.214 V15.2.0 Physical layer Measurements (Release 15), 2018.
- [73] Won-Hyoung Park and Saewoong Bahk. Resource management policies for fixed relays in cellular networks. *Computer Communications*, 32(4):703–711, mar 2009.
- [74] Zhuyan Zhao, Jian Wang, Simone Redana, and Bernhard Raaf. Downlink resource allocation for LTE-advanced networks with type1 relay nodes. *IEEE Vehicular Technology Conference*, (1), 2012.
- [75] Hoon Kim and Youngnam Han. A proportional fair scheduling for multicarrier transmission systems. *IEEE Communications Letters*, 9(3):210–212, mar 2005.
- [76] Zhangchao Ma, Wei Xiang, Hang Long, and Wenbo Wang. Proportional Fair Resource Partition for LTE-Advanced Networks with Type I Relay Nodes. In *2011 IEEE International Conference on Communications (ICC)*, pages 1–5. IEEE, jun 2011.

- [77] Mattia Minelli, Maode Ma, Marceau Coupechoux, and Philippe Godlewski. Scheduling Impact on the Performance of Relay-Enhanced LTE-A Networks. *IEEE Transactions on Vehicular Technology*, 65(4):2496–2508, 2016.
- [78] Paul Arnold, Veselin Rakocevic, Oscar Ramos, and Joachim Habermann. Algorithms for Adaptive Radio Resource Management in Relay-Assisted LTE-A Networks. In *2013 IEEE 77th Vehicular Technology Conference (VTC Spring)*, pages 1–5. IEEE, jun 2013.
- [79] Woo-geun Ahn and Hyung-myung Kim. Proportional fair scheduling in relay enhanced cellular OFDMA systems. In *2008 IEEE 19th International Symposium on Personal, Indoor and Mobile Radio Communications*, volume 2, pages 1–4. IEEE, sep 2008.
- [80] Mazen O. Hasna and Mohamed Slim Alouini. Harmonic Mean and End-to-End Performance of Transmission Systems With Relays. *IEEE Transactions on Communications*, 52(1):130–135, 2004.
- [81] Chang Liu, Xiaowei Qin, Sihai Zhang, and Wuyang Zhou. Proportional-fair downlink resource allocation in OFDMA-based relay networks. *Journal of Communications and Networks*, 13(6):633–638, dec 2011.
- [82] Kifle Woldemedhin, Omer Bulakci, Abdallah Bou Saleh, Simone Redana, and Fabrizio Granelli. Joint backhaul co-scheduling and relay cell extension in LTE-advanced networks uplink performance evaluation. 2012.
- [83] Guenther Liebl, Thiago Martins de Moraes, Akin Soysal, and Eiko Seidel. Fair resource allocation for inband relaying in LTE-Advanced. In *2011 8th International Workshop on Multi-Carrier Systems & Solutions*, volume 1, pages 1–5. IEEE, may 2011.
- [84] Guenther Liebl, Thiago Martins De Moraes, Akin Soysal, and Eiko Seidel. Fair resource allocation for the relay backhaul link in LTE-Advanced. In *IEEE Wireless Communications and Networking Conference, WCNC*, pages 1196–1201. IEEE, apr 2012.
- [85] Zhengchuan Chen, Tao Li, Pingyi Fan, Tony Q.S. Quek, and Khaled Ben Letaief. Cooperation in 5G Heterogeneous Networking: Relay Scheme Combination and

- Resource Allocation. *IEEE Transactions on Communications*, 64(8):3430–3443, 2016.
- [86] Cai Hong Kai, Hui Li, and Liping Qian. Game-theoretic radio resource management for relay-assisted access in wireless networks. *IET Communications*, 12(5):566–572, 2017.
- [87] Zhengchuan Chen, Pingyi Fan, and Dapeng Oliver Wu. Joint Power Allocation and Strategy Selection for Half-Duplex Relay System. *IEEE Transactions on Vehicular Technology*, 66(3):2144–2157, mar 2017.
- [88] Richa Gupta and Suresh Kalyanasundaram. Resource allocation for self-backhauled networks with half-duplex small cells. *2017 IEEE International Conference on Communications Workshops, ICC Workshops 2017*, pages 198–204, 2017.
- [89] Ben-jye Chang, Po-yen Chang, and Ying-hsin Liang. Adaptive Packet Scheduling and Radio RB Allocation for LTE-A toward 5G Relaying Communications. pages 1–7, 2017.
- [90] Lun Tang, Xixi Yang, Xiaolin Wu, Taiping Cui, and Qianbin Chen. Queue Stability-Based Virtual Resource Allocation for Virtualized Wireless Networks with Self-Backhauls. *IEEE Access*, 6:13604–13616, 2018.
- [91] Lanqin He, Lun Tang, Hao Liao, Qianbin Chen, and Yannan Wei. Queue-Aware Dynamic Resource Reuse and Joint Allocation Algorithm in Self-Backhaul Small Cell Networks. *IEEE Access*, 6:61077–61090, 2018.
- [92] Naeimeh Omidvar, An Liu, Vincent Lau, Fan Zhang, Danny H.K. Tsang, and Mohammad Reza Pakravan. Optimal Hierarchical Radio Resource Management for HetNets with Flexible Backhaul. *IEEE Transactions on Wireless Communications*, 17(7):4239–4255, 2018.
- [93] Wooseok Nam, Woohyuk Chang, S.-Y. Chung, and Yong H Lee. Transmit Optimization for Relay-Based Cellular OFDMA Systems. In *2007 IEEE International Conference on Communications*, pages 5714–5719. IEEE, jun 2007.
- [94] Mohamed Salem, Abdulkareem Adinoyi, Mahmudur Rahman, Halim Yanikomeroğlu, David Falconer, Young-Doo Kim, Eungsun Kim, Yoon-Chae

- Cheong, Young-Doo Kim, Eungsun Kim, Yoon-Chae Cheong, Young-Doo Kim, Eungsun Kim, and Yoon-Chae Cheong. An Overview of Radio Resource Management in Relay-Enhanced OFDMA-Based Networks. *IEEE Communications Surveys & Tutorials*, 12(3):422–438, 2010.
- [95] 3GPP. 3GPP TR 36.872 Small cell enhancements for E-UTRA and E-UTRAN - Physical layer aspects (Release 12). Technical report, 3GPP, 2013.
- [96] Jacek Góra and Simone Redana. Resource management issues for multi-carrier relay-enhanced systems. *EURASIP Journal on Wireless Communications and Networking*, 2012(1):124, dec 2012.
- [97] Gunther Auer, George T Karetsos, Paulo Jose Jesus, and Sofoklis Kyriazakos. WINNER II Deliverable D6 . 13 . 7 : Test Scenarios and Calibration Cases IST-4-027756 WINNER II. Technical Report December, 2006.
- [98] 3GPP. TR 36.814 v9.0.0, Further advancements for E-UTRA physical layer aspects, 2010.
- [99] Ralf Irmer, Martin Döttling, Simone Redana, Tobias Frank, David Falconer, Tommy Svensson, Eric Hardouin, Yi Yuan, Mugdim Bublin, Alexander Tyrrell, and Ralf Pabst. WINNER II D6.13.10 V1.0. 1(127):1–127, 2007.
- [100] E Tragos, S A Kyriazakos, and A Mihovska. IST-4-027756 WINNER II D6.13.1 WINNER II Test scenarios and calibration cases issue 1. Technical Report 1, 2006.
- [101] 3GPP. 3GPP TR 25.996 V14.0.0 (2017-03). Technical report, 2017.
- [102] 3GPP2. cdma2000 Evaluation Methodology Revision A. Technical report, 2009.
- [103] Report ITU-R M.2135-1. Guidelines for evaluation of radio interface technologies for IMTadvanced. *Evaluation*, 93(3), 2009.
- [104] 3GPP. R1-092742 3GPP TSG RAN WG1 Meeting #57bis. Summary on calibration step 1c. Technical report, 2009.
- [105] S. Naga Sekhar Kshatriya, Sunil Kaimalettu, Sivakishore Reddy Yerrapareddy, Klutto Milleth, and Nadeem Akhtar. On interference management based on sub-frame blanking in Heterogeneous LTE networks. In *2013 Fifth International Conference on Communication Systems and Networks (COMSNETS)*, pages 1–7. IEEE, jan 2013.

- [106] Paul Arnold, Veselin Rakocevic, and Joachim Habermann. Simulation study on 2 hop-proportional fair scheduling and eICIC in relay type 1 extended LTE-A networks. *2015 IEEE 82nd Vehicular Technology Conference, VTC Fall 2015 - Proceedings*, pages 0–4, 2016.
- [107] 3GPP. 3GPP TR 36.873 V12.7.0 Study on 3D channel model for LTE (Release 12). Technical report, 2017.
- [108] C. Blum and A. Roli. Metaheuristics in combinatorial optimization: overview and conceptual comparison. *ACM Computing Surveys*, 35(3):189–213, 2003.
- [109] Johann Dréo, Alain Pétrowski, and Eric Taillard. *Metaheuristics for Hard Optimization*. Springer-Verlag, Berlin/Heidelberg, 2006.
- [110] Sonia Sharma and Hari Mohan Pandey. Genetic Algorithm, Particle Swarm Optimization and Harmony Search: A quick comparison. *6th International Conference - Cloud System and Big Data Engineering (Confluence)*, pages 40–44, 2016.
- [111] Engku Muhammad Nazri and Stanley Murairwa. Classification of heuristic techniques for performance comparisons. In *2016 12th International Conference on Mathematics, Statistics, and Their Applications (ICMSA)*, pages 19–24. IEEE, oct 2016.
- [112] Rania Hassan, Babak Cohanim, and Olivier de Weck. A comparison of particle swarm optimization and the genetic algorithm. *1st AIAA multidisciplinary design optimization specialist conference*, pages 1–13, 2005.
- [113] Usama Mehboob, Junaid Qadir, Salman Ali, and Athanasios Vasilakos. *Genetic algorithms in wireless networking: techniques, applications, and issues*, volume 20. Springer Berlin Heidelberg, 2016.
- [114] Wern Ho Sheen, Shiang Jiun Lin, and Chia Chi Huang. Downlink optimization and performance of relay-assisted cellular networks in multicell environments. *IEEE Transactions on Vehicular Technology*, 59(5):2529–2542, 2010.
- [115] Luca Chiaraviglio, Delia Ciullo, George Koutitas, Michela Meo, and Leandros Tassiulas. Energy-efficient planning and management of cellular networks. *2012 9th Annual Conference on Wireless On-Demand Network Systems and Services, WONS 2012*, pages 159–166, 2012.

- [116] Juwo Yang, Hui Zhao, Wenbo Wang, and Chengcheng Zhang. An effective SINR mapping models for 256QAM in LTE-Advanced system. *IEEE International Symposium on Personal, Indoor and Mobile Radio Communications, PIMRC*, 2014-June:343–347, 2014.
- [117] Zakaria Hanzaz and Hans Dieter Schotten. Analysis of effective SINR mapping models for MIMO OFDM in LTE system. *2013 9th International Wireless Communications and Mobile Computing Conference, IWCMC 2013*, pages 1509–1515, 2013.